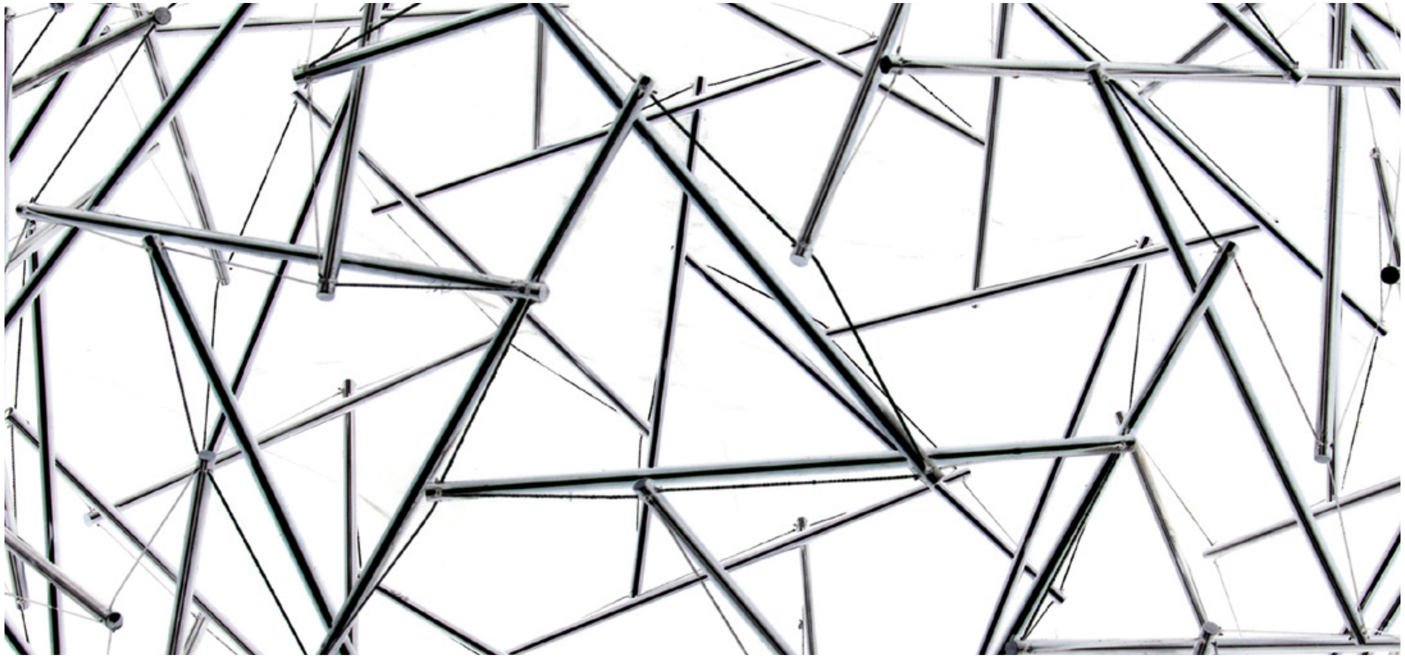

TOWARD A NEW TENSEGRITY SYSTEM

D. NGO

research (5’) + **design** (25’)

1. tensegrity needle tower, kenneth snelson, 1969

For more than 50 years, tensegrity is considered an innovative structural concept and it has the potentials to become a super-efficient structural system. In this system, the coupling between forces and forms is very tight, and this relation is made visible by structural components themselves.

Everyone is fascinated by seeing the very particular type of structural composition in which struts seem to float in the air. This character is also the key point since people, engineers and architects more than the others, are surprised by this new kind of flow of forces. They are used to gravity effect, and in this case, gravity seems to be absent.

2.1. tensegrity sphere

2.2. tensegrity pavilion, ball state university

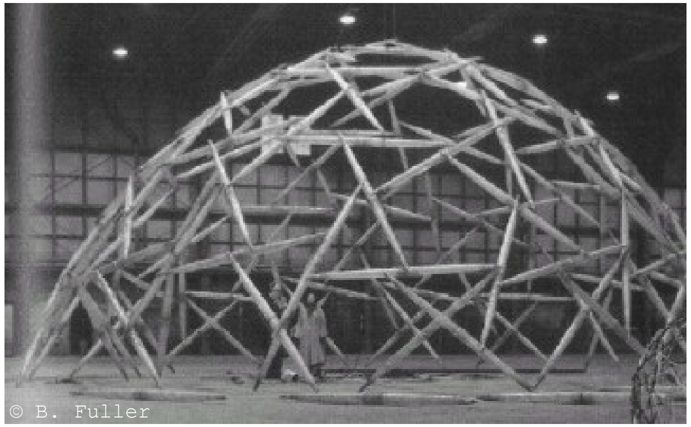

2.3. tensegrity dome, fuller

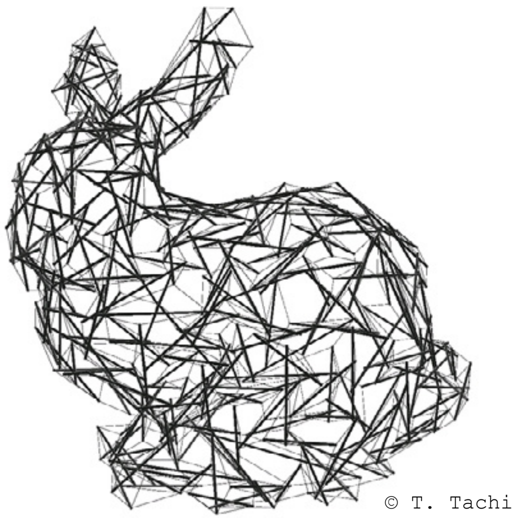

2.2. tensegrity rabit, taichi

The issue of form-finding is central in the study of tensegrity system due to the lack of design and analysis techniques, especially when the system is complex with a large number of struts and cables. The composition of struts in a network of cables could not be manually handled anymore.

On the other hand, spherical and domical structures of tensegrity are enormously sophisticated which can lead to difficulties in fabrication and assembling.

When the structure spans a long distance, it is almost impossible to predict the structural behavior to ensure whether or not they are stable in reality.

How to design a stable tensegrity system for a large span structure to cover a stadium?

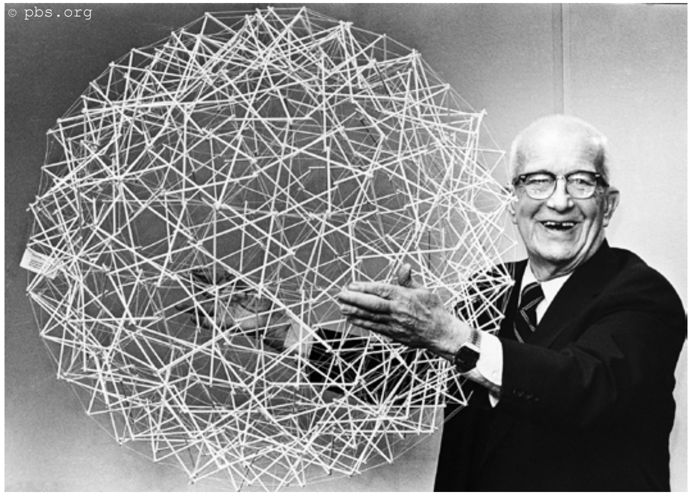

3.1. Buckminster Fuller with his tensegrity sphere

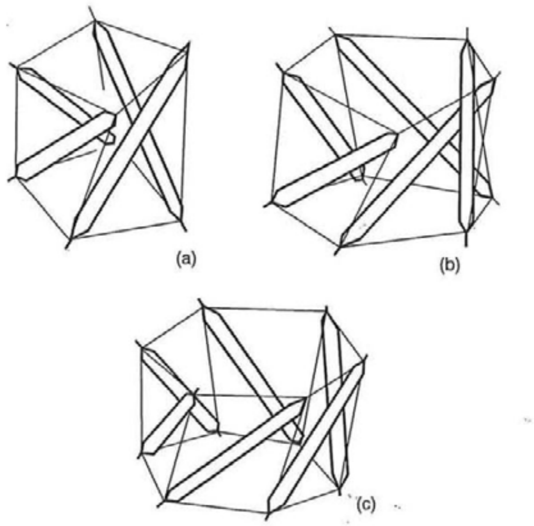

3.2. Tesegrity structures based on twisted prisms. a - 4 struts, b - 5 struts, c - 6 struts

B. Fuller gives the name to the structure. He describes tensegrity is the system in which there are islands of compression in the sea of tension.

A. Pugh gives a more comprehensive definition: *'A tensegrity system is established when a set of discontinuous compressive components interacts with a set of continuous tensile components to define a stable volume in space.'*

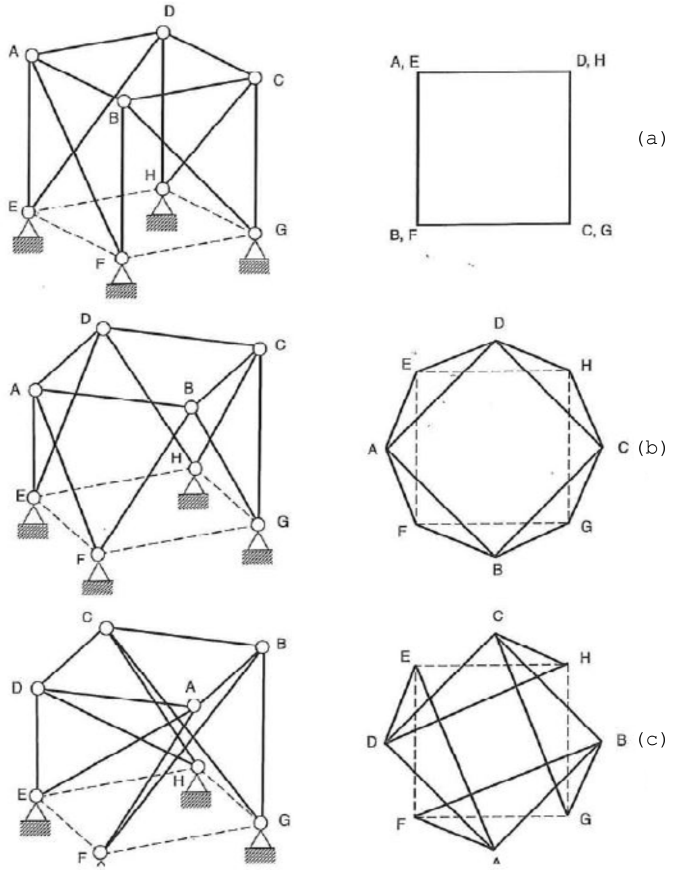

4. Cubic truss

The existence of special configurations that are both statically and kinematically indeterminate is a general feature of trusses based on two interconnected regular polygons with n-sides (in figure 4. n = 4) and, in particular, configurations that admit finite amplitude inextensional mechanisms exist for all trusses with n even and ≥ 4. However, for n odd, there are no such special configurations.

Truss structures with a layout similar to figure 4(b) have been used for several applications, often in preference to the layout in figure 4(a), because their higher degree of symmetry leads to the expectation of a ‘more uniform’ stiffness distribution.

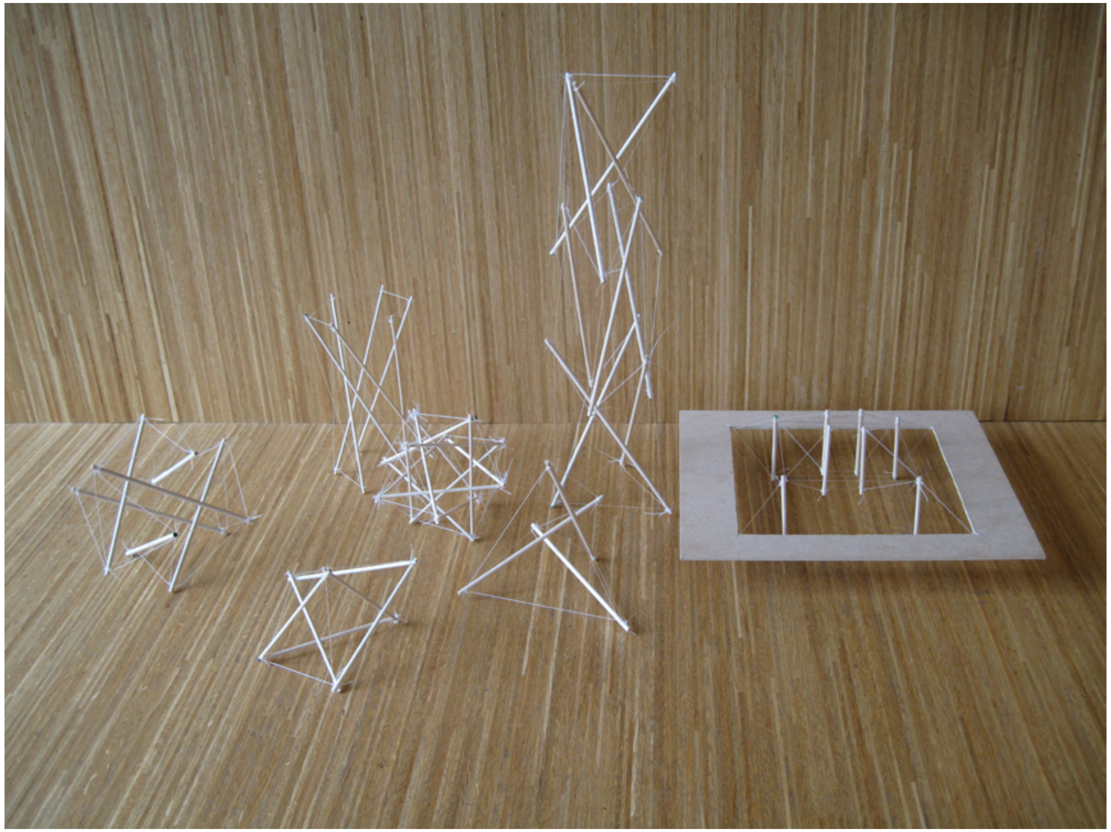

5. A collective of tensegrity models

A proper understanding of Tensegrity can only be gained by building and studying models of the figures. Depending on the type of tensegrity models, the different methods are applied, there is no method especially in favor.

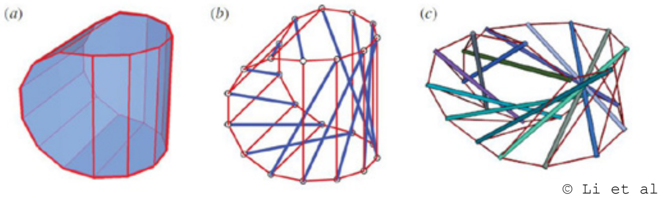

8.1. Construction of Z-based tensegrity based on a sphericon-like polyhedron. (a) The topology of a sphericon-like polyhedron assembled by two perpendicular half-prisms (b) The topology of struts (c) The form-finding result

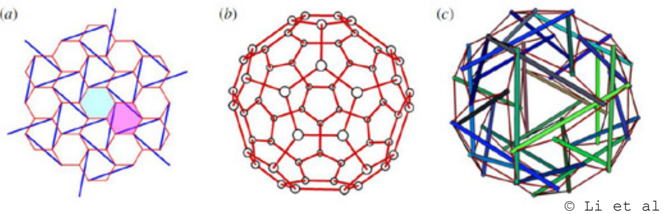

8.2. Construction of Z-based Bucky ball tensegrity. (a) A hexagonal mesh. There are two different modes of adding struts, which are colored by cyan and magenta, respectively (b) The topology of C_{60} Bucky ball (c) The form-finding result

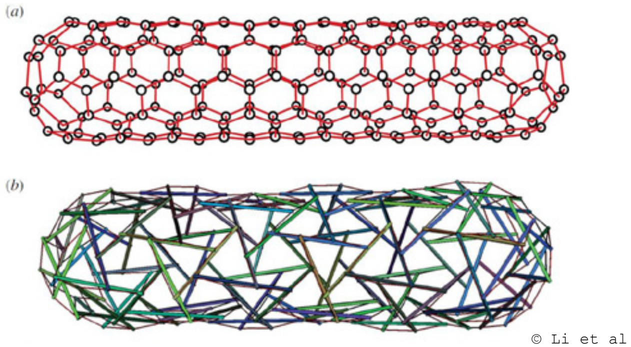

8.3. Construction of Z-based tensegrity resembling a capped carbon nanotube. (a) The topology of a capped (5,5) carbon nanotube (b) The form-finding result

Four Methods of Evolving New Tensegrity Systems

(1) One way of evolving new figures is to postulate a new concept of Tensegrity or to modify an existing idea.

(2) A second method is to discover a new relationship between struts and cables. There are several ways of doing it, as will be suggested later.

(3) A third method is to discover or develop new polyhedral figures which can be used as bases for Tensegrity systems using an already established relationship between struts and cables.

(4) A fourth method is to extend an existing idea or figure.

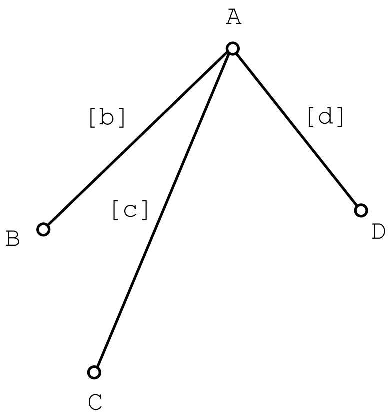

6.1. Topology of a frame

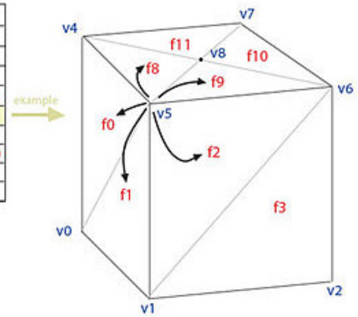

Face List

f0	v0 v4 v5
f1	v0 v5 v1
f2	v1 v5 v6
f3	v1 v6 v2
f4	v2 v6 v7
f5	v2 v7 v3
f6	v3 v7 v4
f7	v3 v4 v0
f8	v8 v5 v4
f9	v8 v6 v5
f10	v8 v7 v6
f11	v8 v4 v7
f12	v9 v5 v4
f13	v9 v6 v5
f14	v9 v7 v6
f15	v9 v4 v7

Vertex List

v0	0,0,0	f0 f1 f12 f15 f7
v1	1,0,0	f2 f3 f13 f12 f1
v2	1,1,0	f4 f5 f14 f13 f3
v3	0,1,0	f6 f7 f15 f14 f5
v4	0,0,1	f6 f7 f0 f8 f11
v5	1,0,1	f0 f1 f2 f9 f8
v6	1,1,1	f2 f3 f4 f10 f9
v7	0,1,1	f4 f5 f6 f11 f10
v8	.5,.5,0	f8 f9 f10 f11
v9	.5,.5,1	f12 13 14 15

© David Dorfman

6.2. Face-vertex topology of a cube

Consider the example in figure 6.1 consisting of three bars and four joints. In one matrix or with two named arrays we can describe the connectivity of this simple framework.

edge	start vertex	end vertex
[b]	A	B
[c]	A	C
[d]	A	D

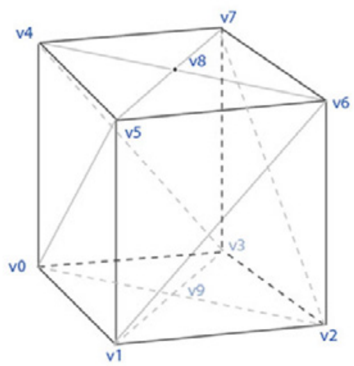

Vertex List

v0	0,0,0	v1 v5 v4 v3 v9
v1	1,0,0	v2 v6 v5 v0 v9
v2	1,1,0	v3 v7 v6 v1 v9
v3	0,1,0	v2 v6 v7 v4 v9
v4	0,0,1	v5 v0 v3 v7 v8
v5	1,0,1	v6 v1 v0 v4 v8
v6	1,1,1	v7 v2 v1 v5 v8
v7	0,1,1	v4 v3 v2 v6 v8
v8	.5,.5,1	v4 v5 v6 v7
v9	.5,.5,0	v0 v1 v2 v3

© David Dorfman

6.3. Vertex-vertex topology of a cube

Looking at figures 6.2 and 6.3, there is an introduction of using a combination of a face-vertex graph in combination with the vertex-vertex graph for the description of a topology of a given geometry. For the equilibrium matrix setup, a network graph will be used with its directional ordered pair written in form D = (V, A), where the order of every 2-element in A determines the start and end joint of a bar.

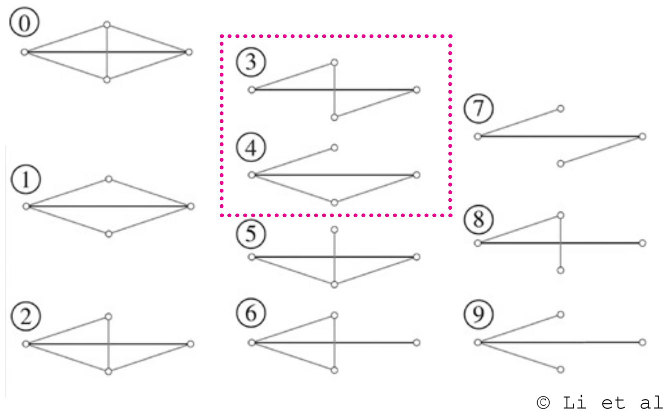

7.1. The topology graph of all elementary tensegrity cells containing one strut and 4 nodes.

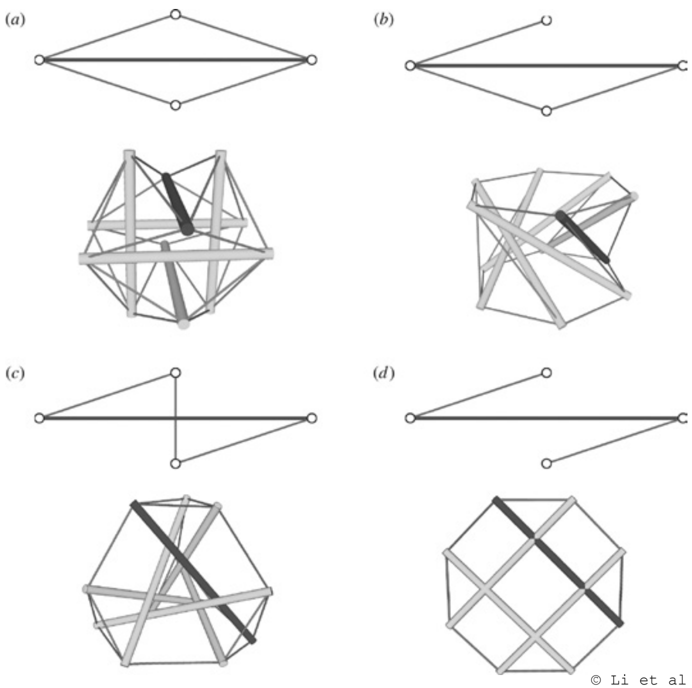

7.2. Typical tensegrity structures assembled from elementary cells
(a) octahedral tensegrity from type-1 cells
(b) cylindrical tensegrity from type-4 cells
(c) truncated tetrahedral from type-3 cells
(d) planar tensegrity from type-7 cells

Figure 7.1 lists all of the ten possible topology graphs of elementary cells containing one strut and four nodes. They are classified into four groups according to the number of cables. The type-0 cell has five cables, and it can be considered as the basis for other cells. By removing one, two, or three cables from the type-0 cell, we obtain elementary cells of the other nine types.

The elementary cells can be used to assemble almost all types of tensegrity structures. For example, the expandable octahedral, cylindrical and truncated regular tetrahedral tensegrity structures can be assembled from type-1, type-4, and type-3, respectively, while planar tensegrity structures can be constructed from the type-7 cell.

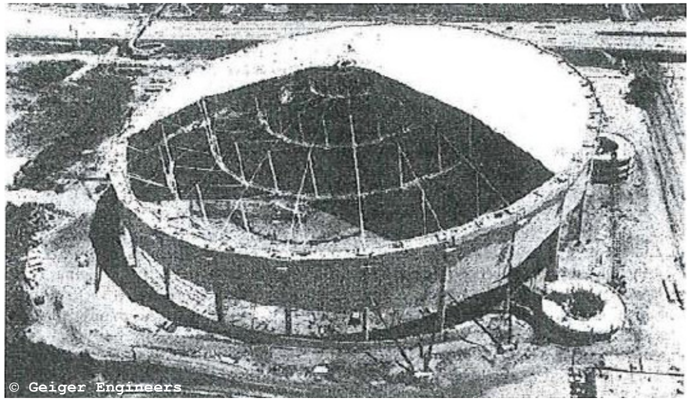

9.1. Sun Coast dome during construction

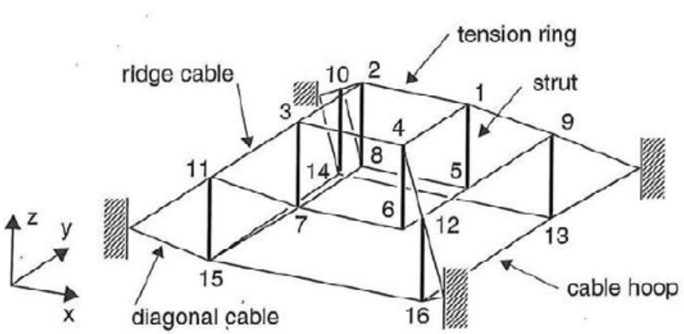

9.2. Small-scale version of structure of Sun Coast dome

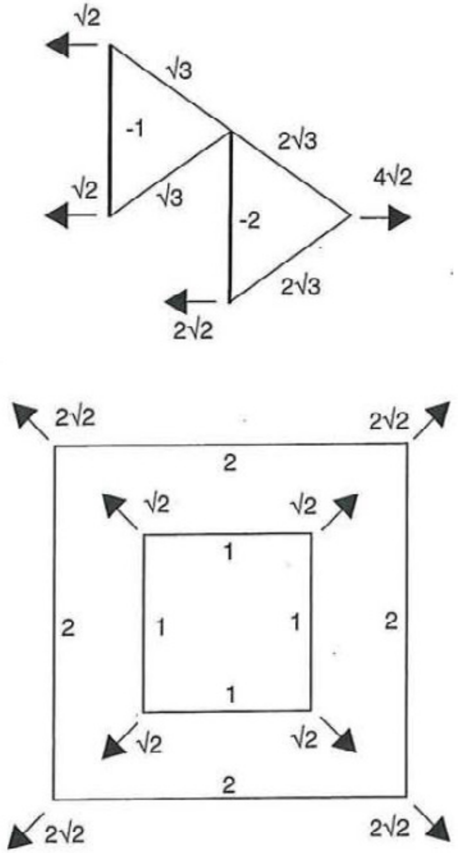

9.3. State of self-stress

In 1984 David Geiger developed the idea of the “Cable-dome” and realized for the Sun Coast Dome in St Peterburg, Florida (diameter 210 m). Figure 9.1 shows the dome during construction. This is a lightweight membrane roof supported by a pre-stressed cable-and-strut structure that was invented by David Geiger (Geiger, Stefaniuk, and Chen 1986). Geiger's structure was a successful, practical realization of an earlier tensegrity dome concept invented by Buckminster Fuller (1964).

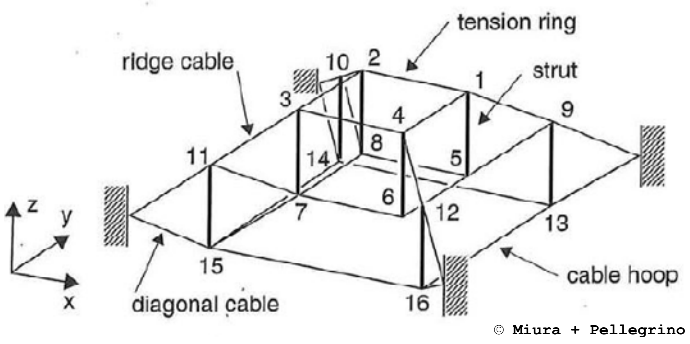

10.3. Small-scale version of structure of Sun Coast dome

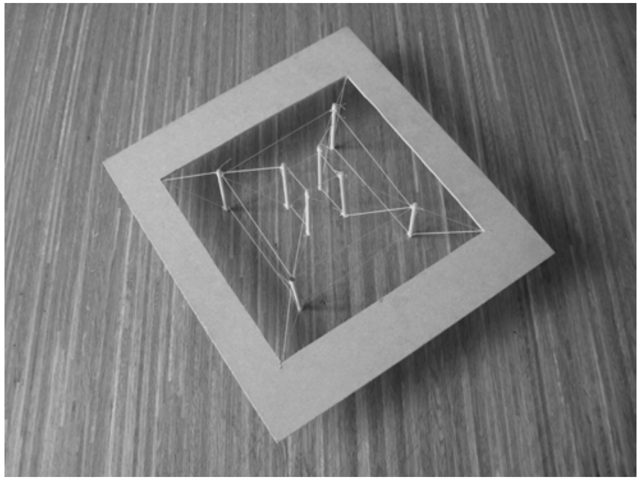

10.2. Physical model of the simple dome

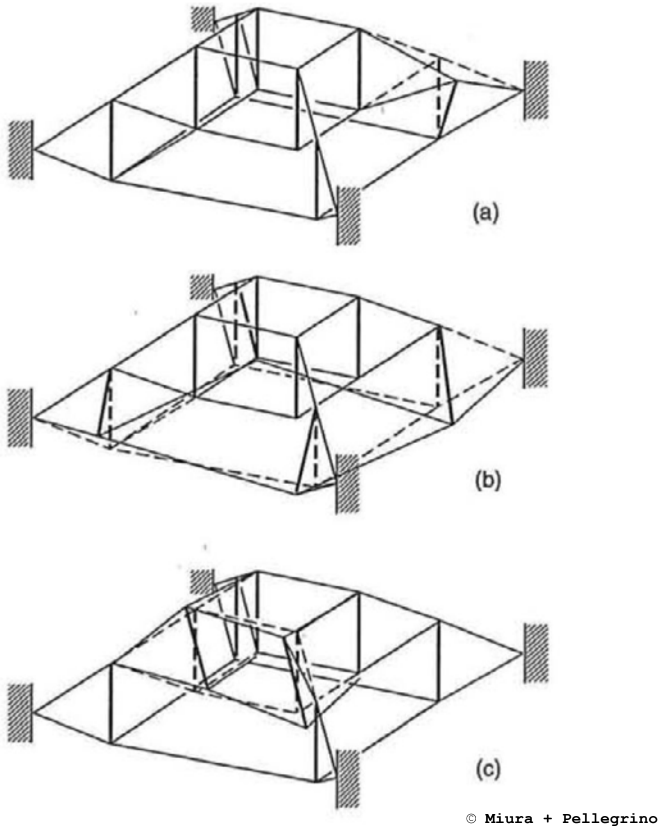

10.1. Mechanisms of the simple dome

For s = 1, m = 13, which can be divided into following four groups:

- Out-of-plane displacement of the mid-ridge joints. There are four independent mechanisms of this type, which involve displacements of joints 9, 10, 11, 12. For instance, in one of these four mechanisms:
- joint 9 moves by equal amounts in the direction x and –y.
- Rotation of the two tensions and the hoop about the z-axis, see figure 10.1. These three mechanisms are independent.
- In-plane distortion of the square ‘four-strut’ links formed by two corresponding elements of the top and bottom inner rings, and the two struts which connect them. The four joints at the corner of the square move in a diagonal direction, alternatively in and out as shown in figure 10.1.

11. La Plata Stadium, Buenos Aires, Agentina

Location: La Plata, in Buenos Aires, Argentina
Capacity: 53,000 seats
Opened year: 2003
Diameter: two 85 m circles, with 48 m between their two centers
Architect: Roberto Ferreira
Roof area: 29,036 m^2
Cladding: tensile roof featuring Birdair’s steel cable systems and PTFE, a Teflon®-coated woven fiberglass membrane
Compression ring: consisting of 45 octahedron/tetrahedron modules

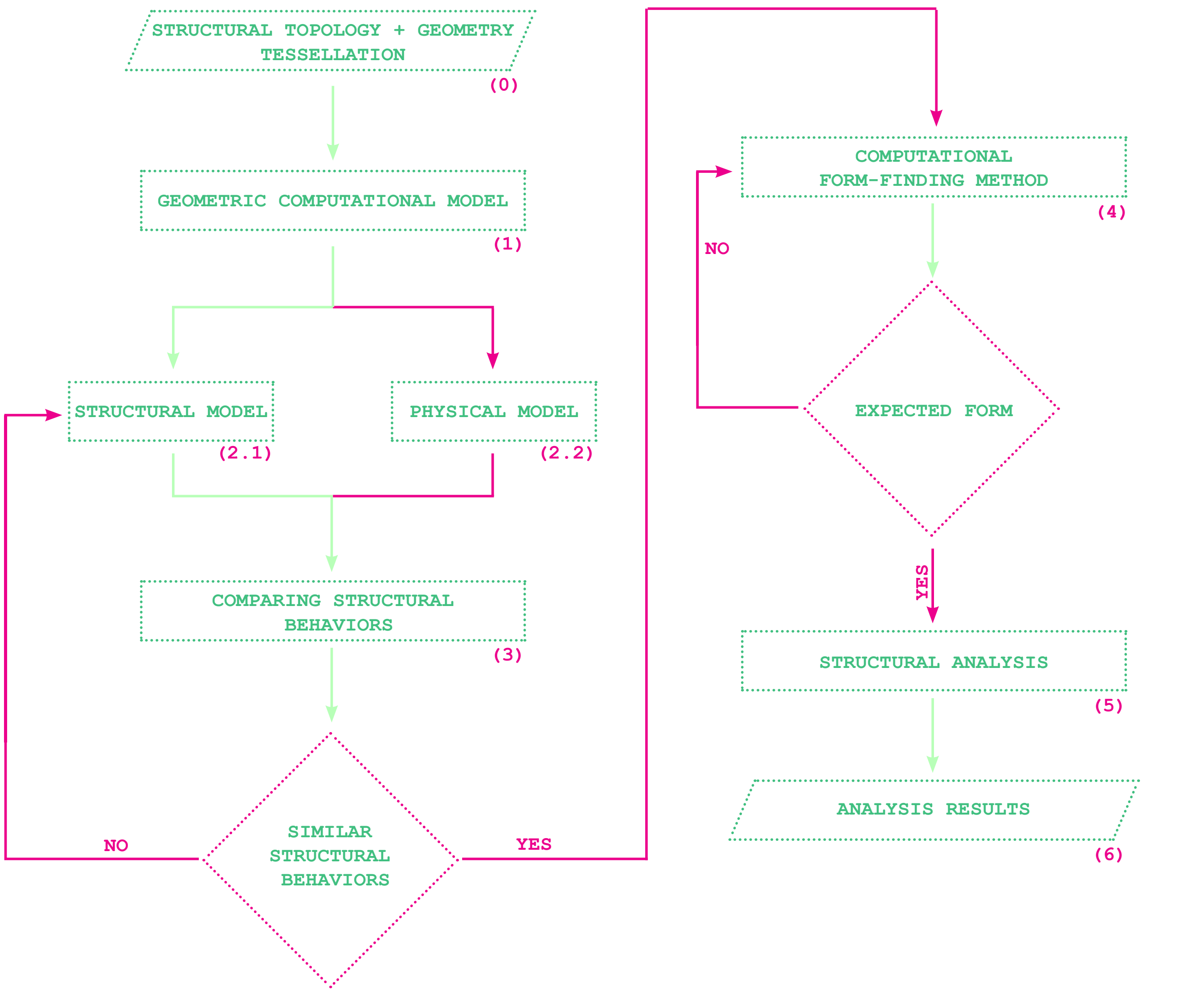

12. Design method

The implementation of the workflow is shown by these steps in diagram 12.1 which identifies several stages in the construction of a computational structural model. Sometimes, it costs a enormous amount of time to go back and forth within options before figuring out the appropriate way to go.

This section is a summary of the design method for a computational and structural model of complex tensegrity structures using Rhinoceros, Grasshopper and Oasys GSA in combination.

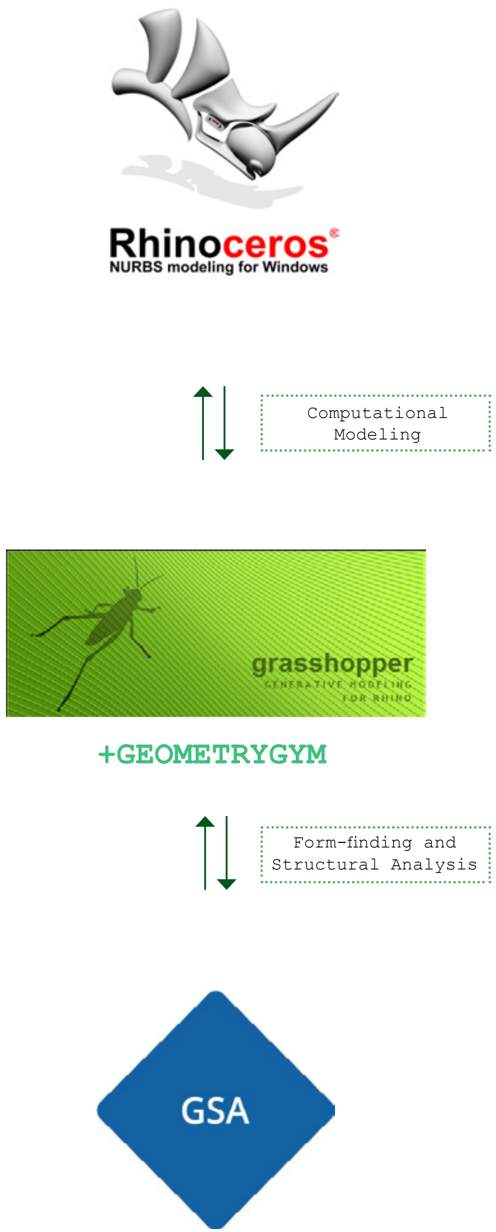

13. Programs in use

Bucky’s dome and Geiger’s dome were investigated previously, and these designs were realized in large-scale projects such as stadium or concert hall. But they are all fully closed domes, without any openings. To achieve a good design for an open-air stadium, it should have a large opening in the center as a typical typology; otherwise, they will become a place for indoor sports which is a different type.

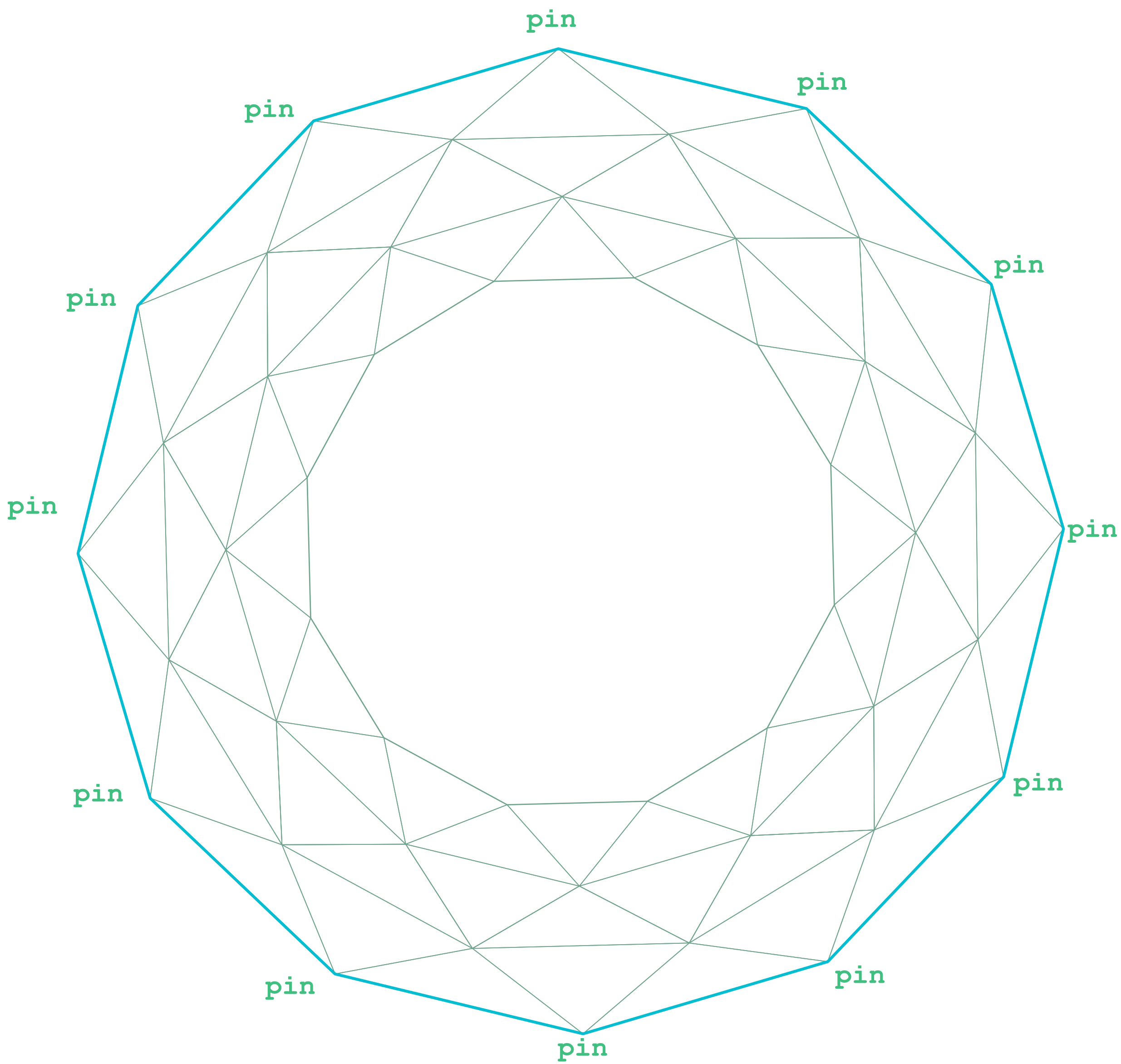

14.1. Plan of Bucky's dome + central opening

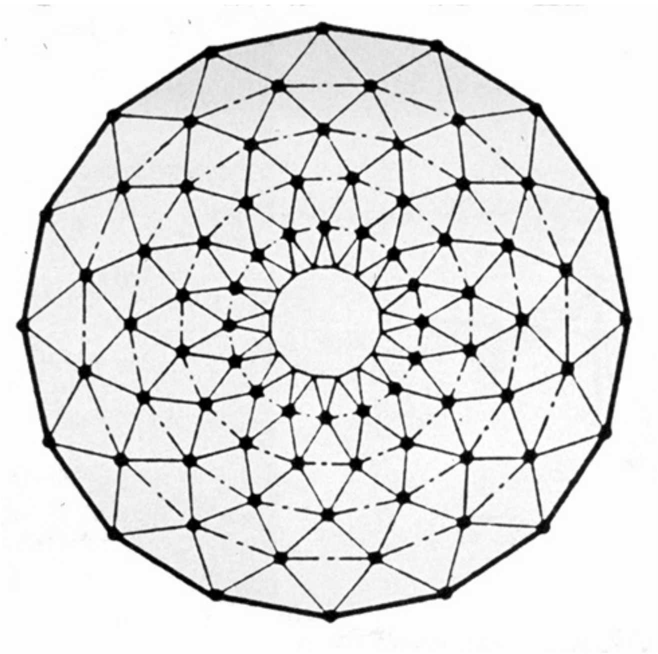

14.2. Bucky's dome, B. Fuller, 1964

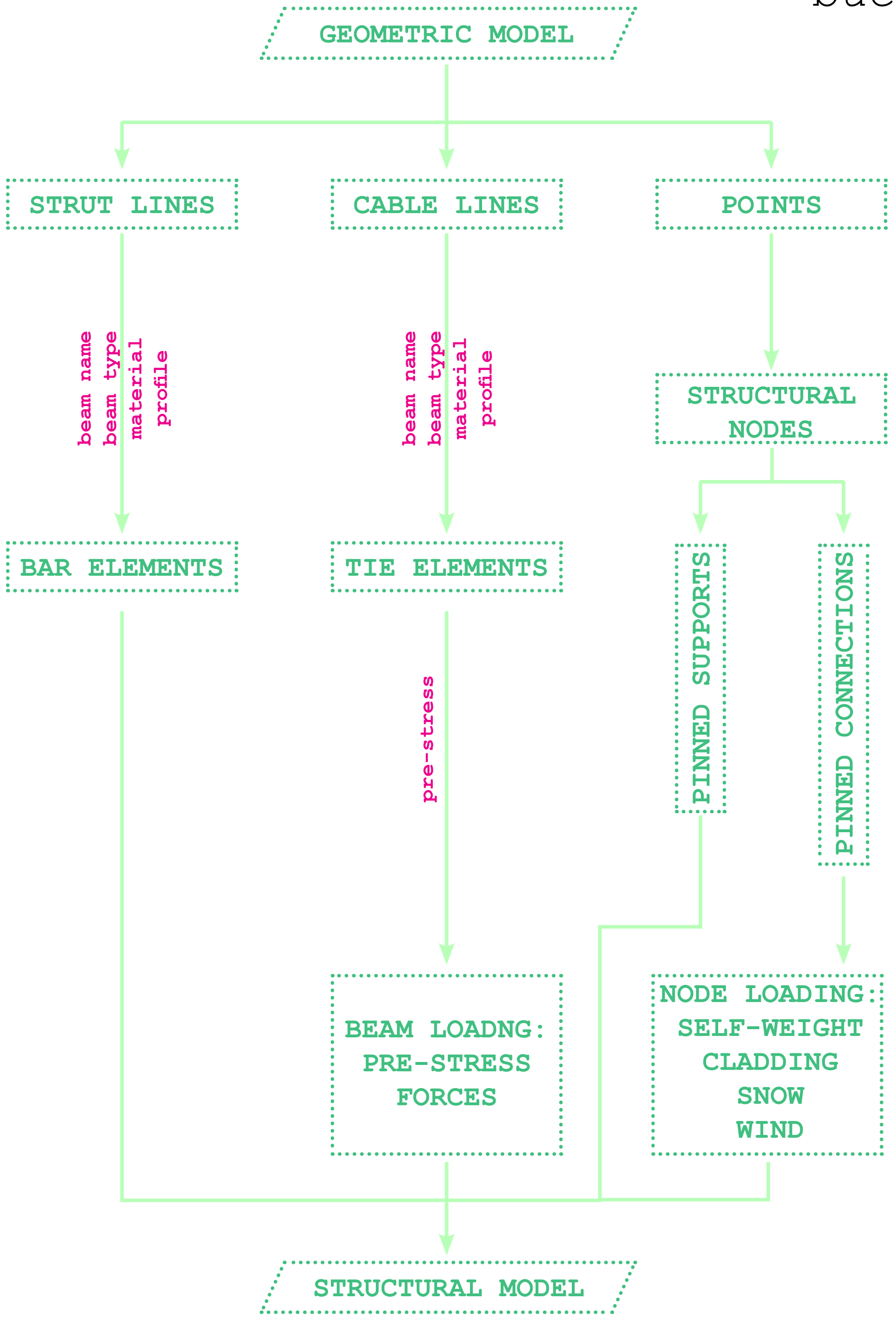

15. From geometric to structural model

Using GeometryGym - a plugin of Grasshopper, all structural elements (nodes, beams, supports, sectional properties, materials) are defined beforehand in Grasshopper as a parametric model. Then this model is exported to Oasys GSA which is only considered a calculation platform in this case. There is a possibility to even conduct the calculation in Grasshopper, but since structural performances of tensegrity systems are complex, it is better to do it in Oasys GSA.

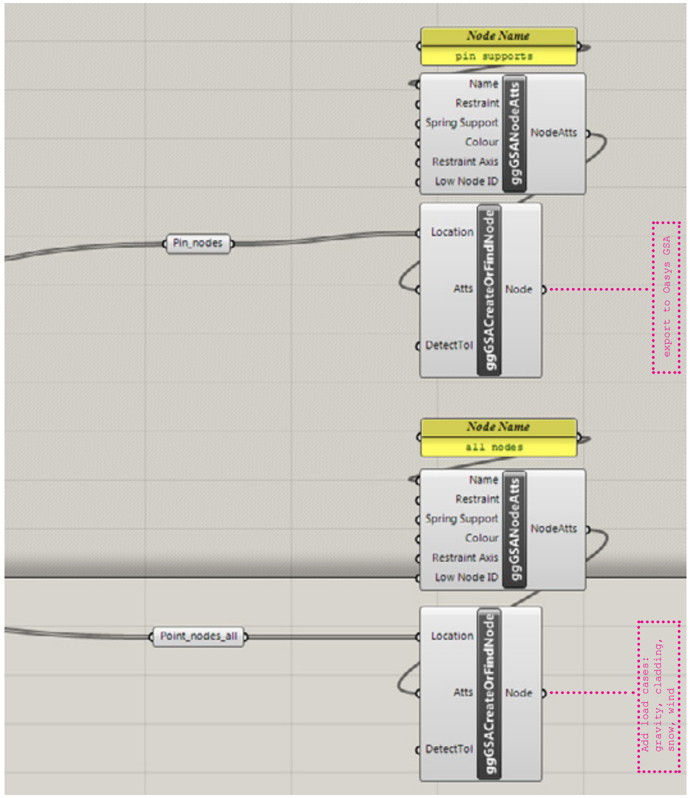

(a) Creating structural nodes and supports

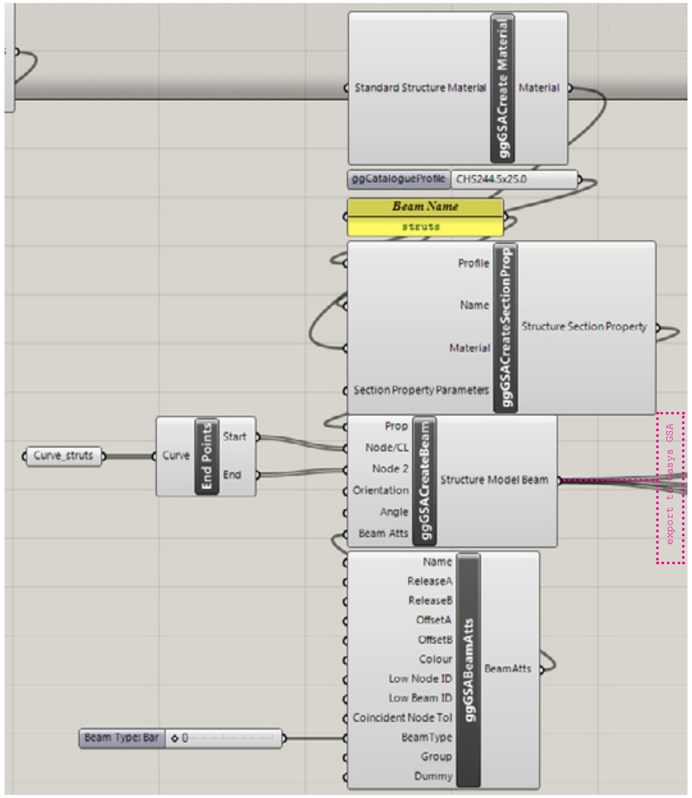

(b) Creating structural properties for struts

(e) Double click this component to export the model

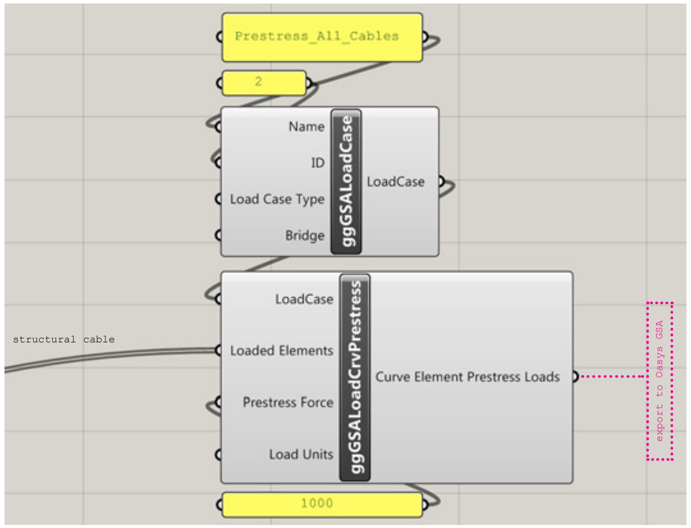

(c) Creating load case: Pre-stress forces in cables

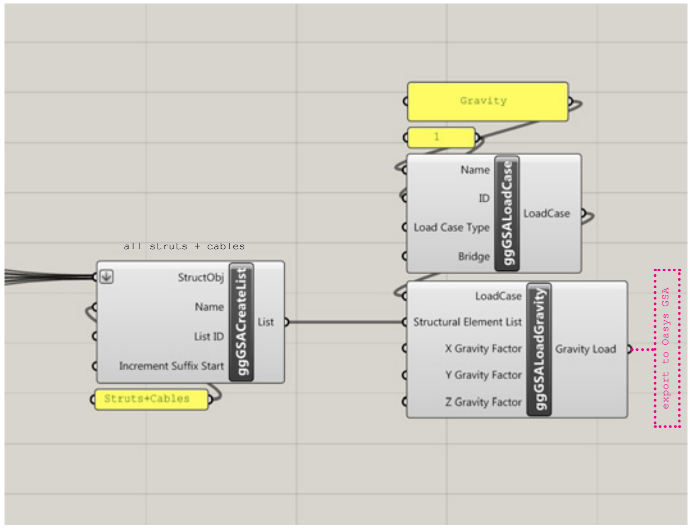

(d) Creating load case: Gravity

The structural model is constructed in grasshopper using plug-in GeometryGem to set all structural properties (nodes, beams, supports, load cases) and export to Oasys GSA for running calculation only.

16. Building structural model using GeometryGym in Grasshopper

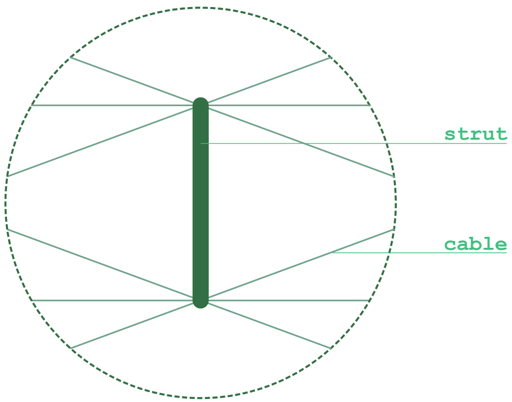

(a) Cell topology

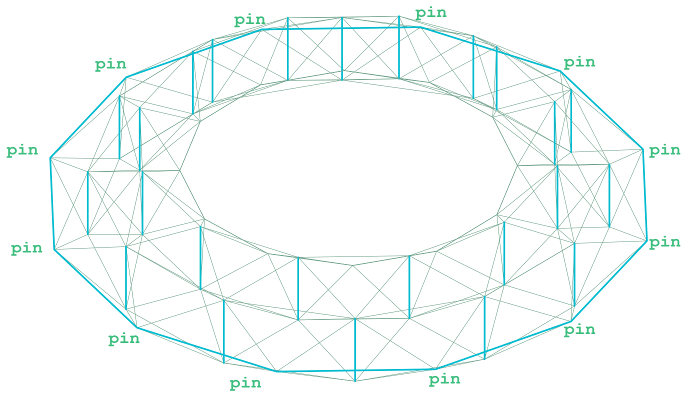

(b) Bucky's dome with a central opening

17.1. Bucky's dome with a central opening

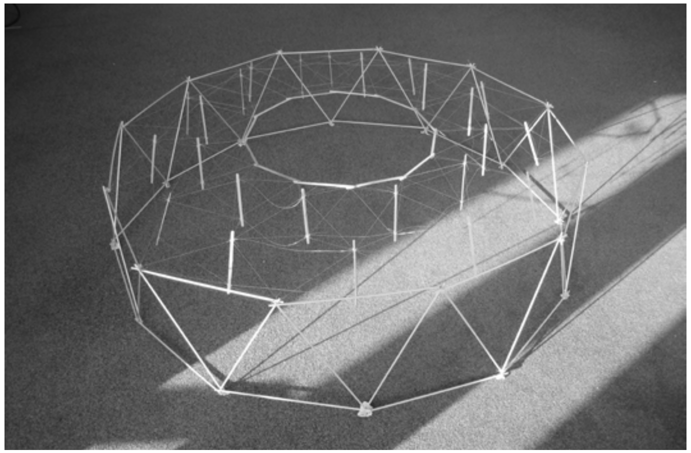

17.2. Physical model

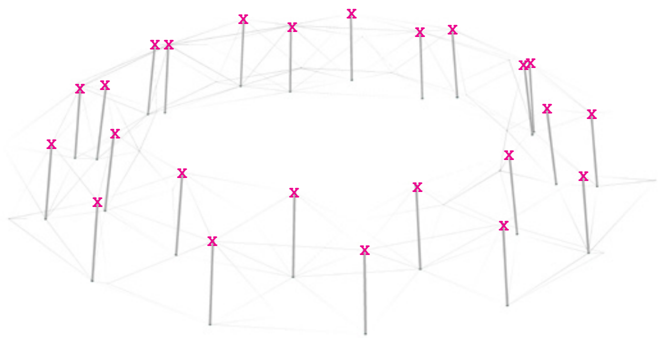

17.3. Form-finding result

The physical model was built similar to the digital model. The model has been constructed bottom-up from the compression ring first and then adding struts one by one, from the outer ring to the inner ring.

The physical model performed as expected in structural principles following the Geiger's dome analysis of Pellegrino. In the physical model, it is observed that there are a number of cables which are not in loading so they can be removed. But on the other hand, for safety reason, they can stay in case other cables are broken in unexpected situations. The compression is clearly in loading. It can be seen that there are several struts bent (because of buckling, not bending forces, it is all axial forces). All structural members are subjected to axial forces following exactly the principle of tensegrity. No strut touches the others, and they are all floating in the network of cables.

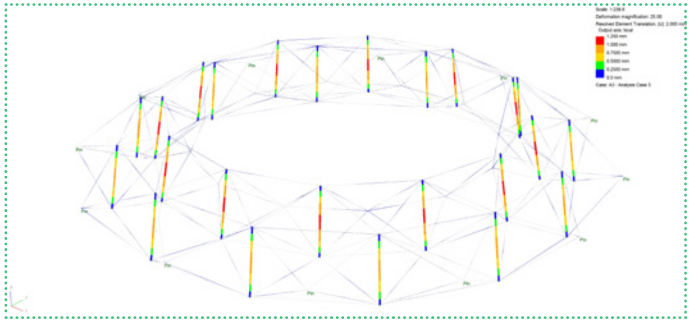

(a) Beam displacements | Max: 1.25mm

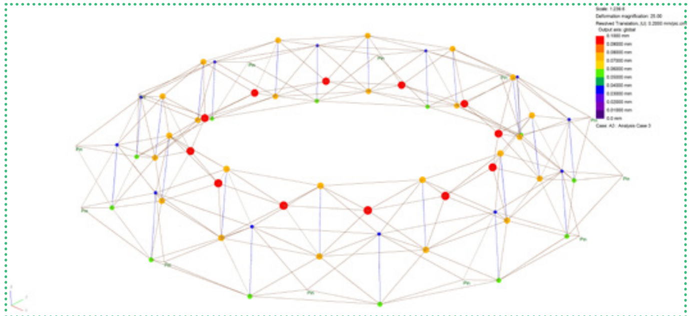

(b) Node displacements | Max: 0.1mm

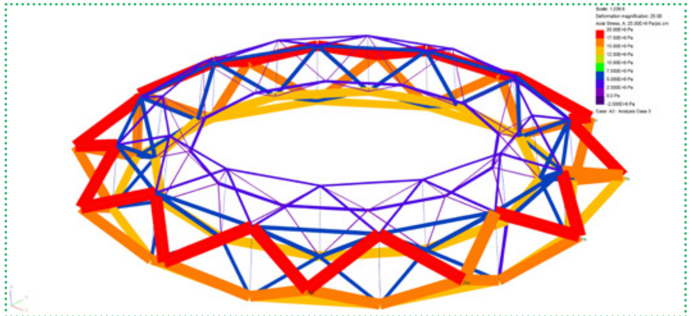

(c) Axial stresses | Max: 20e9 Pa

18.1. Structural performance under Pre-stress forces and Gravity

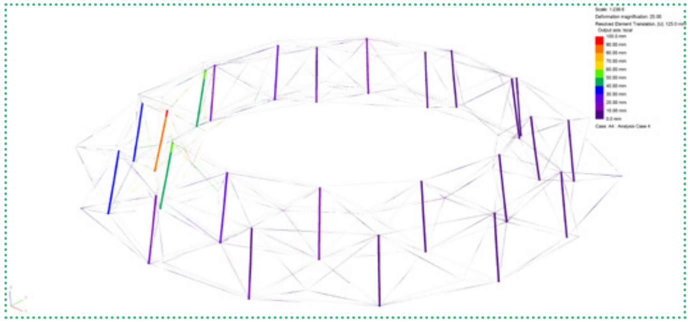

(a) Beam displacements | Max: 100 mm

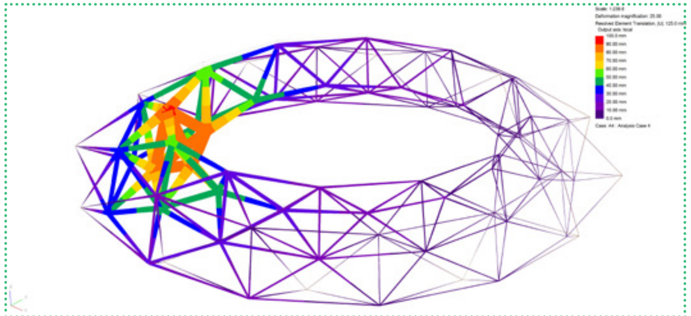

(b) Beam displacements | Max: 100 mm

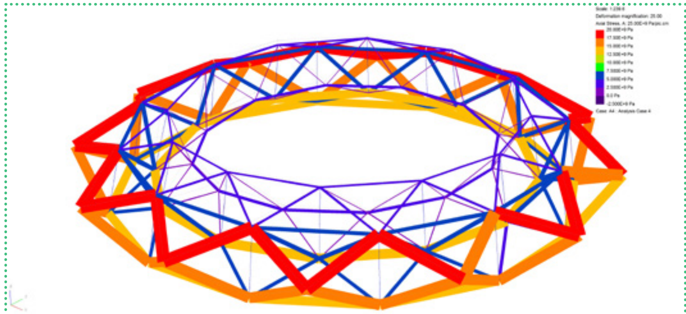

(c) Axial stresses | Max: 20e9 Pa

188.2. Structural performance under Pre-stress forces, Gravity and Node loading

Form-finding

After conducting form-finding with option 'ignore form-finding properties' in Oasys GSA, the tops of struts slightly deformed inwards, which is similar to the physical model. So this form-finding technique is the right choice for more complex ones.

Gravity

There is pure compression in struts and pure tension in cables. The entire structure became very rigid after form-finding, and it mostly works in tension strength. The inner ring deforms the most (0,1mm). From the outer ring to the inner ring, the magnitudes of pre-tensional forces decrease.

Nodal Loading

When a nodal load (-1000kn) is applied, the surrounding areas are affected in all directions. This behavior is also similar to the physical model. The rigidity of tensegrity structures depends on the pre-stress forces in cables that gives the structure the state of self-stress. Soap film and force density method cannot be applicable in this type of tensegrity, only 'ignore form-finding properties' works. This technique takes the deformed shape and internal loading from form-finding as the input for the next analysis.

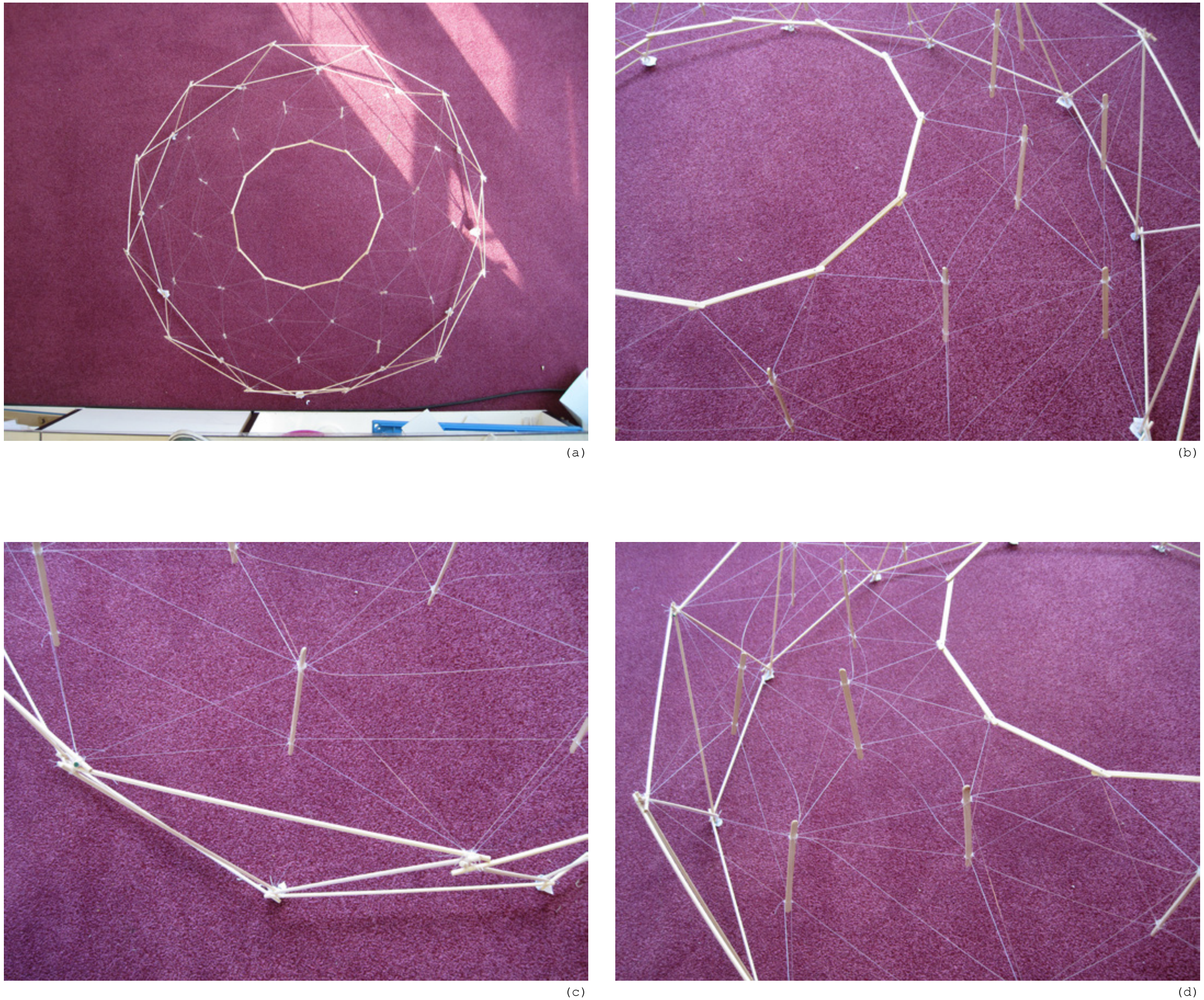

Physical models are always coupling with structural models to reflect on the results of each other.

19. Physical model of Bucky's dome with a central opening

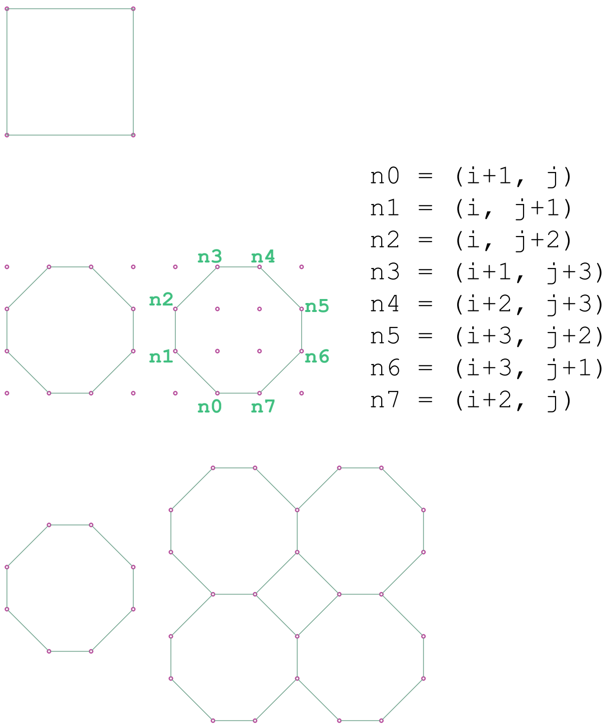

20.1. Tessellation from a generic grid of vertices

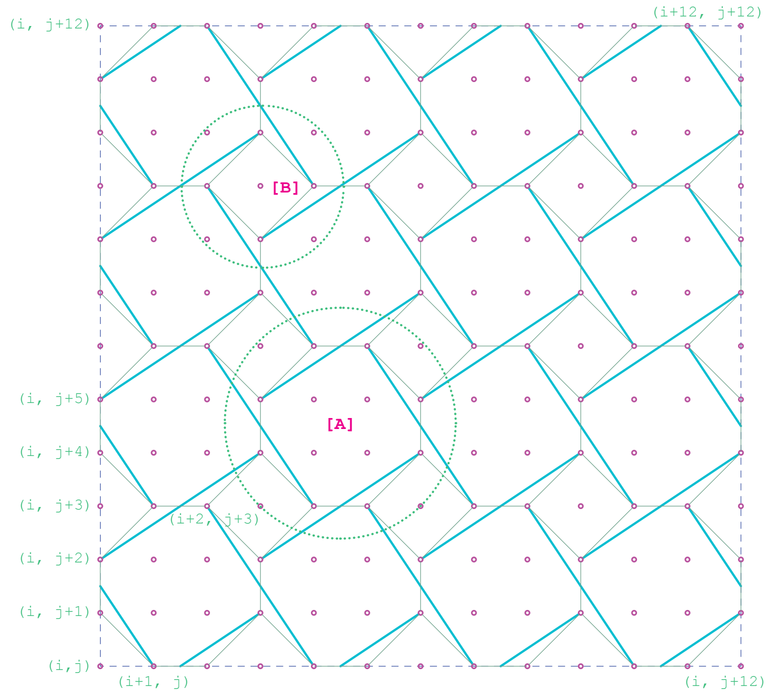

20.2. Numbering the generic quadriangular grid which is the base for defining the network of struts and network of cables.

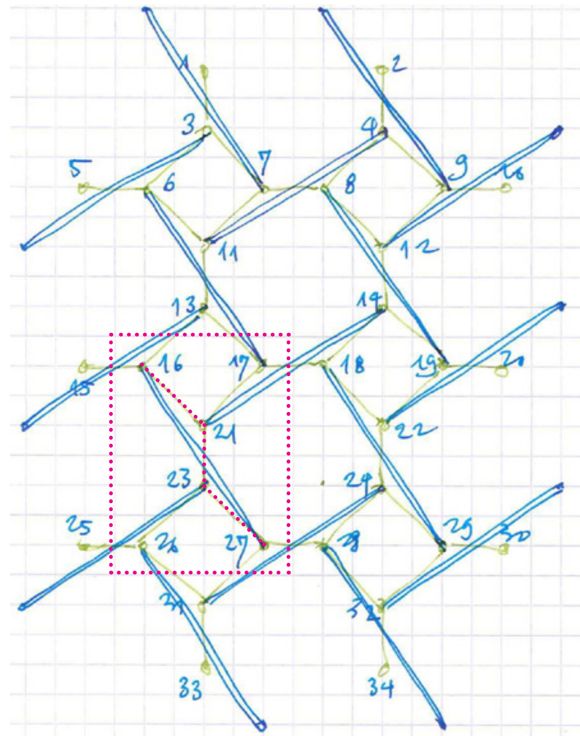

20.3. A network of struts within a network of cables with octagonal pattern, based on Z-topology

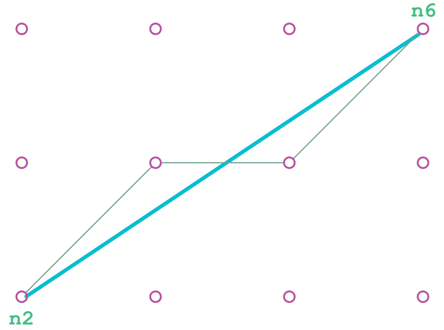

n2 = (i, j+2)
n6 = (i+3, j+4)

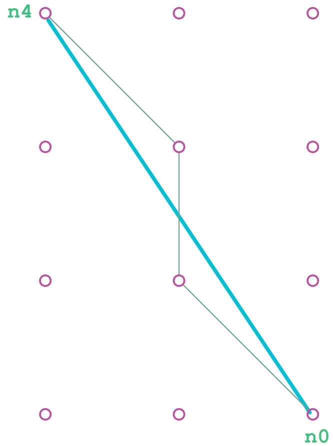

n0 = (i+4, j)
n4 = (i+2, j+3)

21.1. Procedural descriptions of struts and cables based on generic quadriangular grid

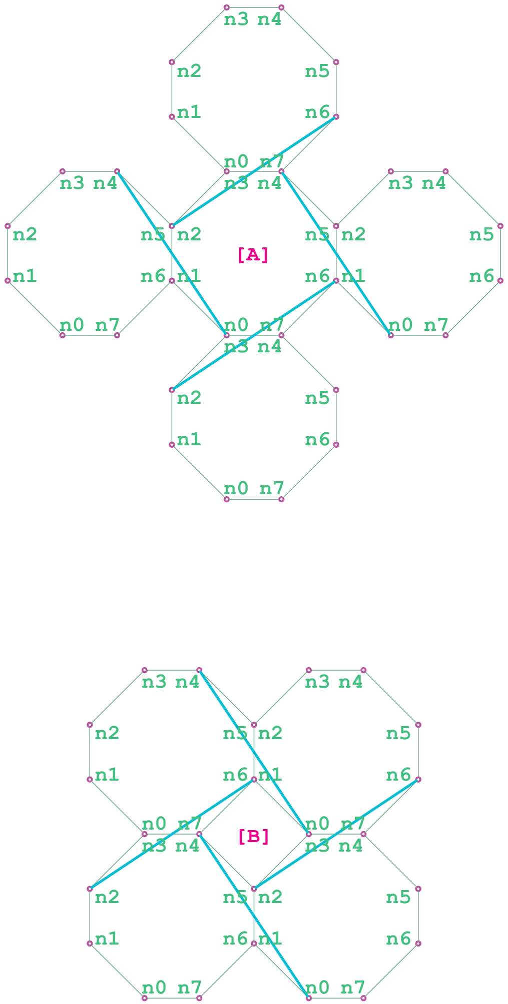

21.2. Two typical compositions of struts around an octagon or a square in the tessellation.

Defining locations of struts programmatically, based on quadrangular grid of vertices, for coding in Python.

Figure 19.2 show polygons and their neighbors in octagonal tessellation, and the way of determining struts.

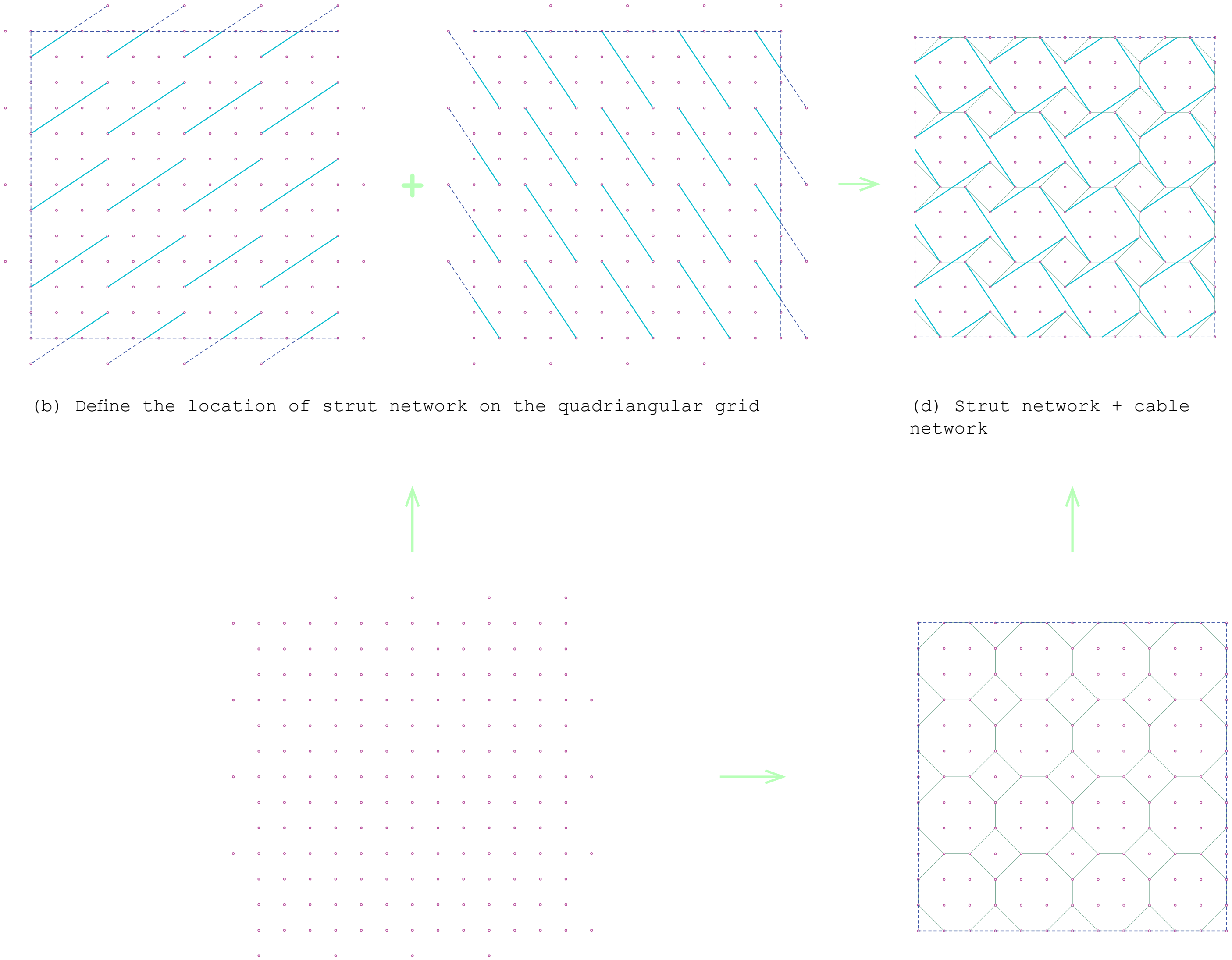

(b) Define the location of strut network on the quadriangular grid

(d) Strut network + cable network

(a) Quadriangular grid based on grid of points

(c) Define the location of cable network on the quadriangular grid

In the end, they are assembled together to form a single-surface tensegrity structure. There is no need to figure out the z-topology or adjacent hexagons to define strut network which is no longer depending on the network of cable but the generic quadrangular grid.

22. The network of struts and network of cables are independently defined based on the generic quadrangular grid of points.

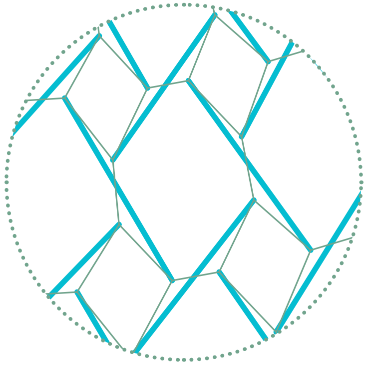

(b)

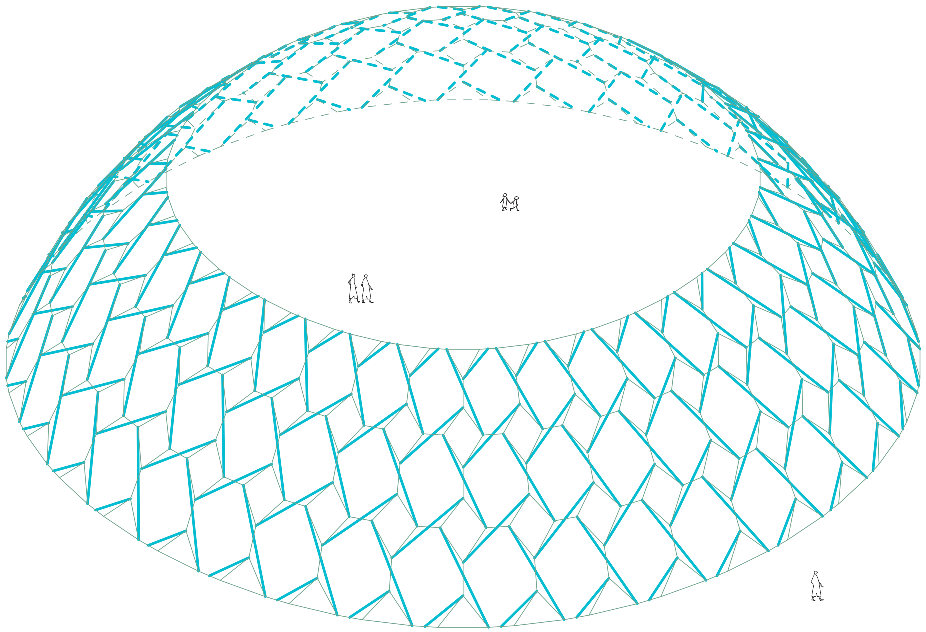

(a)

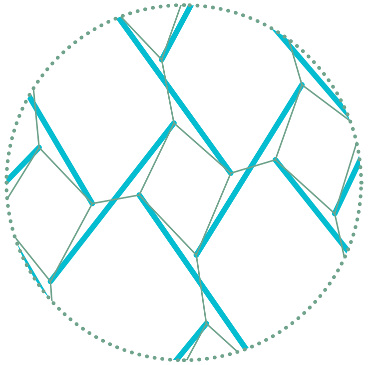

(c)

23. Tesselatizing and tensegritizing a simple dome with a central opening for an octagonal pattern (8-gon) | Single-surface tensegrity

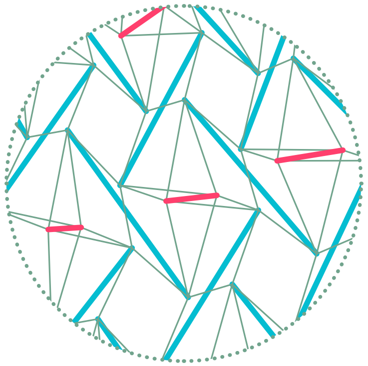

(b)

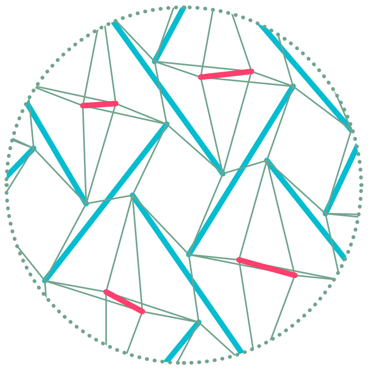

(c)

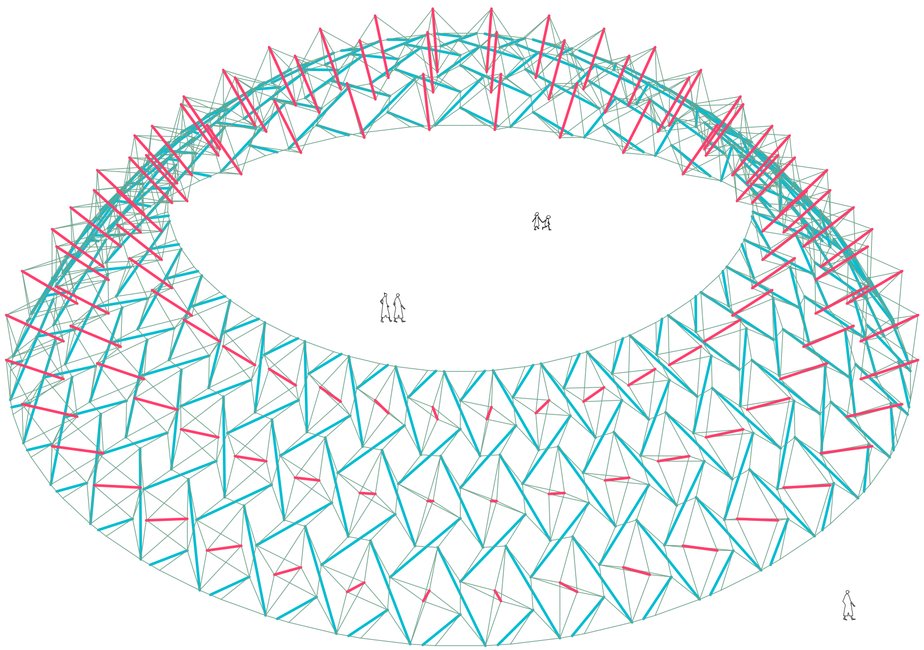

(a)

24. Adding normal struts (in pink) in the center of hexagonal cells to increase the thickness of the shell and handle out-plane loading applying to octagonal pattern (8-gon)
The in-plane struts (In blue) remain in the same reference surface
extra cables are added to connect normal struts to in-plane struts

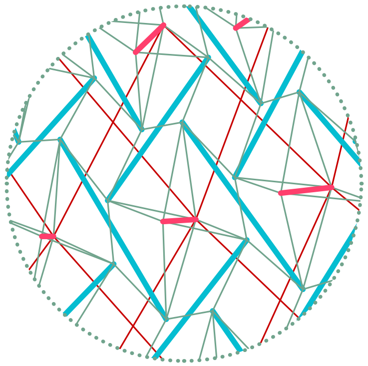

(b)

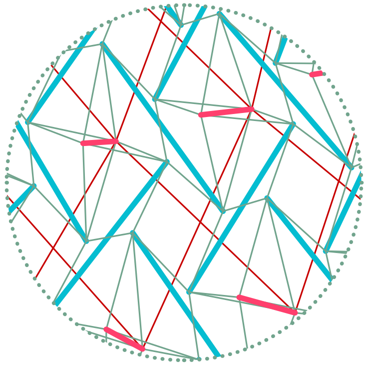

(c)

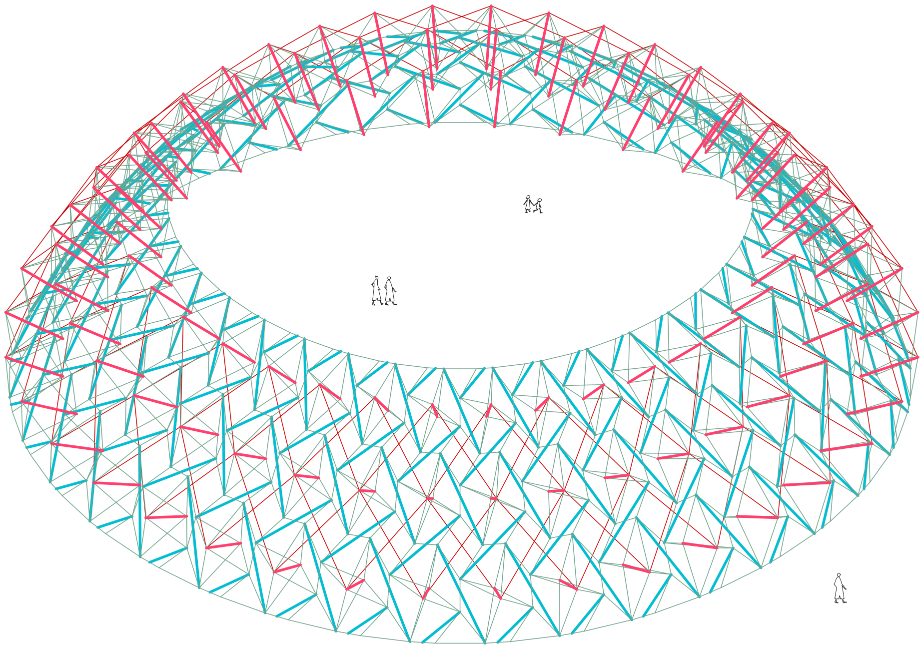

(a)

25. Adding outer bracing cables (thin lines in pink) to limit the rotation of pin-jointed connections
Applying to octagonal pattern (8-gon)
These bracing cables connect tops of normal struts in order

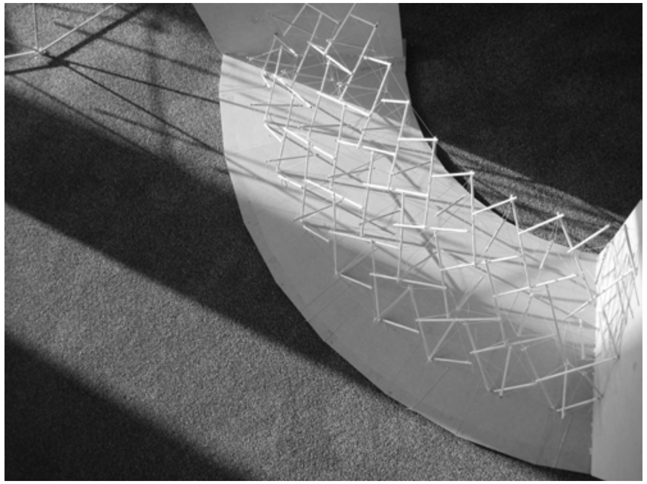

26. physical model

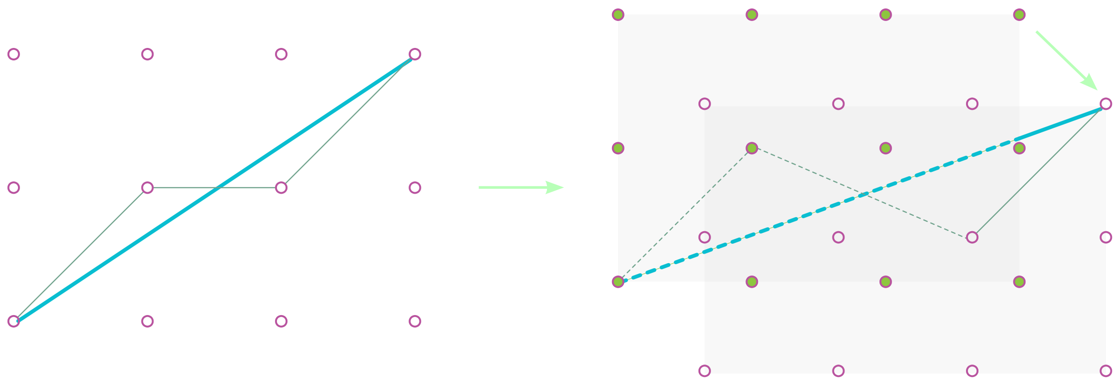

27.1. Based on Z-topology
(Mentioned in previous chapters)

MAKE IT SPATIAL!?

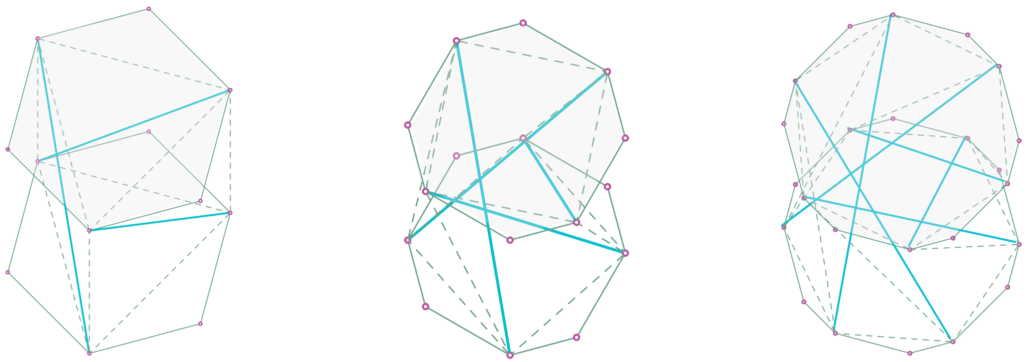

3 struts

4 struts

6 struts

27.2. Based on cylindrical tensegrity structures - 2n-gonal tesselation (n>2)
(The most popular tensegrity systems)

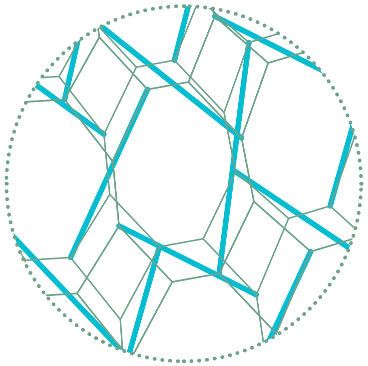

(b)

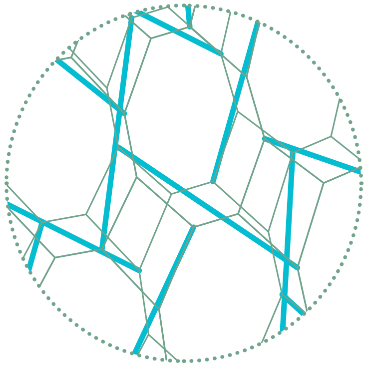

(c)

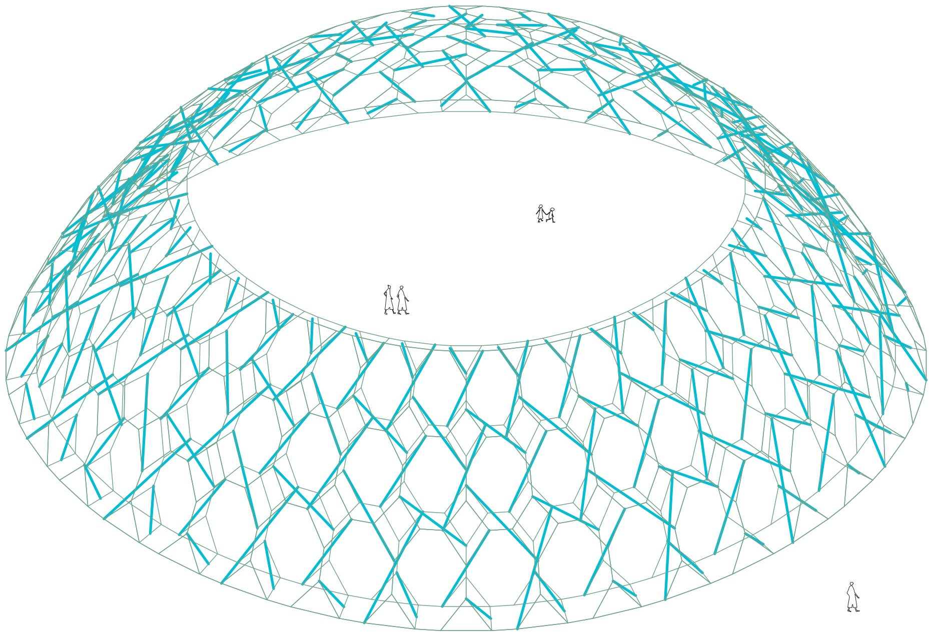

(a)

28. Using two reference surfaces with the same way of tessellating

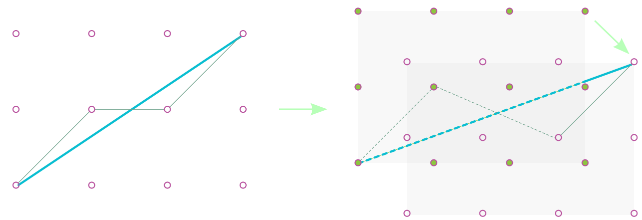

Applying the method of single-surface tensegrity structures with z-topology, but in this case, two ends of a strut are located on two different surfaces. By doing this, the structure has the thickness, becomes more spatial. And touching between struts is avoided.
In this figure, the tesselation is an octagonal pattern.

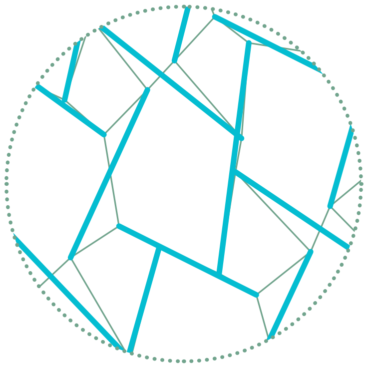

(b)

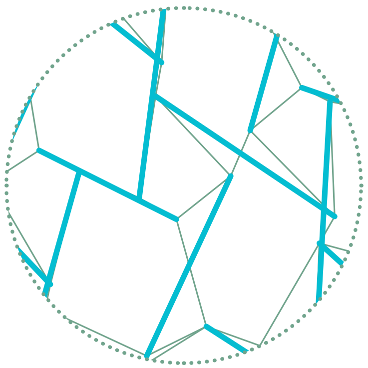

(c)

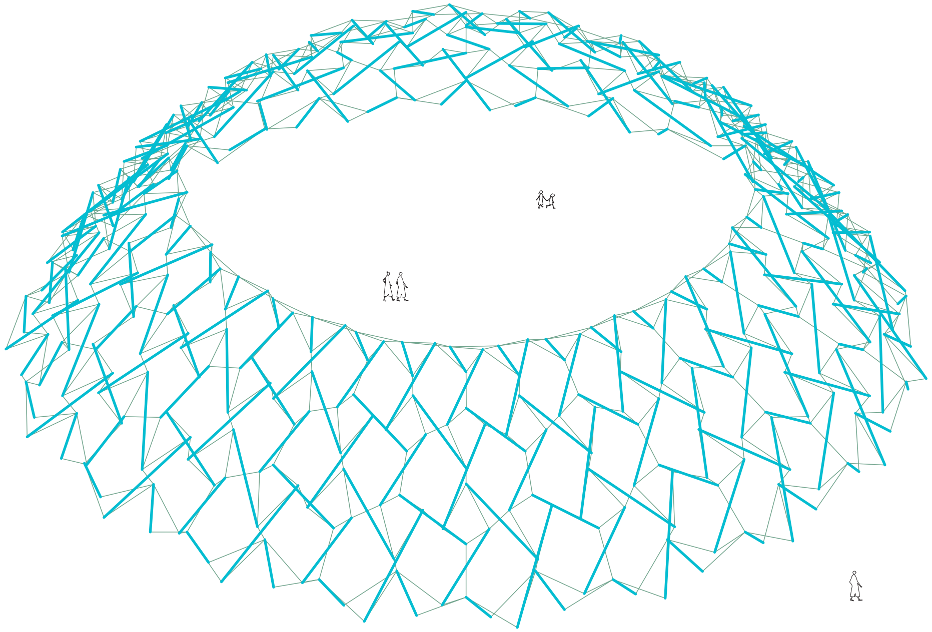

(a)

29. After having the network of struts, two reference cable networks are merged into one.

In terms of topology, the system becomes similar to single-surface tensegrity structures again, but the geometry is different, and better in structural performance. In this case, the tessellation is octagonal pattern.

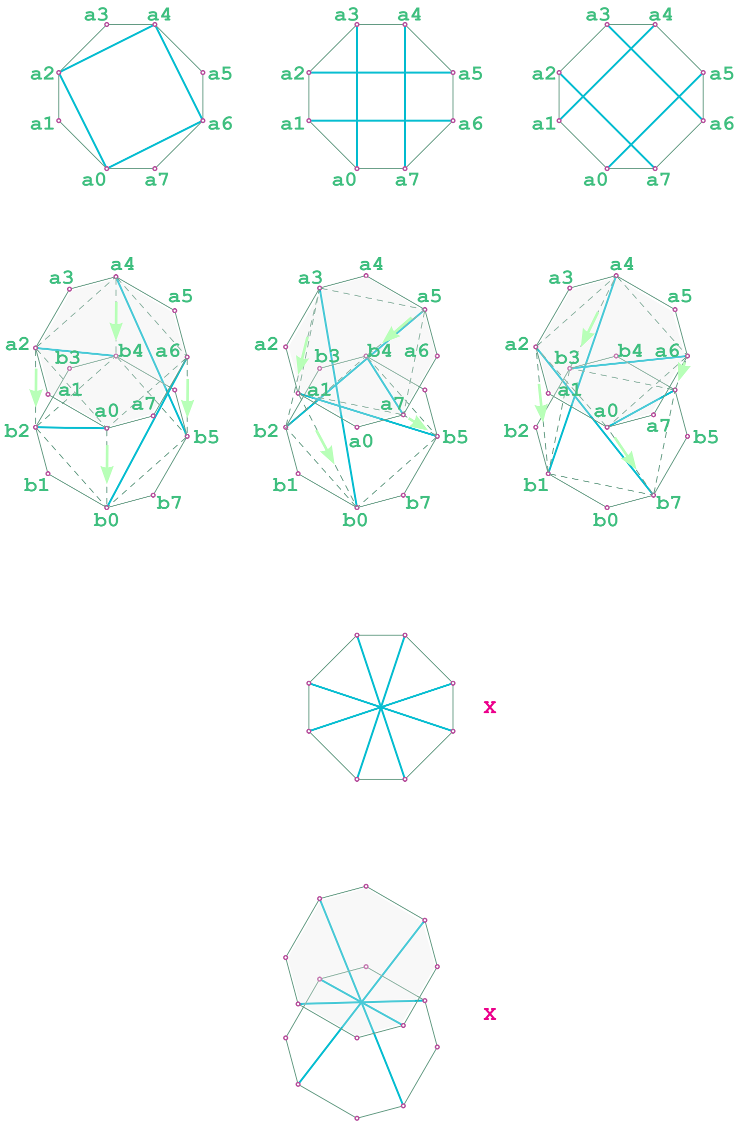

30.1. Within an octagonal tessellation, the system of quadrex tensegrity (quadrangular prism) can be constructed. n = 4
(x) Eliminated option because of touching struts in their centre points

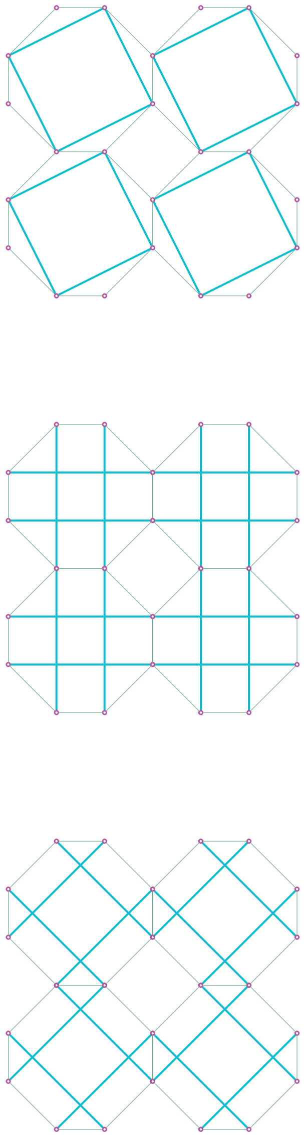

30.2. Three different ways of placing struts in cable networks, which is creating different tessellations.

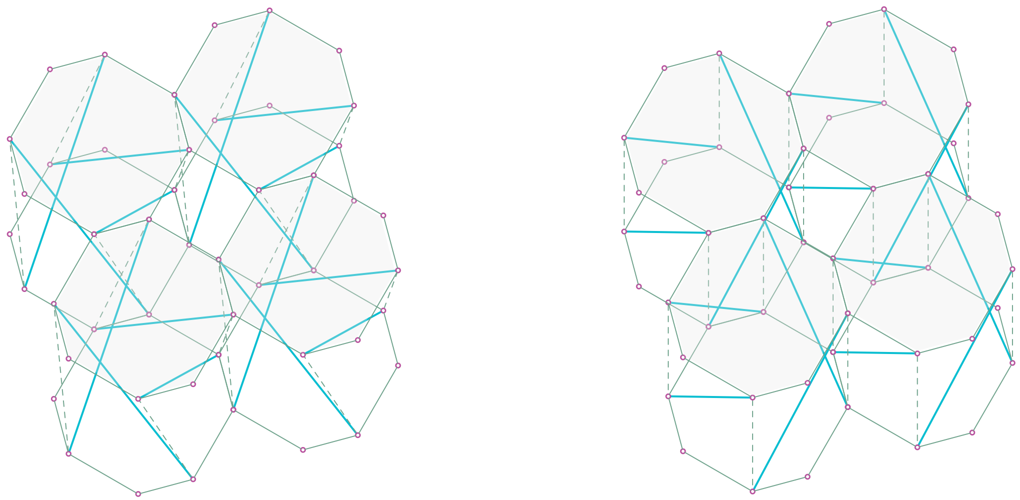

31. The cell of this system is a quadrex tensegrity inside an octagonal cylindrical geometry. They will be then combined in the way that struts do not touch each other.

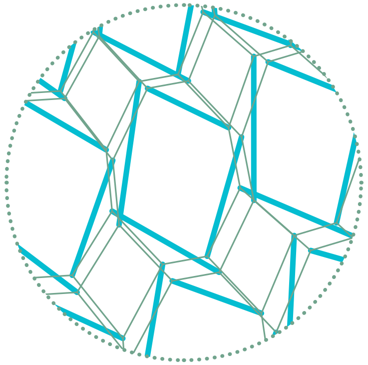
(b)

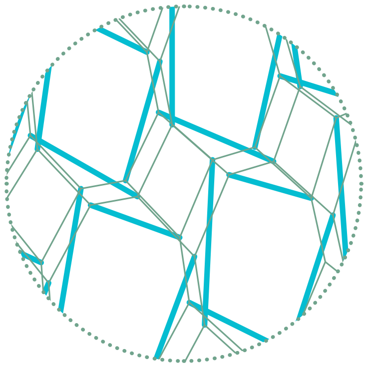
(c)

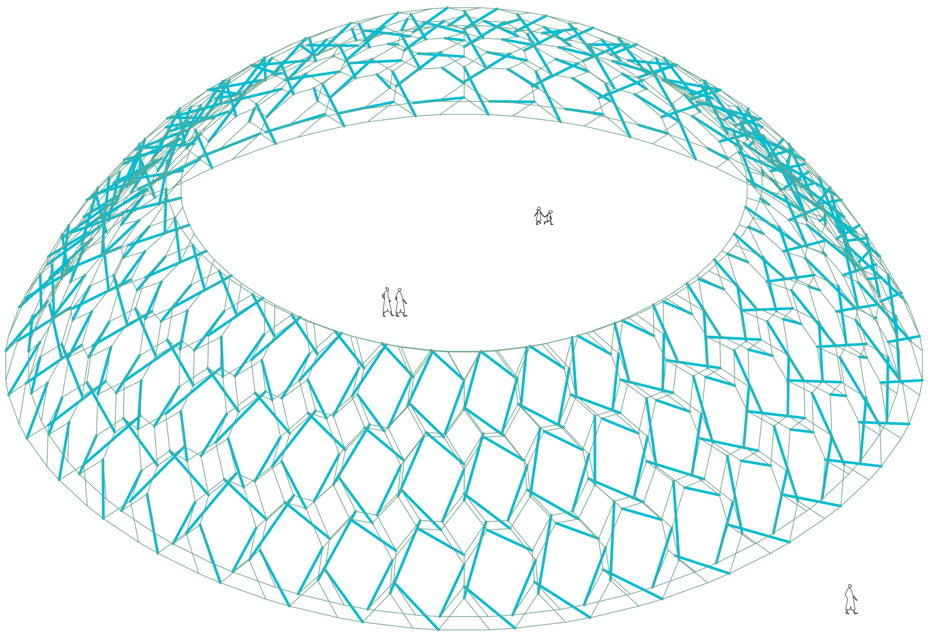
(a)

32. Applying to the dome with a central opening. There are a certain amount of cables which will be added to connect two reference tessellations. In this case, these reference tessellations are not merged. With an octagonal pattern, a network of quadrex tensegrities is achieved.

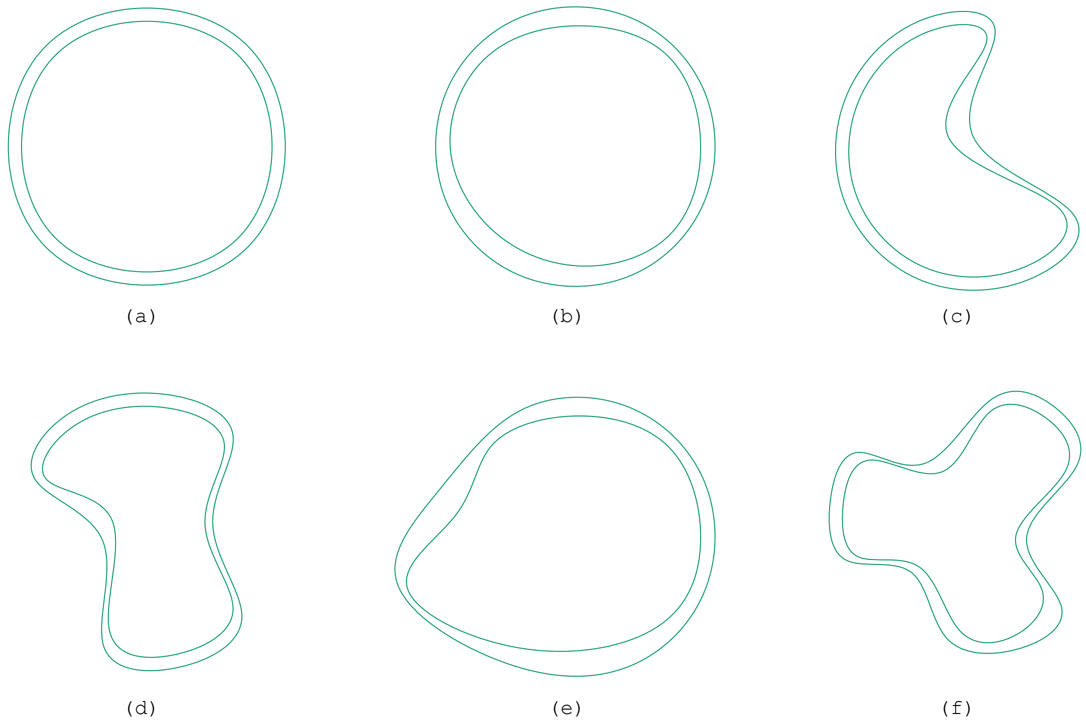

33. The double-surface tensegrity structures can be applied to given free-form, with two reference surfaces are slightly different, to locally change the thickness of the tensegrity shell, following structural purpose, architectural quality, and so on.

Procedure: Tessellating and tensegritizing of octagonal pattern based on quad-rangular grid, Z-topology, type A.

```
Inputs:
srf  #first reference surface
srfx #second reference surface
udiv #u count, udiv % 3 == 0
vdiv #v count, vdiv % 3 == 0
Outputs:
nods #list of structural nodes
cabs #list of lines of cables
stra, strb  #list of lines of struts

#Define the generic quadrangular grid of vertices which have (u, v) coordinates
for i in range (0, udiv - 2, 3):
    for j in range (0, vdiv - 2, 3):
        n0 = (i/udiv, (j+1)/vdiv, 0)
        n1 = (i/udiv, (j+2)/vdiv, 0)
        n2 = ((i+1)/udiv, (j+3)/vdiv, 0)
        n3 = ((i+2)/udiv, (j+3)/vdiv, 0)
        n4 = ((i+3)/udiv, (j+2)/vdiv, 0)
        n5 = ((i+3)/udiv, (j+1)/vdiv, 0)
        n6 = ((i+2)/udiv, j/vdiv, 0)
        n7 = ((i+1)/udiv, j/vdiv, 0)
        n8 = (i/udiv, (j+1)/vdiv, 0)

#Make the network of vertices to reference surfaces
        Evaluate (n0, n2, n4, n6) on srfx as (newn0,…,newn6)
         Evaluate (n1, n3, n5, n7) on srf as (newn1,…, newn7)
         AddPoint (newn0,…,newn7) to nods

#Define the network of cables or Constructing network of octagons
        AddLine ((newn0, newn1), (newn1, newn2), (newn2, newn3), (newn3, newn4),
(newn4, newn5), (newn5, newn6), (newn7, newn0)) to cabs

#Define the list of struts a
for i in range (0, udiv - 2, 3):
    for j in range (0, vdiv - 2, 3):
        a0 = (i/udiv, (j+2)/vdiv, 0)
        a1 = ((i+3)/udiv, (j+4)/vdiv, 0)
        Define a0 on srf as newa0
        Define a1 on srfx as newa1

        AddLine (newa0, newa1) to stra

#Define the list of struts b
for i in range (0, udiv - 2, 3):
    for j in range (0, vdiv - 2, 3):
        b0 = ((i+2)/udiv, (j+3)/vdiv, 0)
        b1 = ((i+4)/udiv, j/vdiv, 0)
        Define b0 on srf as newb0
        Define b1 on srfx as newb1

        AddLine (newb0, newb1) to strb
```

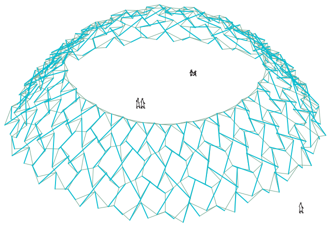

Procedure: Tessellating and tensegritizing of octagonal pattern based on quad-rangular grid, cylindrical topology, type B. (for cell 3.25(a))

```
Inputs:
srf #first reference surface
srfx #second reference surface
udiv #ucount, udiv % 3 == 0
vdiv #v count, vdiv % 3 == 0
Outputs:
nods #list of structural nodes
cabs #list of lines of cables
strs #list of lines of struts

#Define the generic quadrangular grid of vertices which have (u, v) coordinates
for i in range (0, udiv - 2, 3):
    for j in range (0, vdiv - 2, 3):
        a0 = (i/udiv, (j+1)/vdiv, 0)
        a1 = (i/udiv, (j+2)/vdiv, 0)
        a2 = ((i+1)/udiv, (j+3)/vdiv, 0)
        a3 = ((i+2)/udiv, (j+3)/vdiv, 0)
        a4 = ((i+3)/udiv, (j+2)/vdiv, 0)
        a5 = ((i+3)/udiv, (j+1)/vdiv, 0)
        a6 = ((i+2)/udiv, j/vdiv, 0)
        a7 = ((i+1)/udiv, j/vdiv, 0)
        a8 = (i/udiv, (j+1)/vdiv, 0)

#Make the network of vertices to reference surfaces
        Evaluate (a0,…,a7) on srfx as (xnewa0,…,xnewa7)
         Evaluate (a0,…,a7) on srf as (newa0,…,newa7)
         AddPoint (newa0,…,newa7) to nods

#Define the network of cables or Constructing network of octagons
        AddLine ((newa0, newa1), (newa1, newa2), (newa2, newa3), (newa3, newa4),
(newa4, newa5), (newa5, newa6), (newa7, newa0)) to cabs #cable network on srf
         AddLine ((xnewa0, xnewa1), (xnewa1, xnewa2), (xnewa2, xnewa3),
(xnewa3, xnewa4), (xnewa4, xnewa5), (xnewa5, xnewa6), (xnewa7, xnewa0)) to cabs
#cable network on srfx
         AddLine ((newa0, xnewa1), (newa1, xnewa2), (newa2, xnewa3), (newa3,
xnewa4), (newa4, xnewa5), (newa5, xnewa6), (newa7, xnewa0)) to cabs #connect two
networks of cables

#Define the network of struts
         AddLine ((newn0, xnewn2), (newn2, xnewn4), (newn4, xnewn6), (newn6,
xnewn0)) to strs #for each strut, one end is in srf, the other is in srfx
```

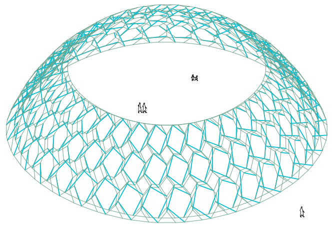

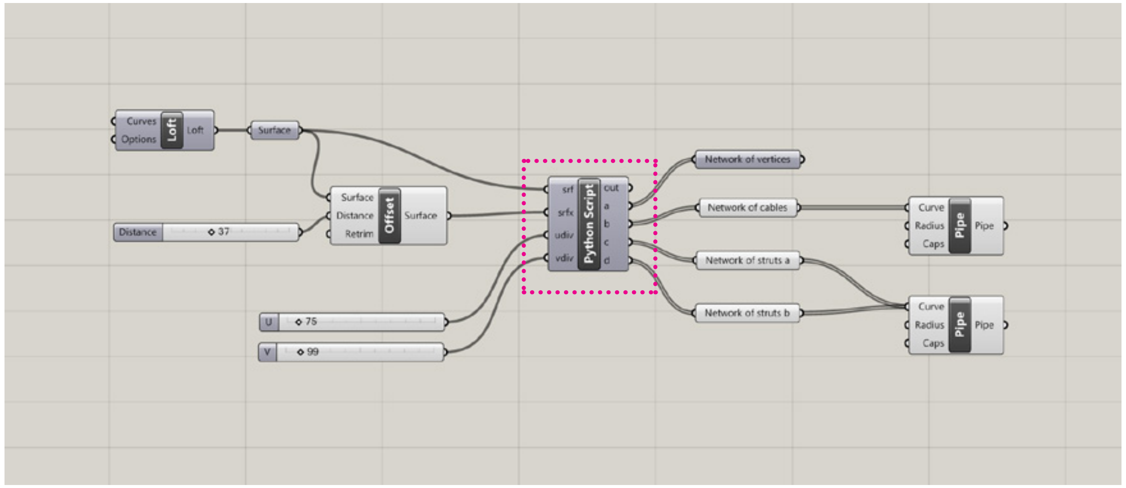

35. Grasshopper script

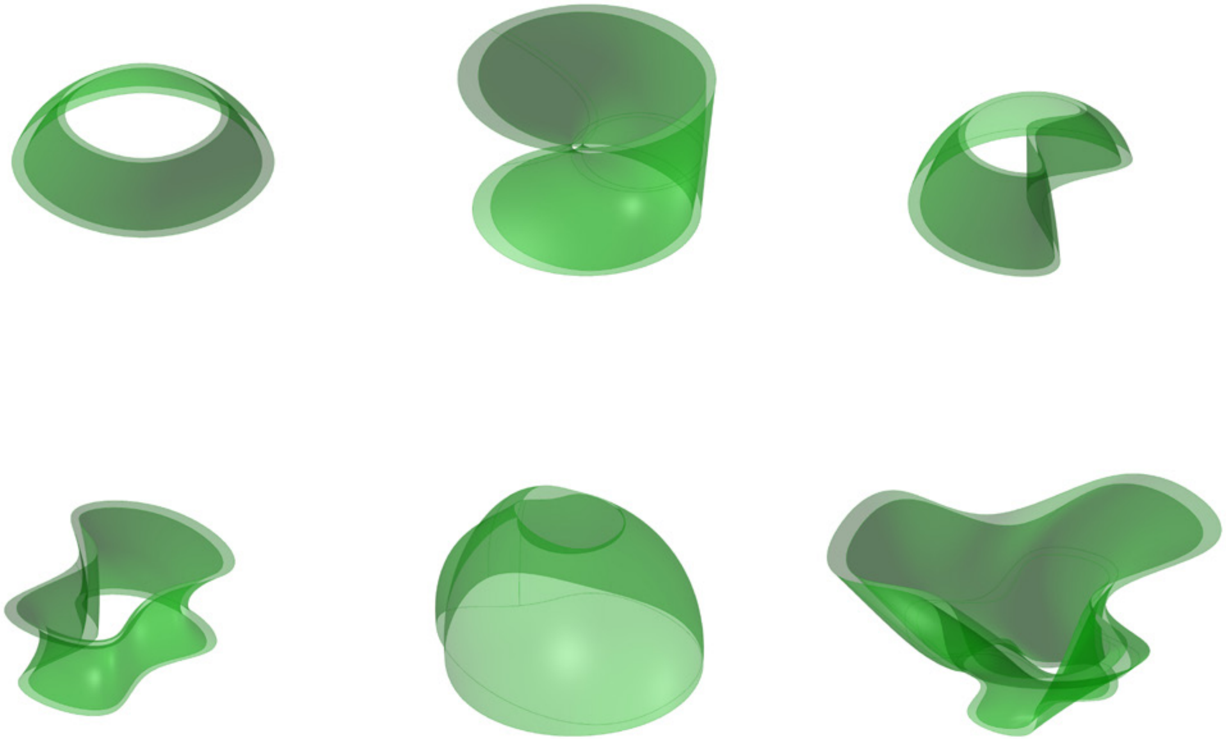

(f)

36. Double-surface tensegrity as a result of programming using Python in Grasshopper

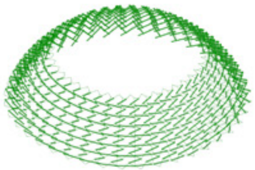

(a)

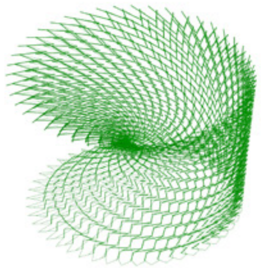

(b)

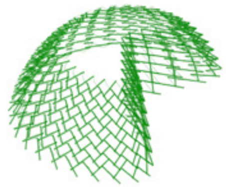

(c)

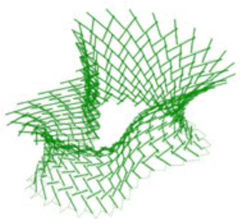

(d)

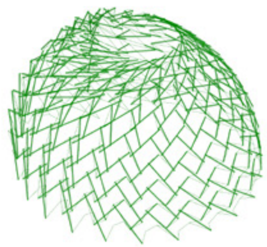

(e)

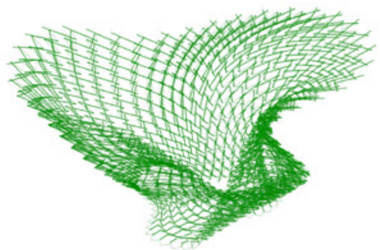

(f)

37. Double-surface tensegrity as a result of programming using Python in Grasshopper

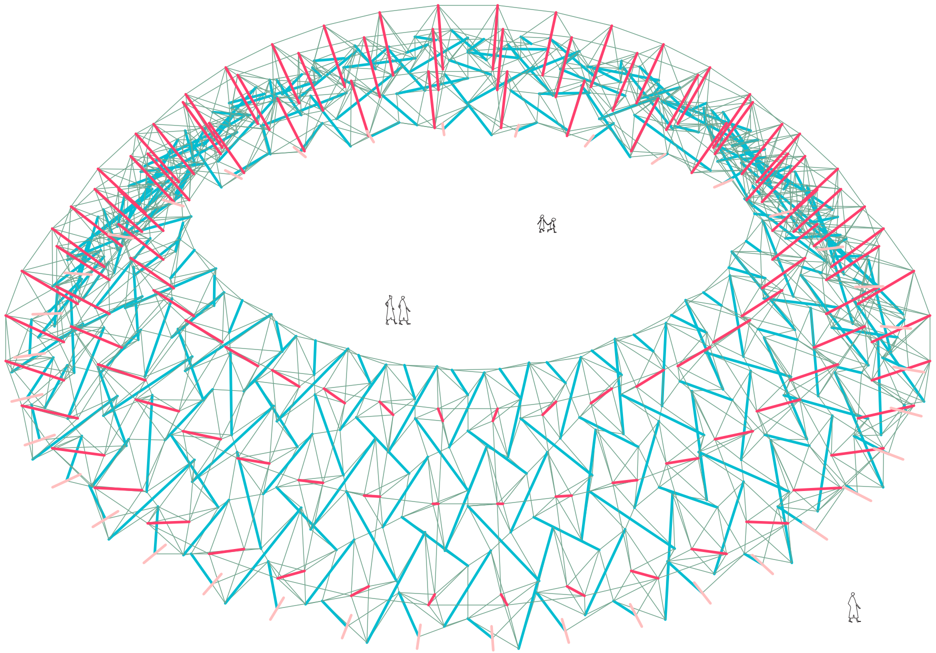

38. Double-surface tensegrity structures. octagonal tessellation. z-base topology. normal struts. bracing cables.

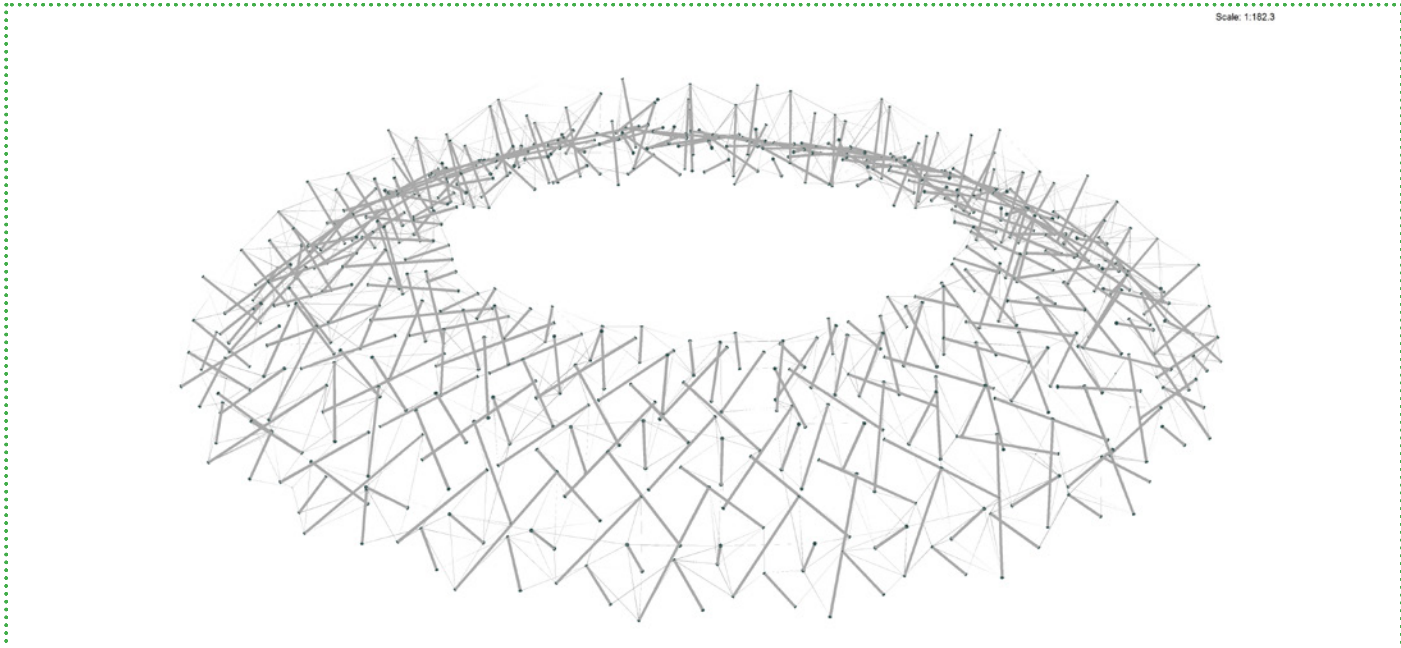

39. Form-finding result

After form-finding, there are internal loads inside cables that lead to tensioning in a cable network. Consequently, discontinuous struts are in compression because of pre-stress forces. This step can be repeated several times until the system achieves a certain stiffness.
At this point, we conduct the last form-finding which is the combination of the last internal loads from last form-finding and self-weight before doing structural analysis. After this form-finding, the model will not deform under similar load cases.

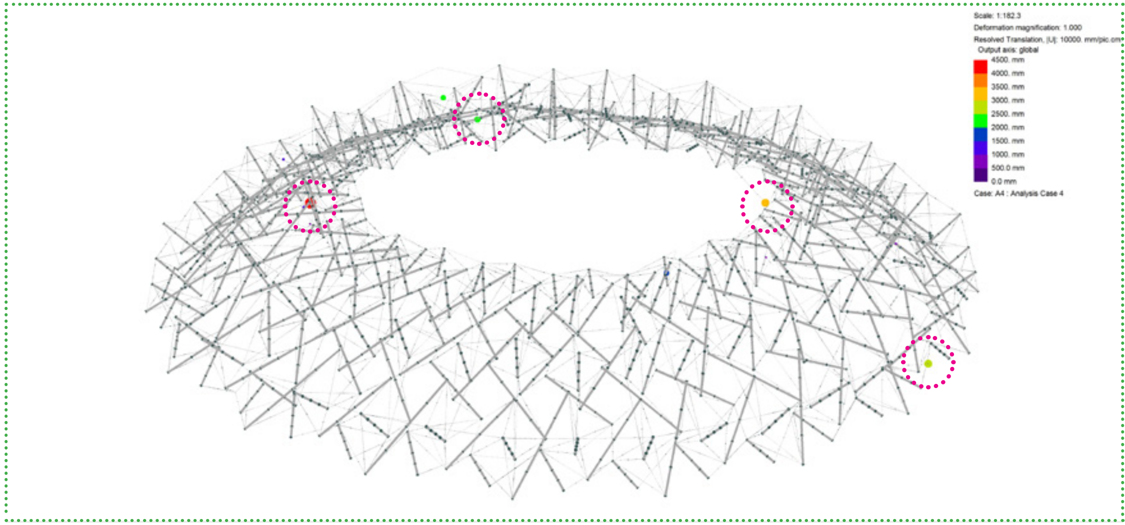

40.1. Nodal displacements

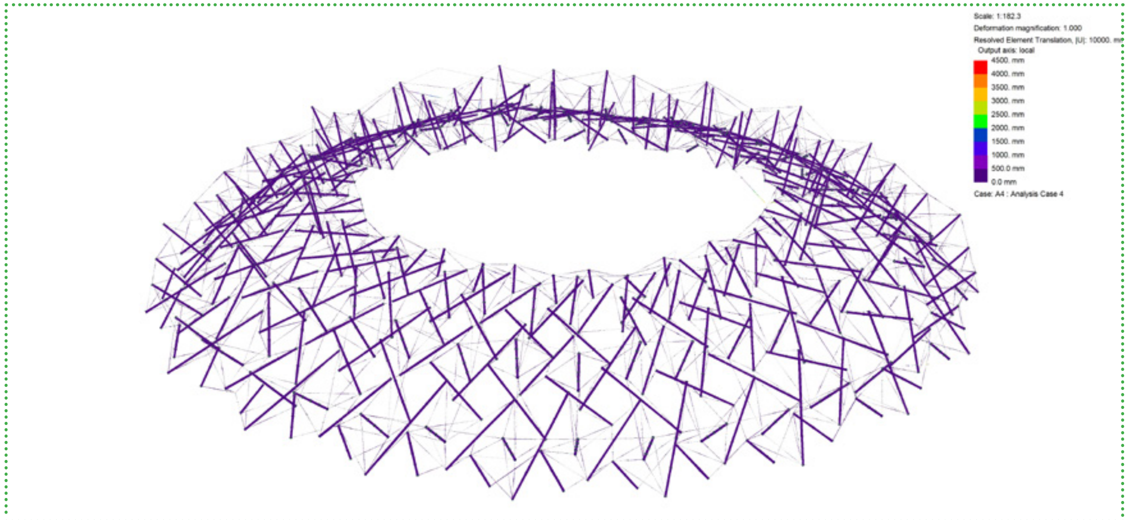

40.2. Beam displacements

The geometry received after the form-finding process deformed quite a lot compared to the original shape, but the general form is reserved. This shape can be improved by adjusting pre-stress forces in the cables.
The model became very stiff and handled the nodal load well.
There is some minor imperfection which does not seem to affect the global performance of the entire system. So it is time to move on with the design for Feyenoord.

Throughout 40 centuries of sports architecture construction, across five continents, the innovations of stadium engineering lie in the size of the stadium, stand's supporting structures and most recently the roof megastructures. From the ancient Greek to the 1900s, almost all stadiums around the world did not have a roof to cover people watching sports games.

41. Evolution of stadium engineering

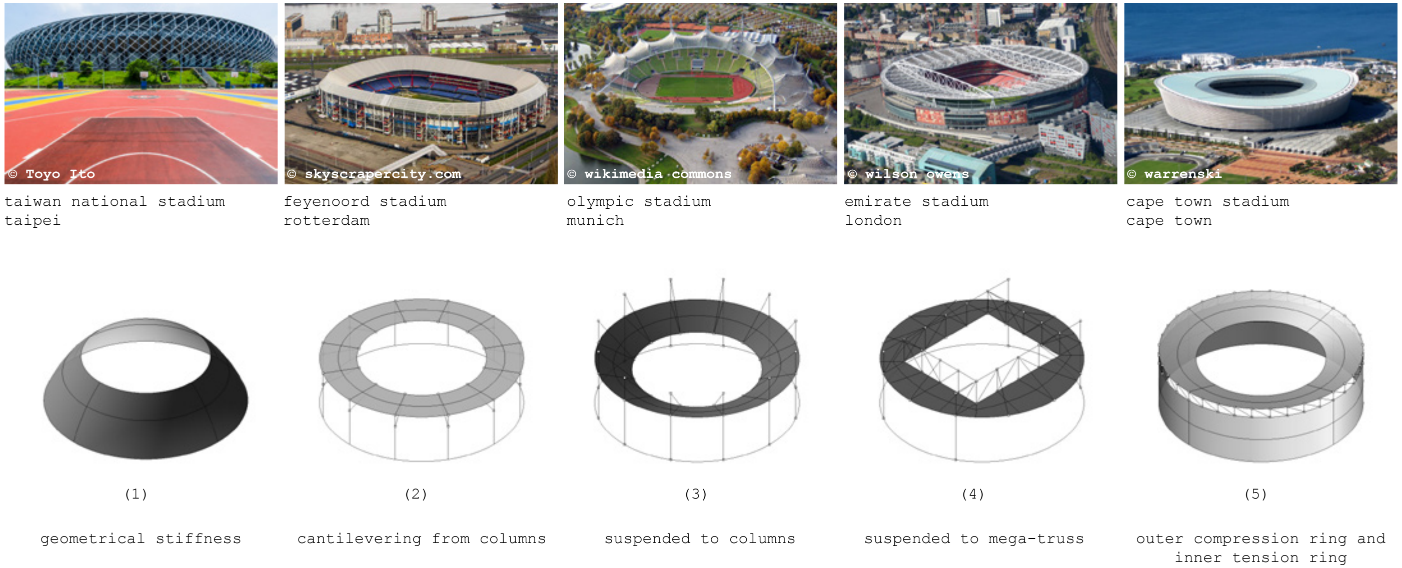

42. Stadium roof structural typology

In contemporary stadium design of the roof, there are mainly five typologies which are commonly applied nowadays:

(1) Geometrical stiffness
(2) Cantilevering from mega-columns
(3) Suspending from mega-columns
(4) Suspending from mega-trusses
(5) Tensioning to the mega-compression ring

43.1. Feyenoord stadium, Google Earth, 2017

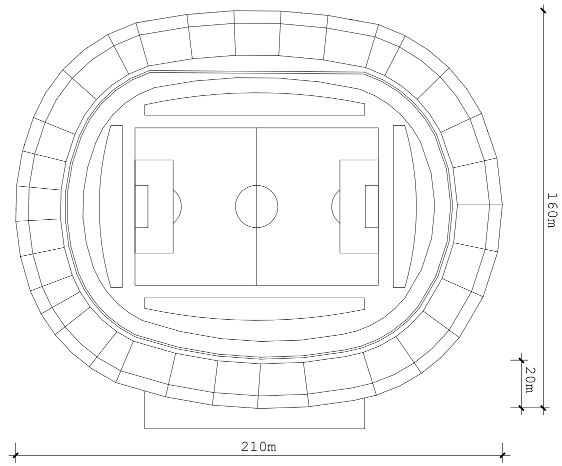

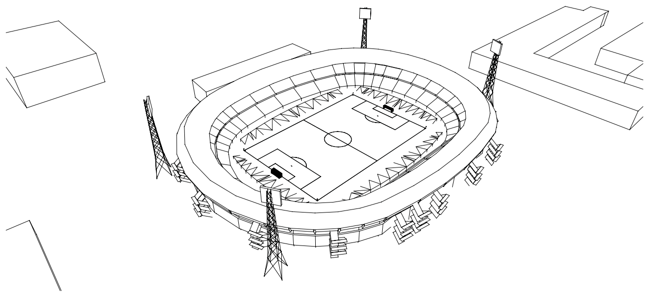

43.2. Stadium's size

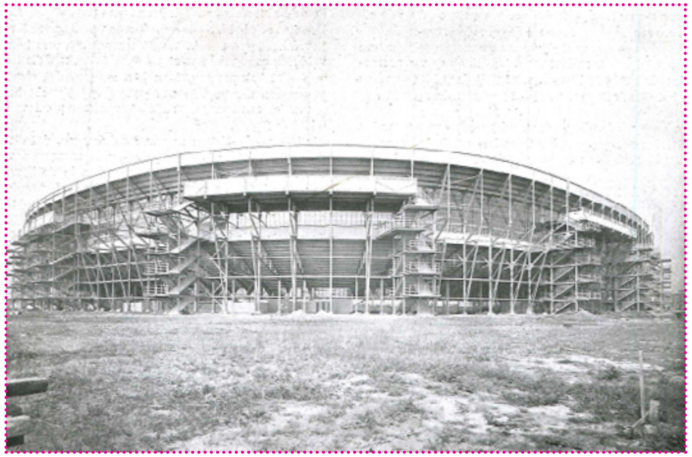

44.1. Feyenoord stadium, Bouwkundig weekblad magazine, 1936

44.2. Feyenoord stadium, Remy de Milde, flickr, 2011

In the 1930s, Leen van Zandviet, Feyenoord's president came up with the idea of building an entirely new stadium, unlike any other on the continent, with two free hanging tiers, and no obstacles blocking the view. This was an extremely innovative use of technology for structure in architecture, which inspires several great stadiums around Europe, Camp Nou is a famous example. After almost 80 years in service, De Kuip needs a new expression. There is obviously an urge for a new story which could continue the innovative tradition.

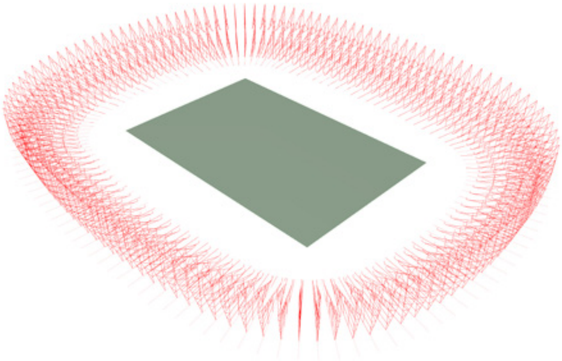

(a) Slender, minimum steel frames

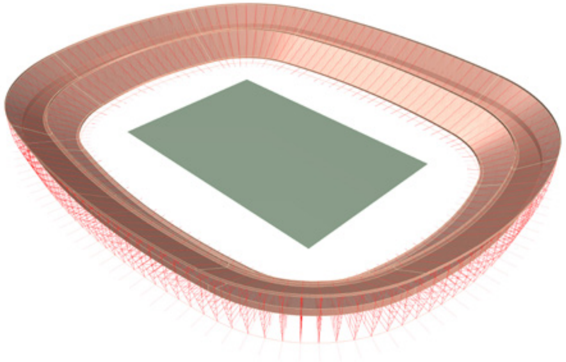

(b) Two hanging tiers

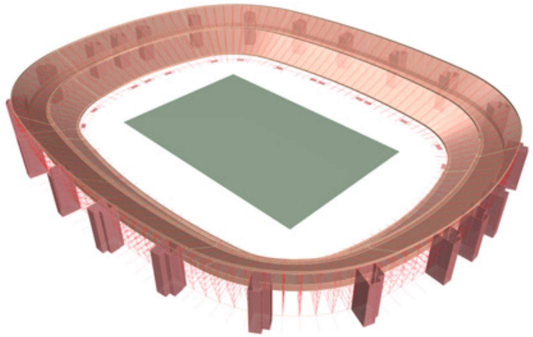

(c) Emergency stairs outside

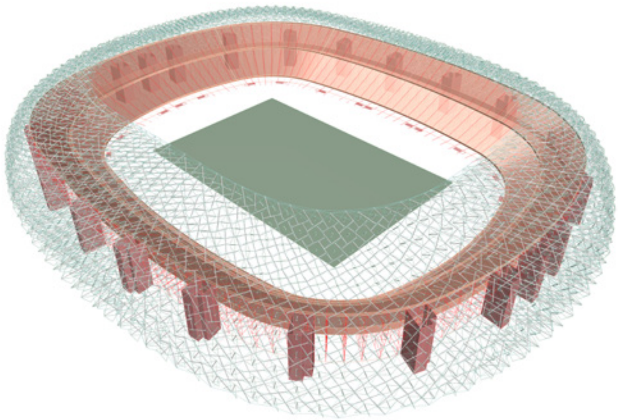

(d) New tensegrity roof

45. Adding new tensegrity structure to the original stadium rooted from 1936

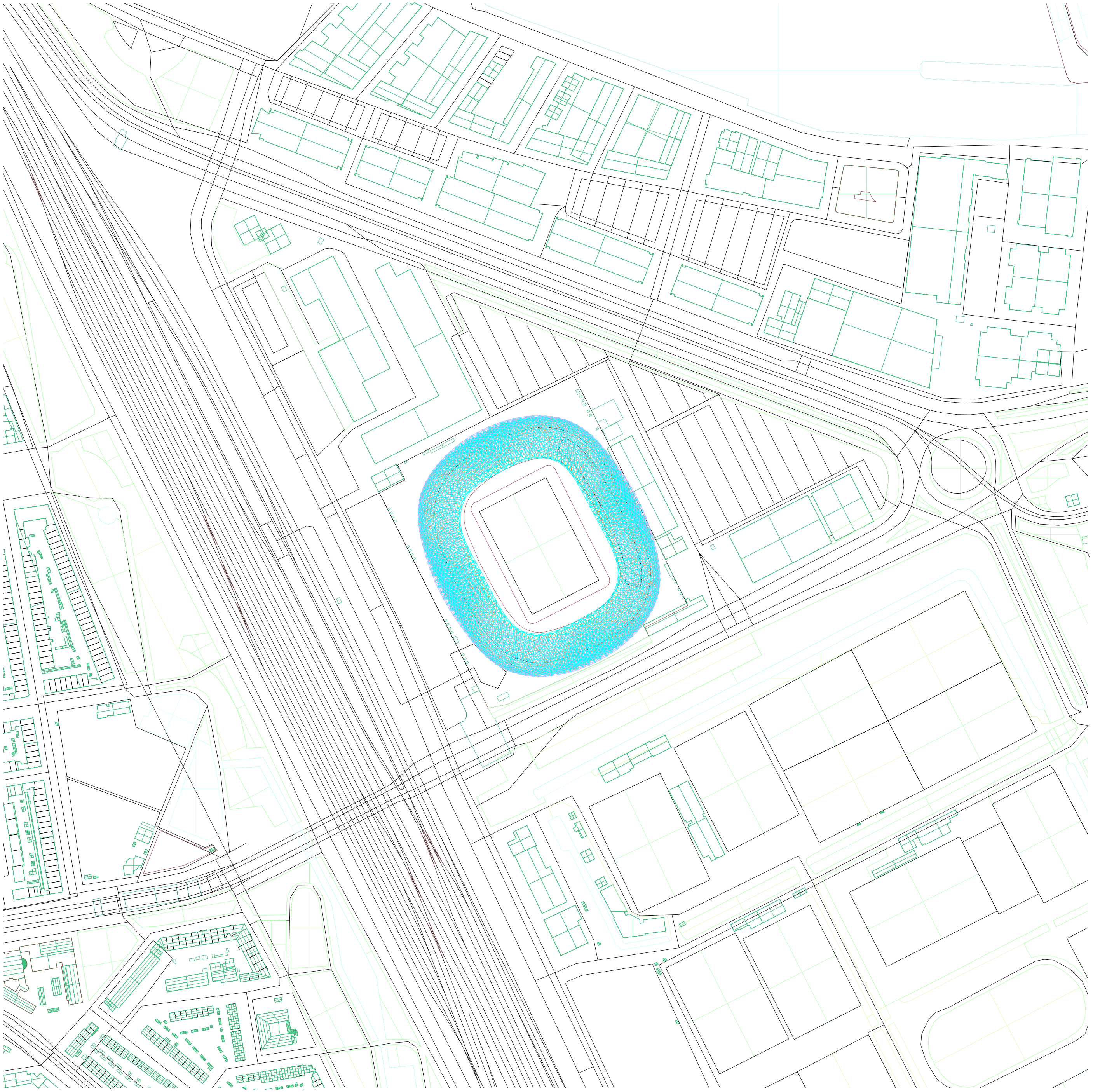

46. The new roof on site

(a) Two reference surfaces

(b) Two reference surfaces are slightly different, creating vairied height

(c) Tessellatizing

(d) Tensegritizing

(e) Merging two reference surfaces

(f) Adding normal struts

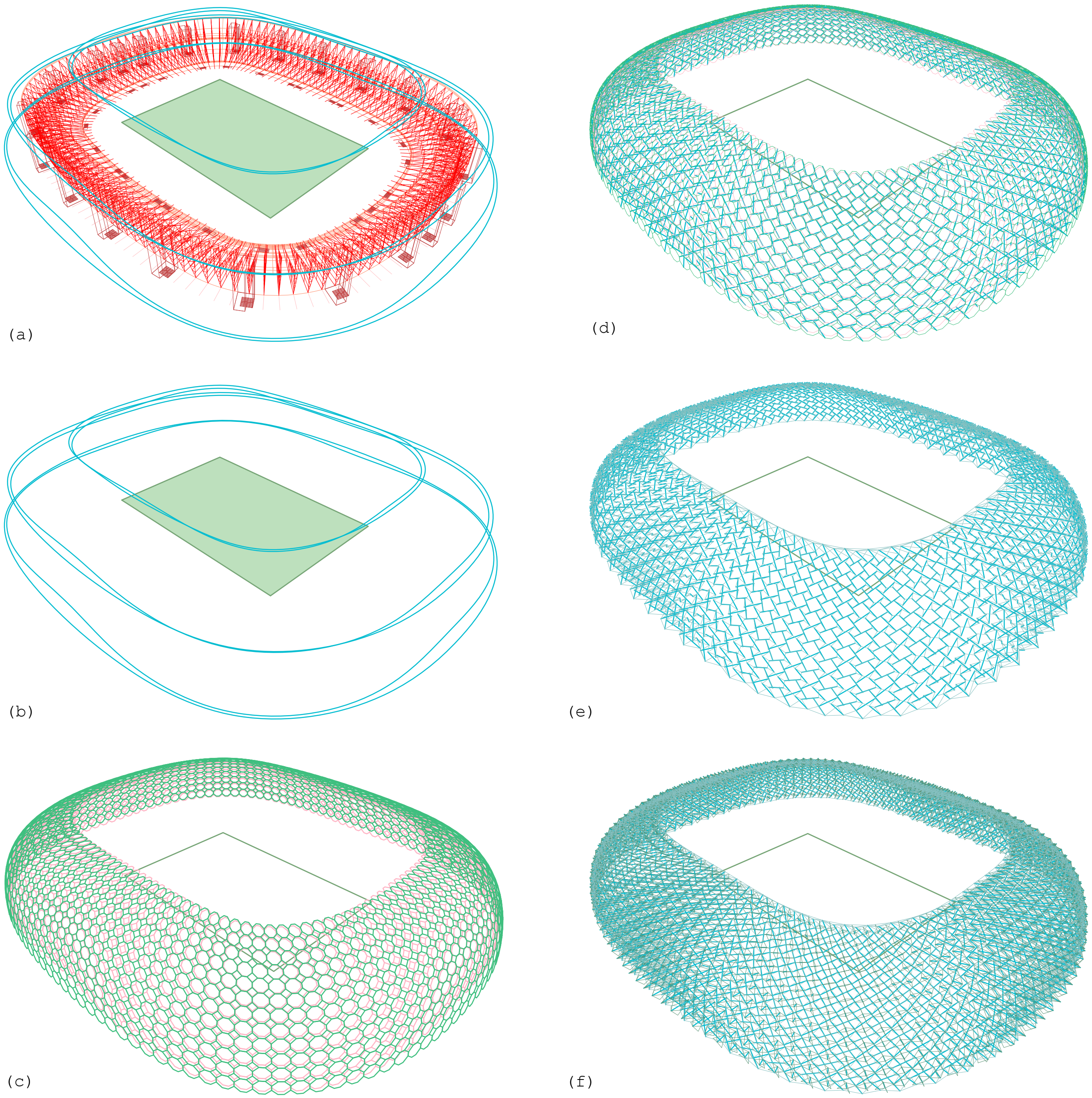

47. Constructing the tesegrity roof

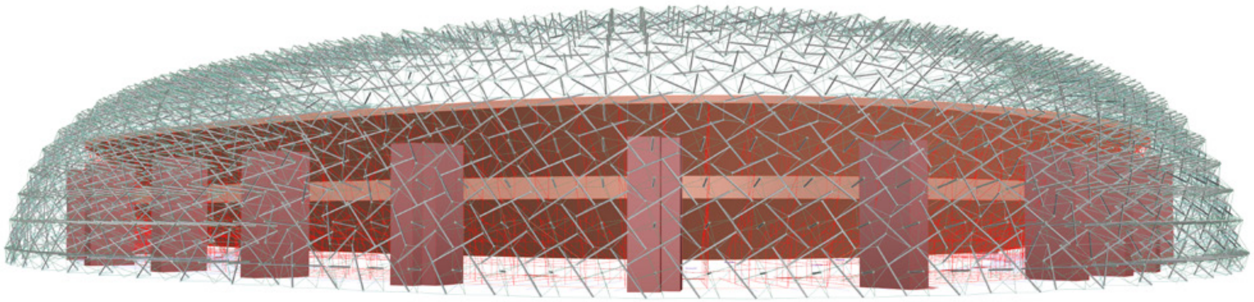

48. The original and the new are blending

The entire structural skin forms
a formless shell which creates
a ambiguous boundary between an
architecture and its environment.

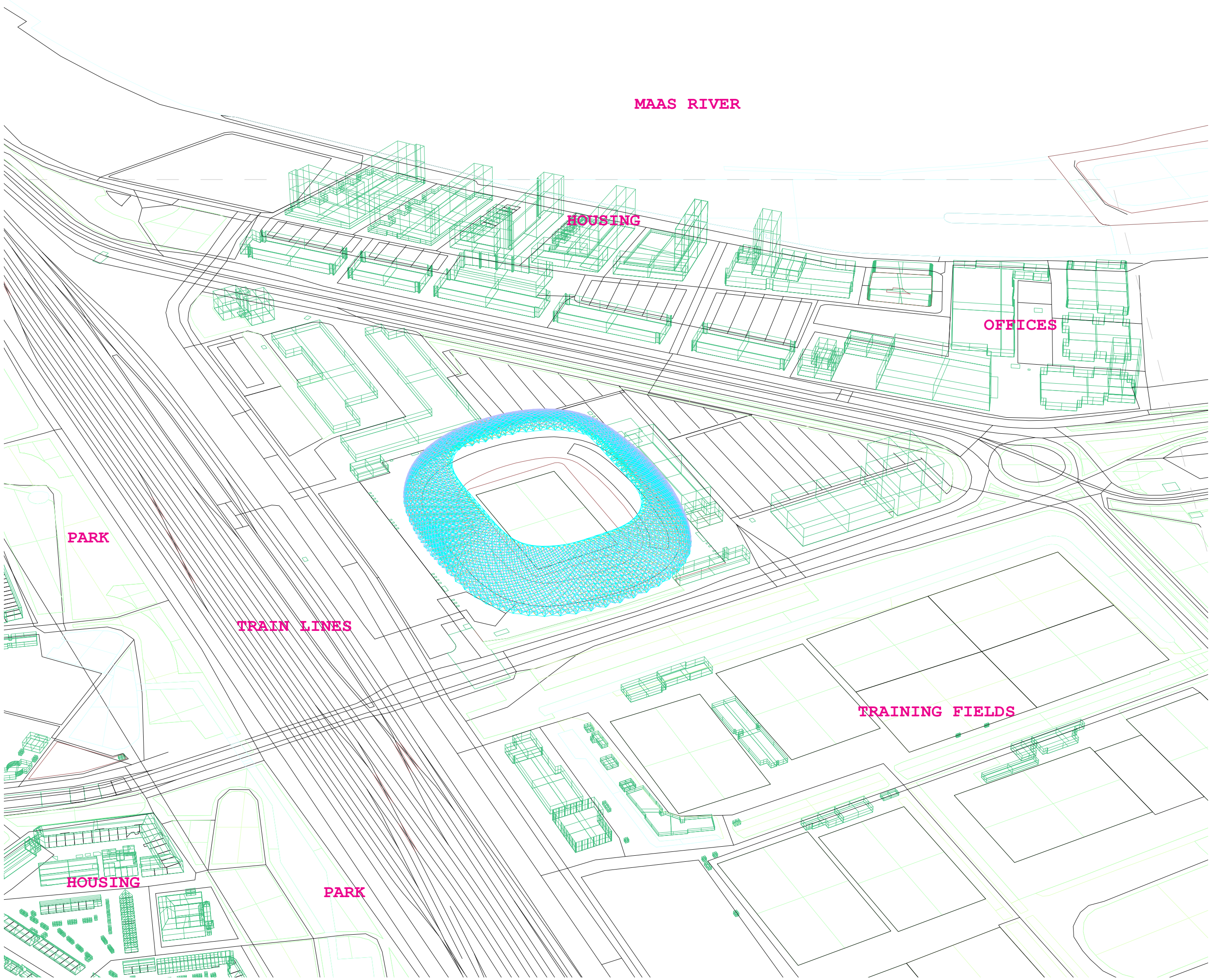

49. Bird-eye perspective

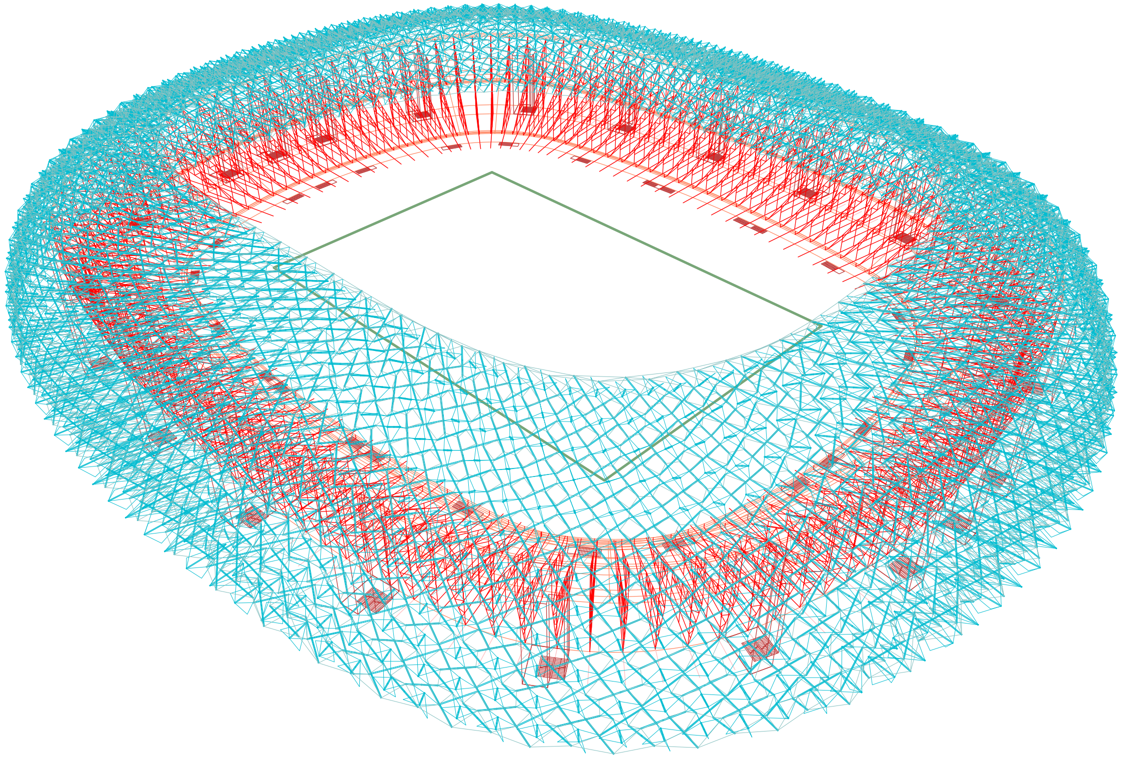

50. The original + The new

The entire structure: 200m x 240m x 37,5m
Cantilivering 37,5m
The central opening: 155m x 115m
4200 struts, 2,16-9,98m - CHS139,7X10
Cables: Ø10
Material: Steel (E = 2,05*E+11 PA)

51. original structure shinning within the floating cloud

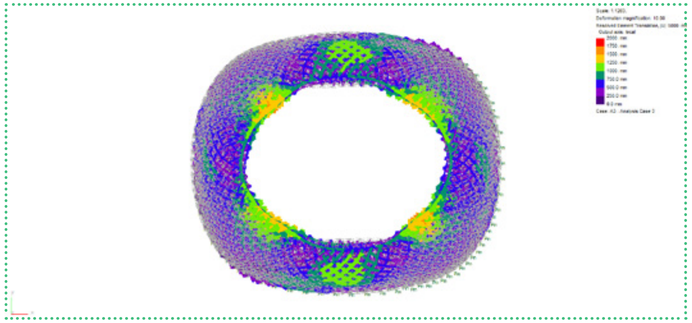

(a) Plan

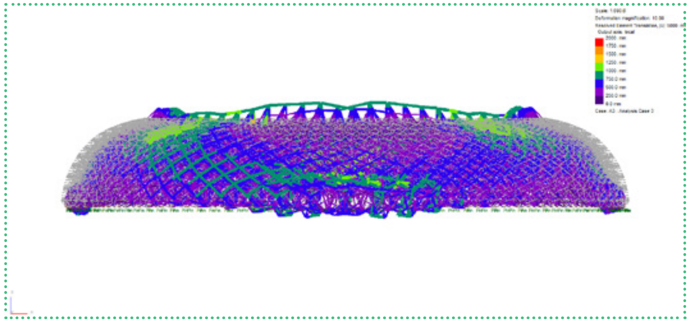

(b) Elevation

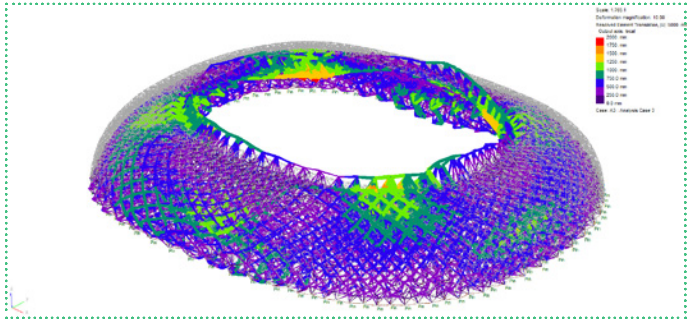

(c) Perspective

52.1. During form-finding

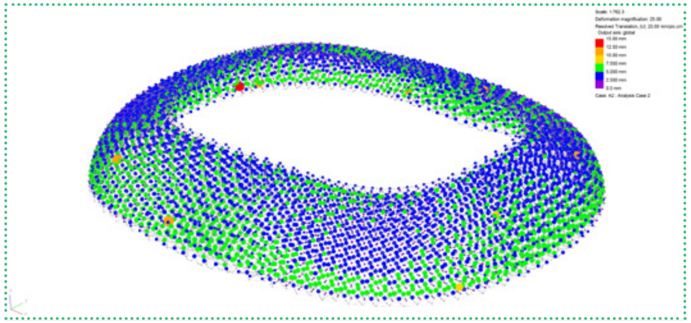

(a) Node displacements

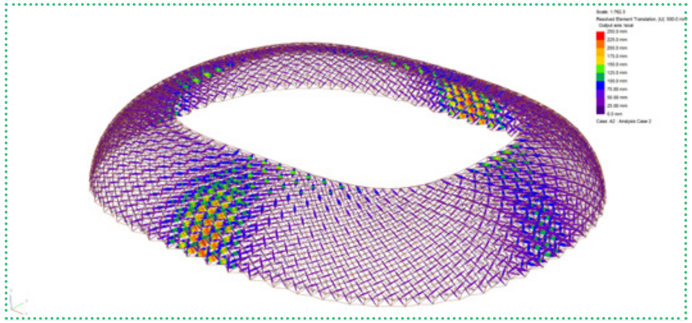

(b) Beam displacements

52.2. After form-finding

47.1. While form-finding is being conducted, the inner ring tends to from a circle which is the minimal figure to find its own state of self-stress while form-finding. But in the end, in the equilibrium, the final shape will be close to the original designed geometry.

47.2. Full-scale model deformed because of gravity during and after form-finding. In the end, after form-finding, the structure became very stiff as well. This is because of pre-stress forces, as well as the large number of structural element. The geometry found is smoother and closer to the original version compared to form-finding of simplified version.

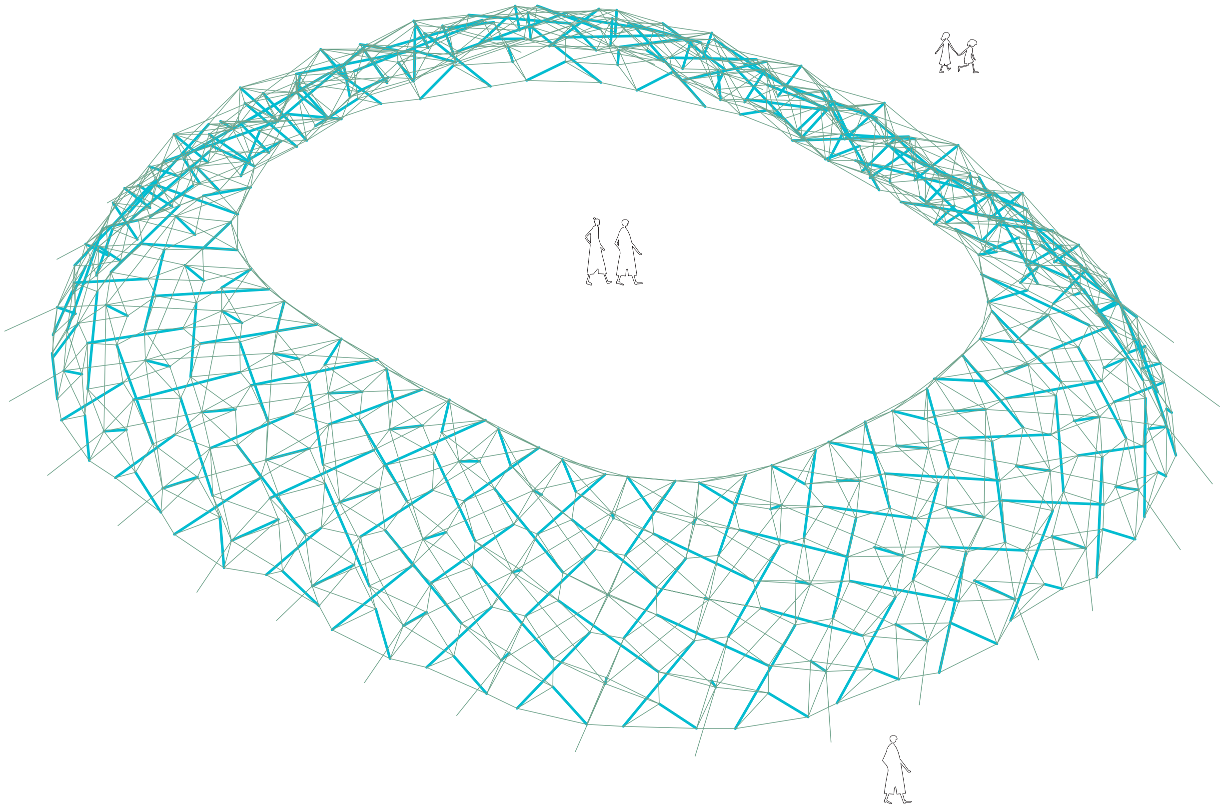

53. Simplified version of the structure

The entire structure: 20m x 24m x 3,7m
Cantilivering 3,7m
The central opening: 15,5m x 11,5m
211 spatial struts, 0,72-2,67m - CHS48,3X5
91 normal struts, 0,56-1,34m - CHS48,3X5
Cable: Ø10
Material: Steel (E = 2,05*E+11 PA)

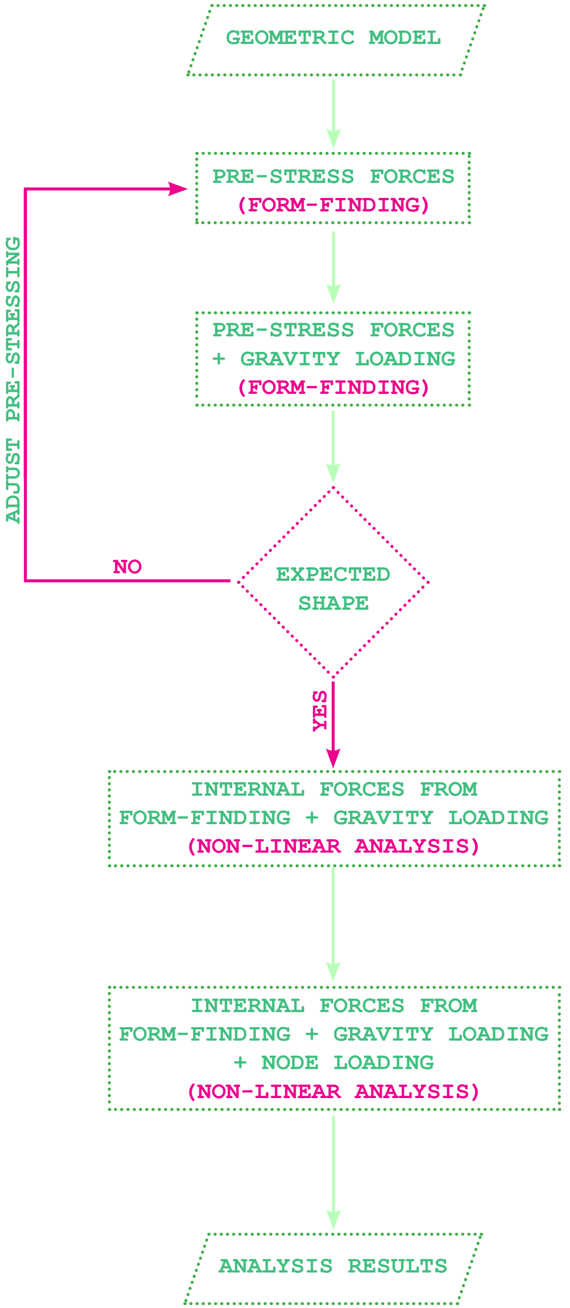

54.1. Form-finding work-flow

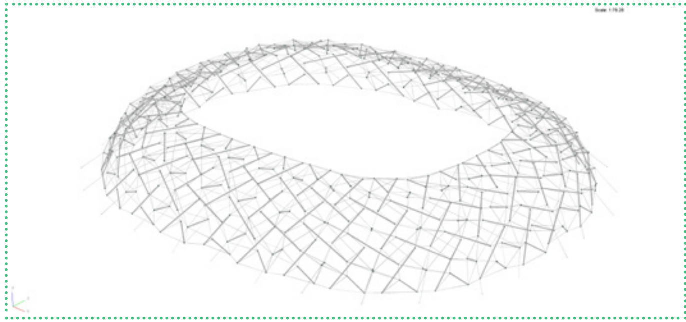

54.2. Designed form

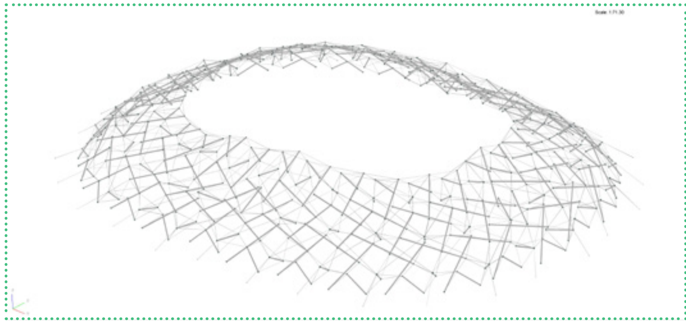

54.3. Form-found 1

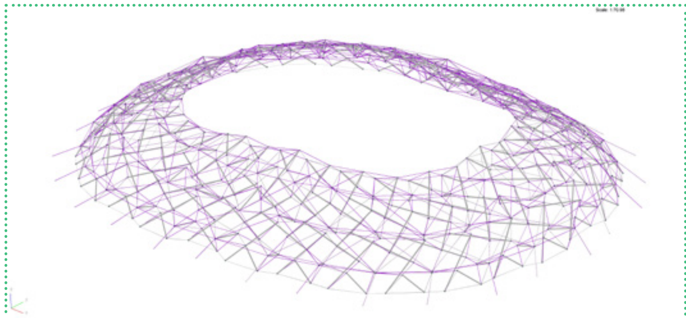

54.4. Form-found 2

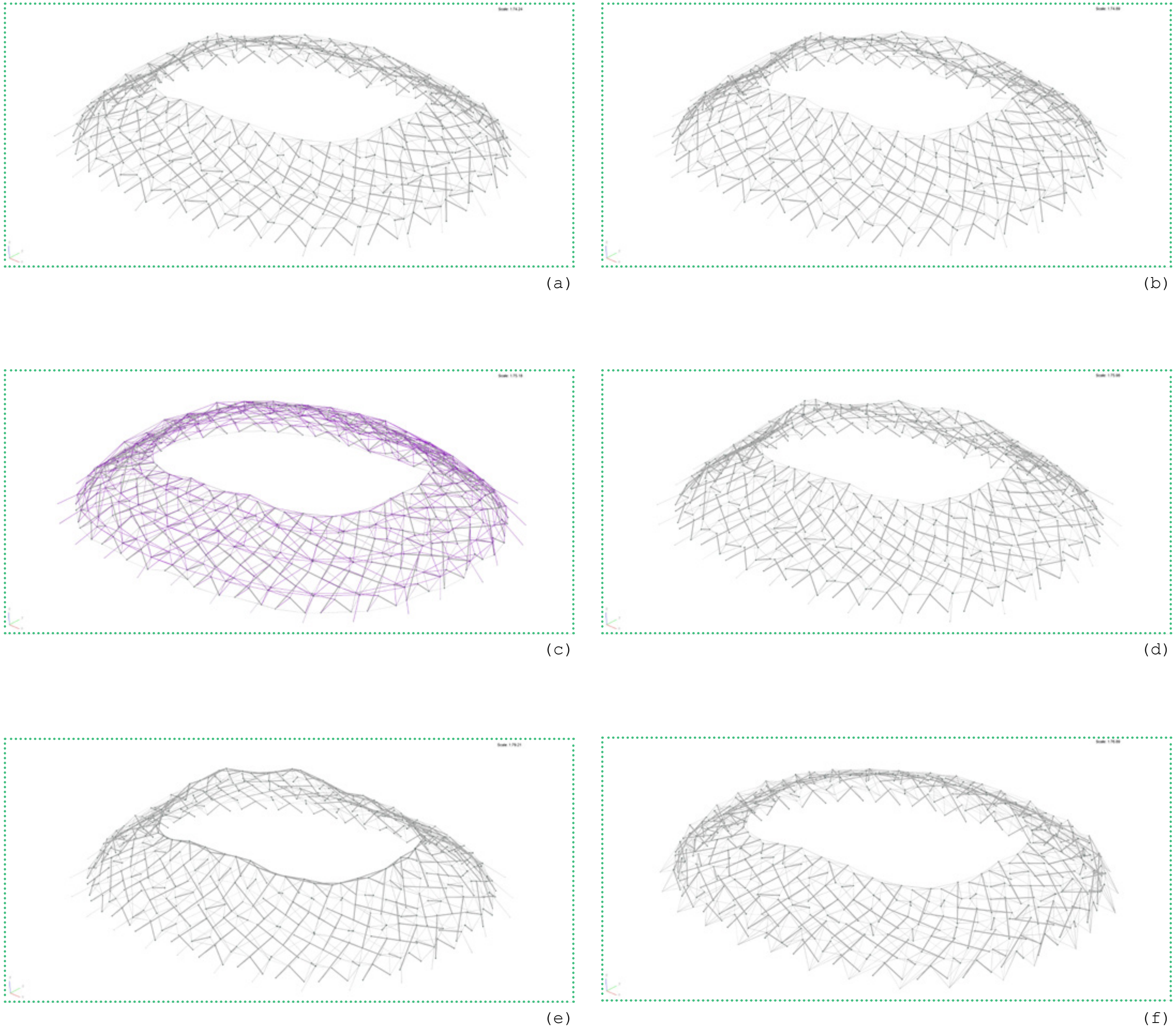

The form-found shapes depend on the pre-stress forces. One has to repeat the form-finding process several times to make the structure less flat, becoming more domical geometries. the inner ring needs to be made out of a stiff 3d-frame which should be as lightweight as possible.

55. Form-finding results

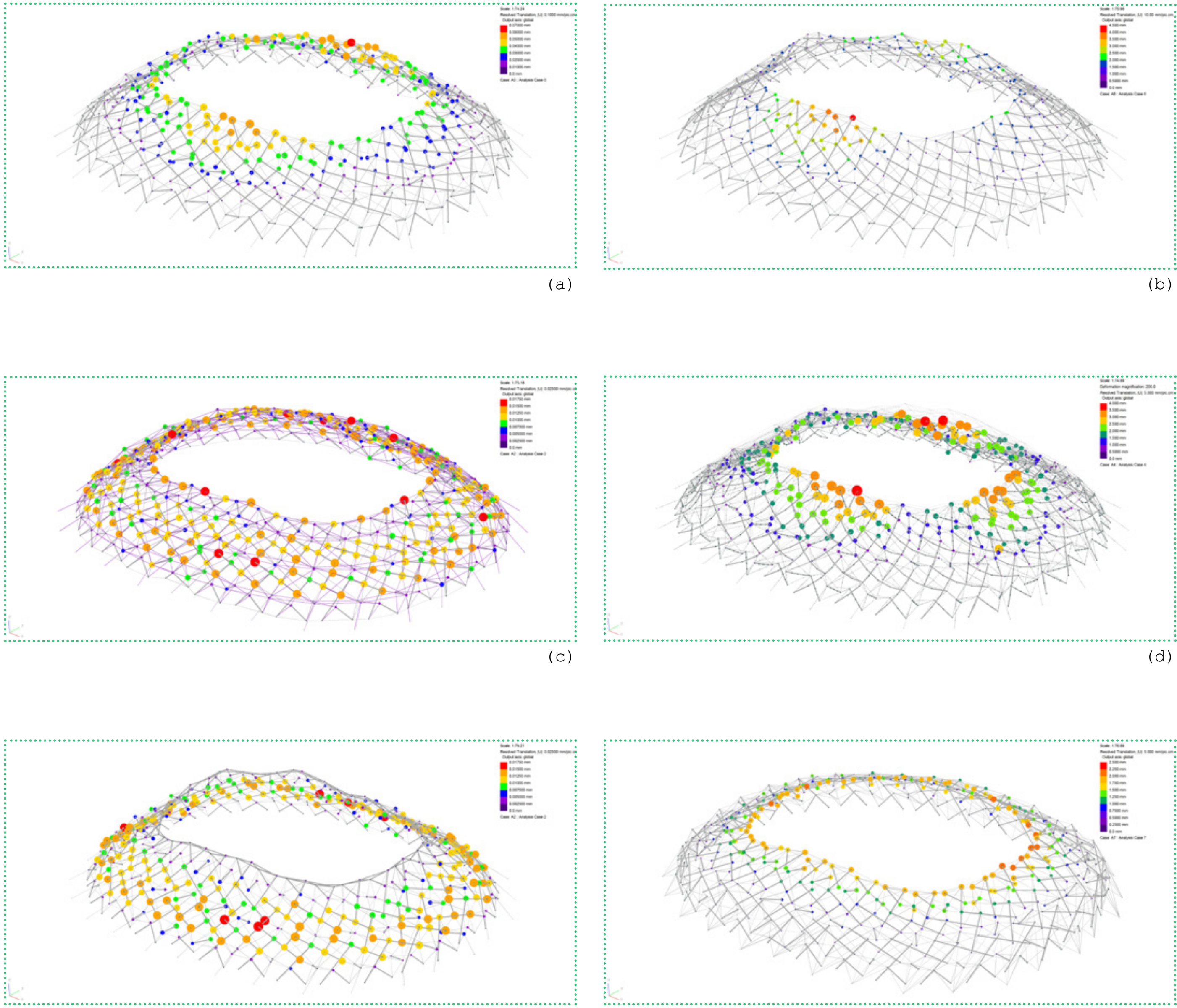

(a) (b) (c) (d) (e) (f)

56. Node displacements caused by gravity

After form-finding processes in Oasys GSA, the structures became very stiff, and it handled very well the gravity load. The displacements are relatively small, much smaller than the limts (l/250 = 3700/250 = 14.8mm).

The areas around the inner ring are the weakest areas. It is expected because of the large central opening.

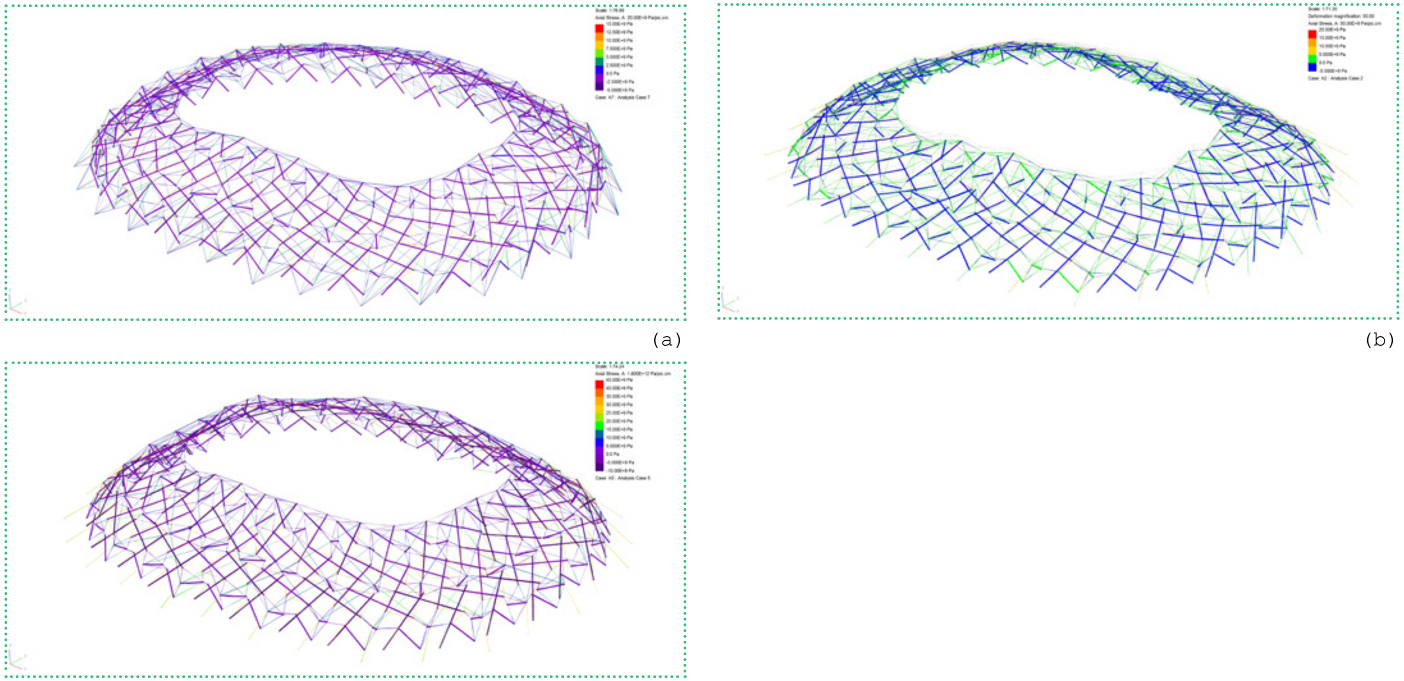

(a) (b) (c)

54.1. Axial stresses caused by gravity

When a nodal load is applied, the surrounding areas are affected in all directions. This behavior is also similar to the physical model. The rigidity of tensegrity structures depends on the pre-stress forces in cables which gives the structure the state of self-stress.

Soap film and force density method cannot be applicable in this type of tensegrity, only 'ignore form-finding properties' works. This technique takes the deformed shape and internal loading from form-finding as the input for the next analysis.

Both struts and cables are subjected to axial stresses. in these models, maximum axial stresses are relatively small compared to young's modulus of steel: 2,05e+11 pa.

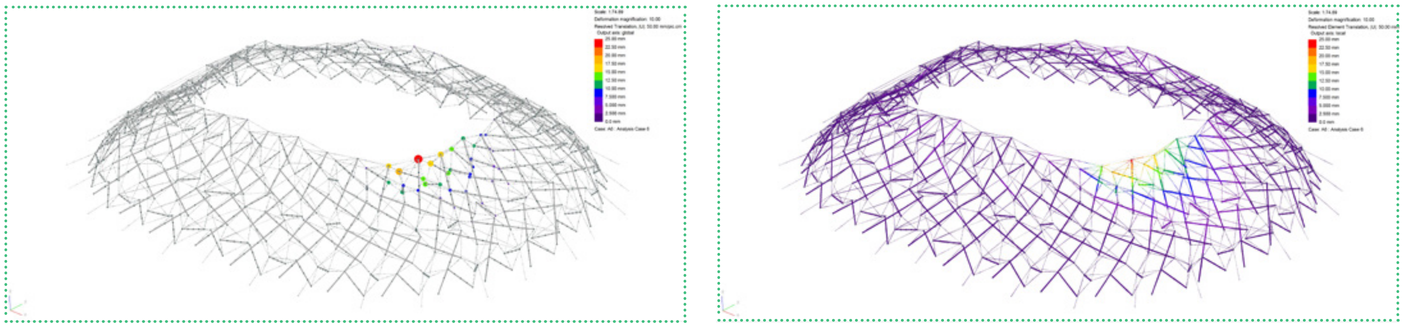

(a) Node deformations (b) Beam deformations

57.2. Displacements caused by nodal loading

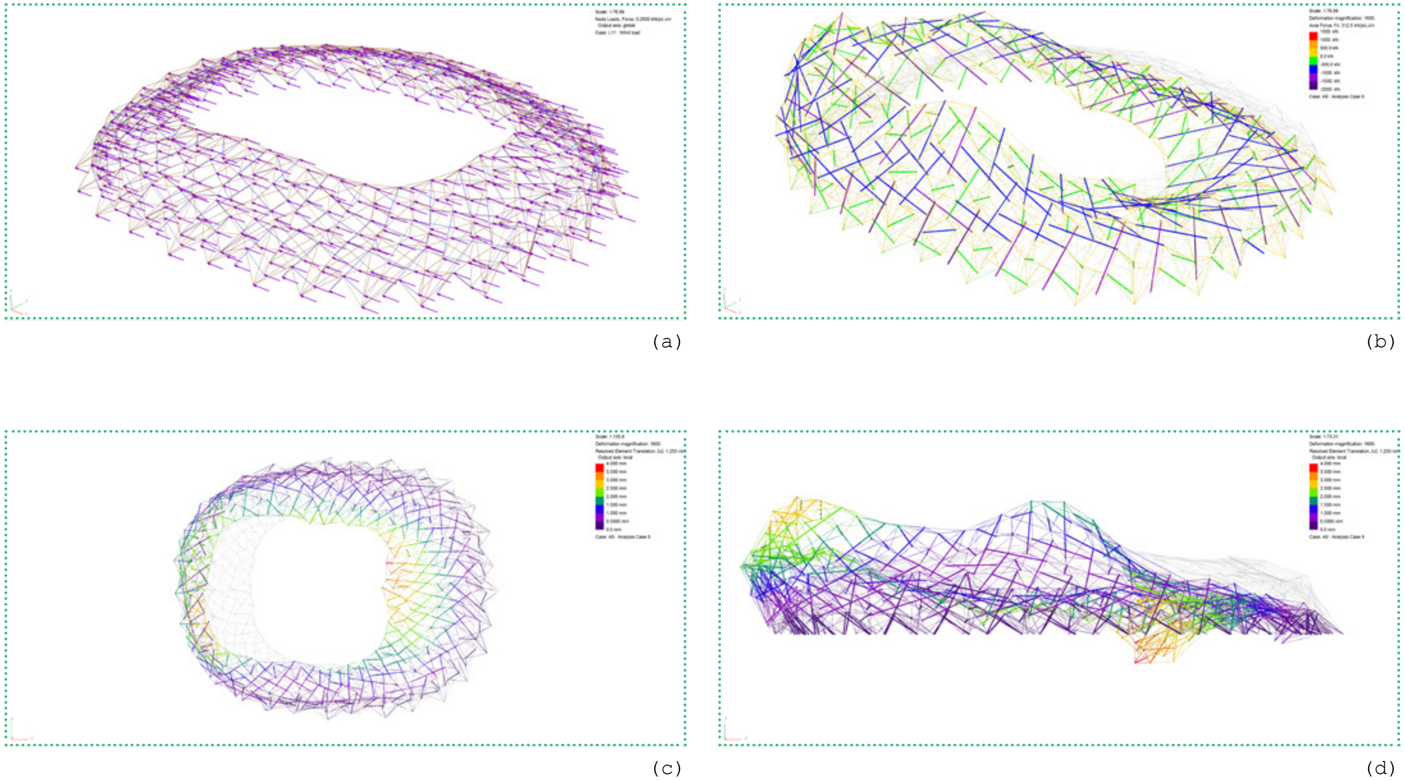

58. Wind loaidng

Checking the affect of lateral, asymetrical loading is crucial for such a flexible system like tensegrity. the roof performed very well. The displacement is relatively small compared to the span.

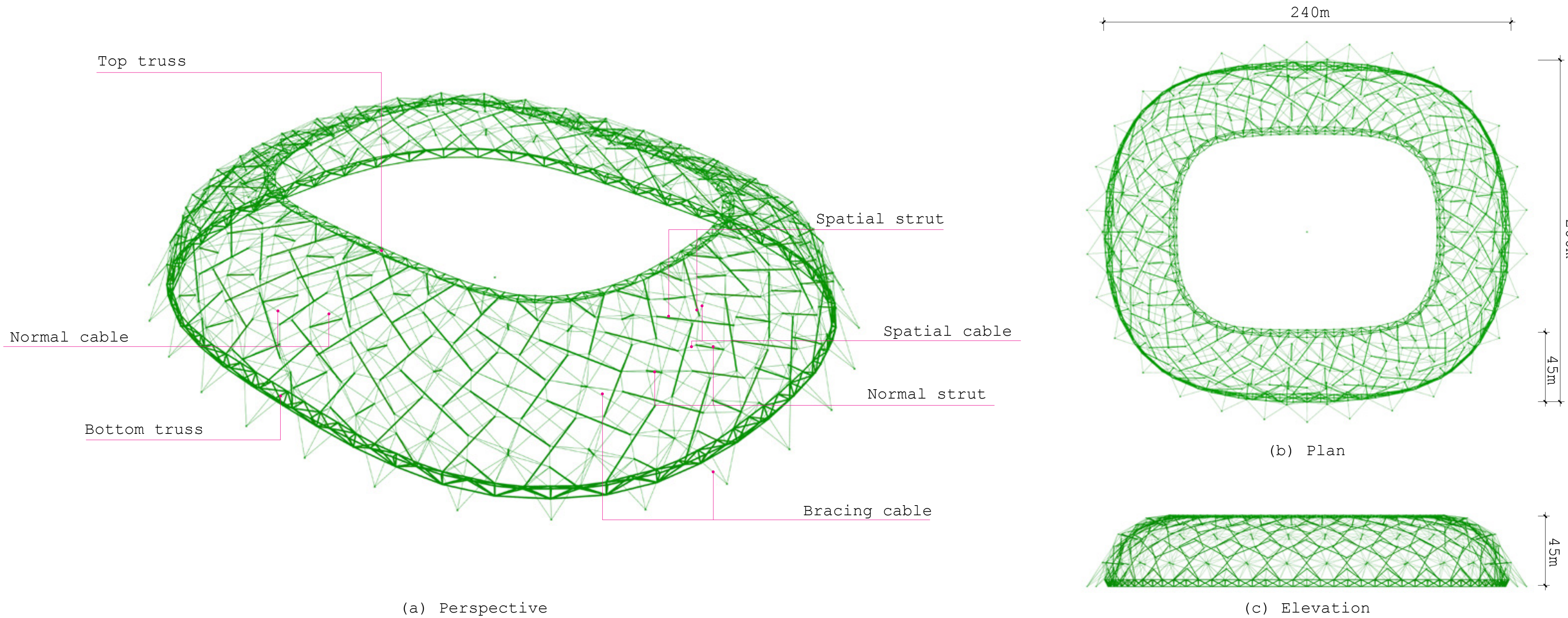

59. Final structural model

(LC1) Internal loads from form-finding

(LC2) Self-weight

(LC3) Dead load: cladding

(LC4) Snow load

(LC5) Wind load

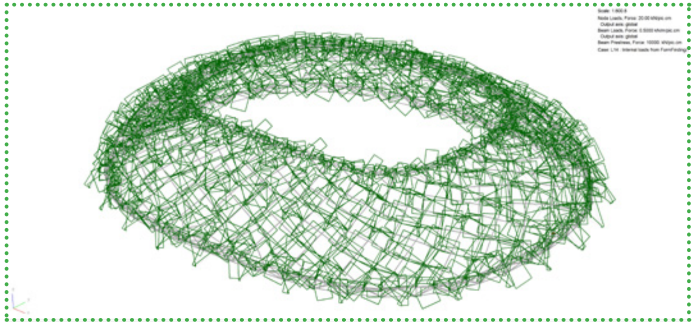

60.1. Internal loads from form-finding

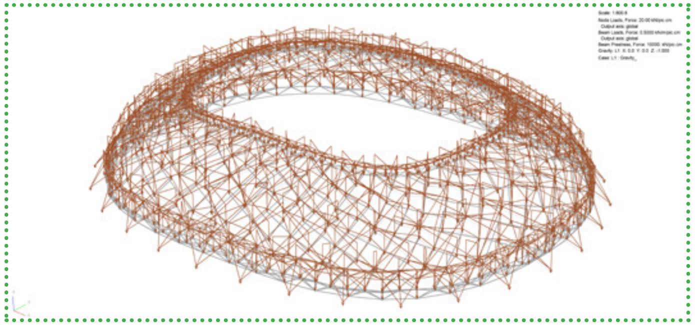

60.2. Self-weight diagram

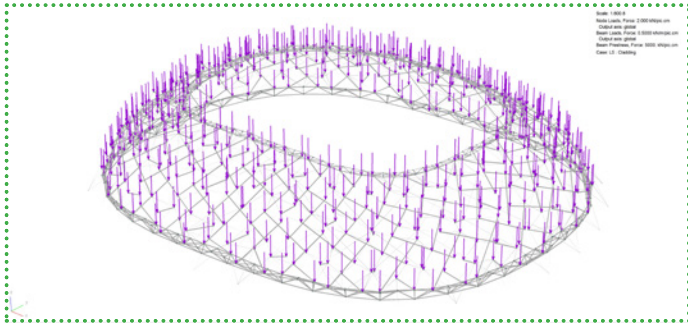

60.3. Cladding load diagram

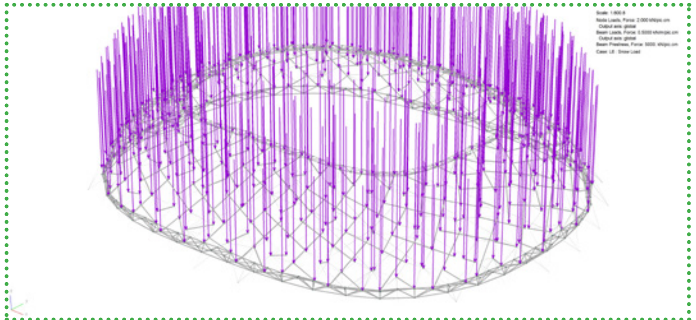

60.4. Snow load diagram

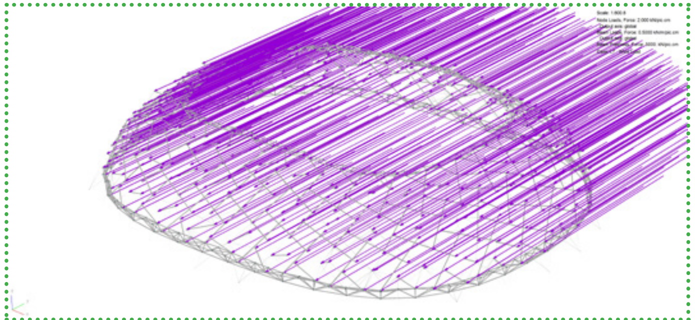

60.5. Wind load diagram, simplified the direction to horizontal y direction

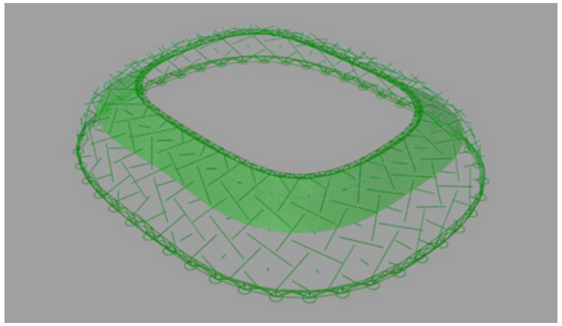

60.6. Cladding layer is underneath the structure

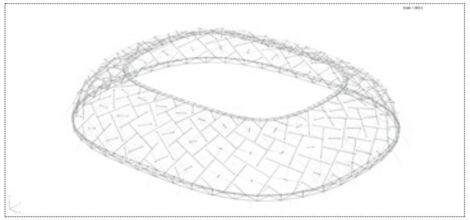

61.1. Original form

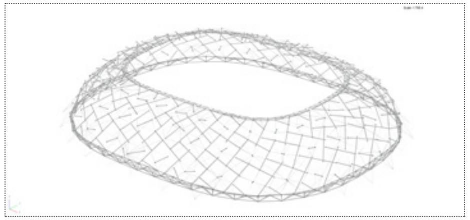

61.2. Form-found

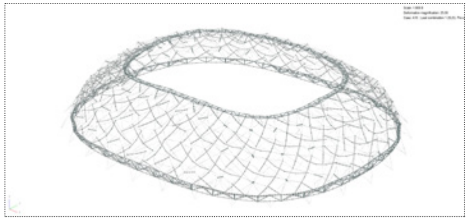

61.3. Pre-stress

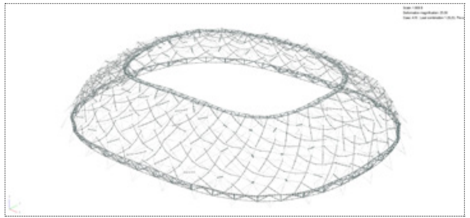

61.4(a). Load combination 1 (SLS)

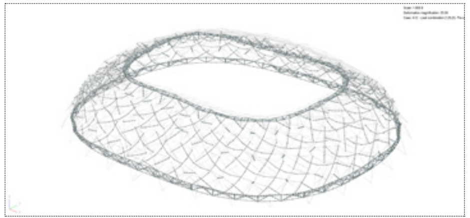

61.5(a). Load combination 2 (SLS)

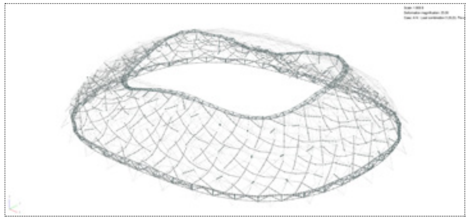

61.6(a).Load combination 3 (SLS)

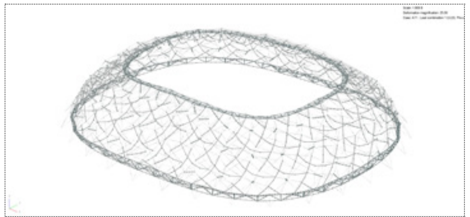

61.4(b). Load combination 1 (ULS)

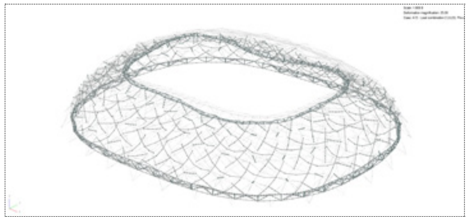

61.5(b) Load combination 2 (ULS)

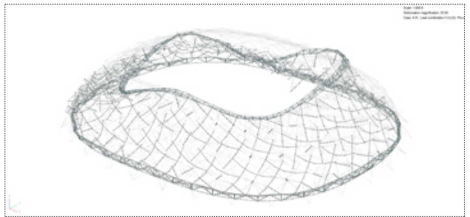

61.6(b). Load combination 3 (ULS)

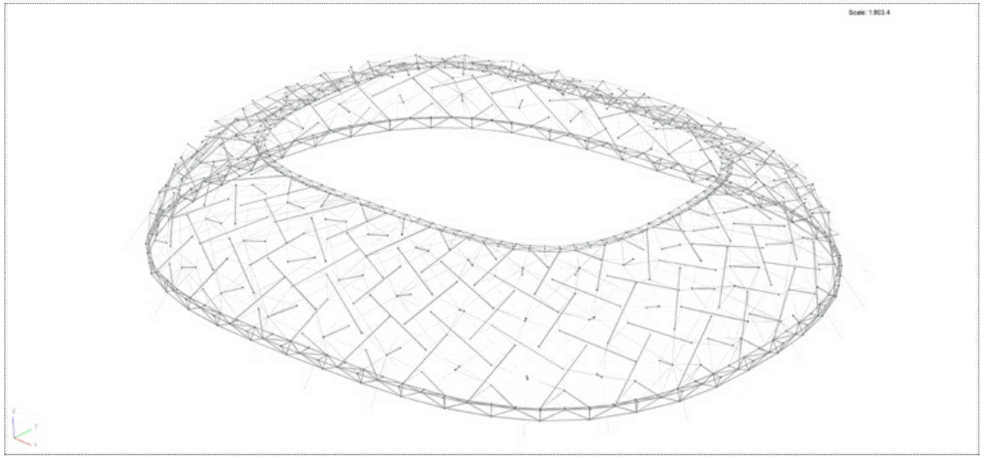

62.1. Original form

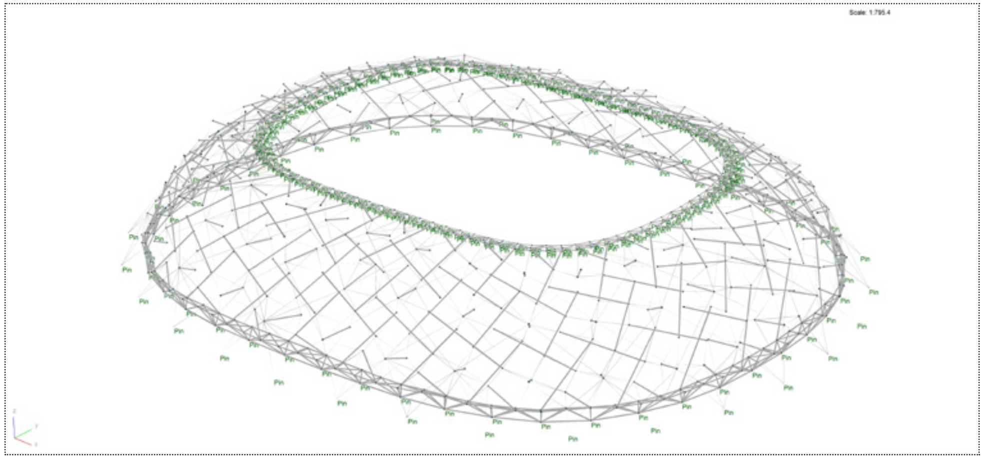

62.1. Form-finding model

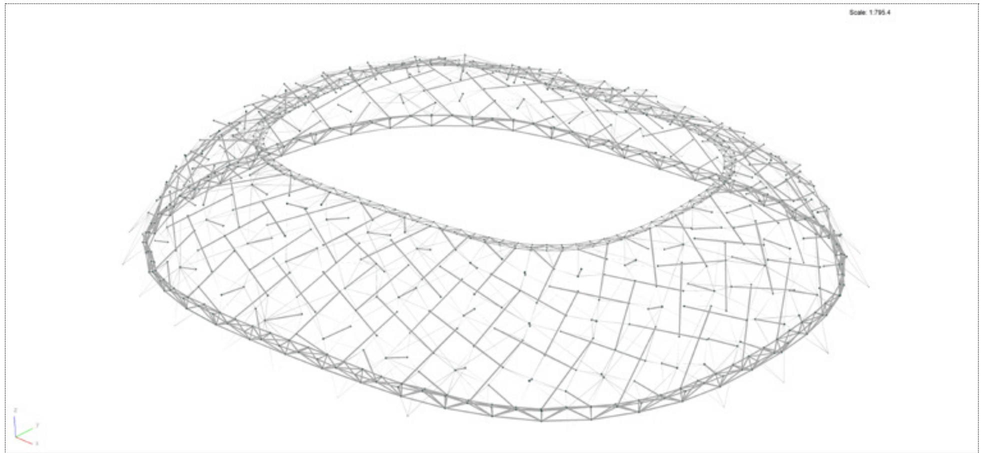

62.2. Form-found

After (7), top truss nodes are unpinned for the last form-finding (8).

(1) Form-finding 1: Cable pre-stress forces (500 kN)
(2) Form-finding 2: Cable pre-stress forces (500kN) + Gravity
(3) Form-finding 3: Cable pre-stress forces (500 kN)
(4) Form-finding 4: Cable pre-stress forces (500 kN)
(5) Form-finding 5: Cable pre-stress forces (500 kN)
(6) Form-finding 6: Cable pre-stress forces (500 kN)
(7) Form-finding 7: Cable pre-stress forces (500 kN)
(8) Form-finding 8: Cable pre-stress forces + Gravity + Dead loads. After this, the model will not deform under gravity and dead loads

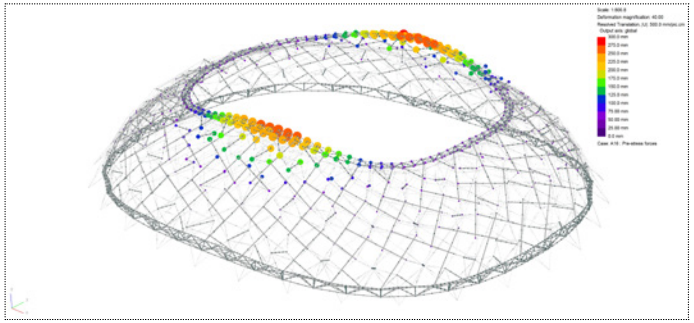

(a) node displacement

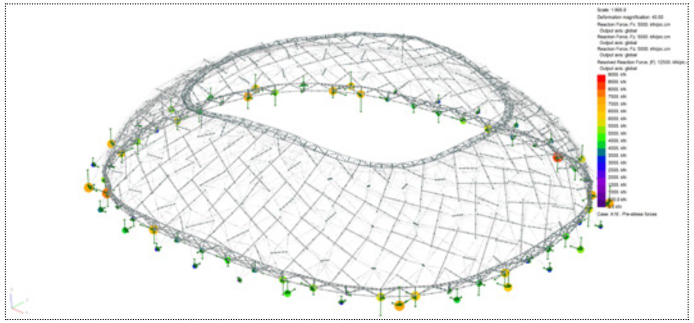

(b) support reaction

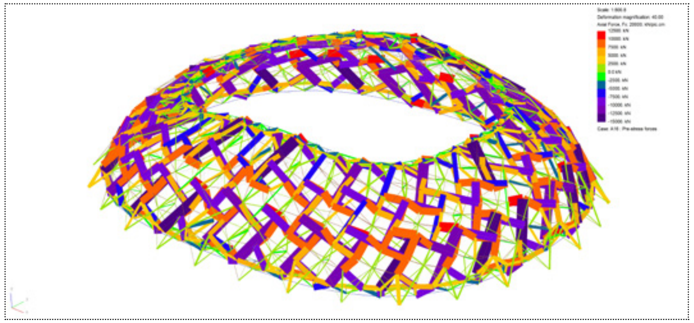

(c) axial force

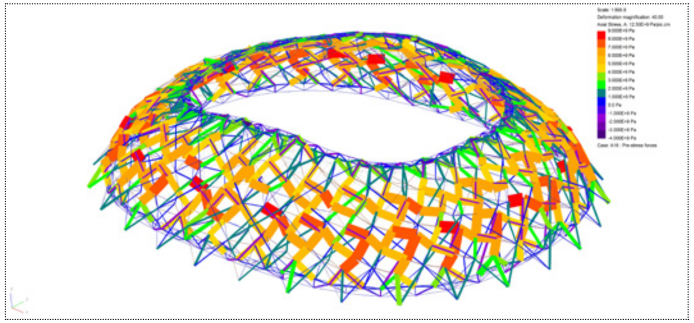

(d) axial stress

Considering pre-stress forces only, the structure would deform in a way that it is going up agaist gravity. Then to combine with gravity and cladding loads, they form will be stablize and closer to the designed geometry.

63. Pre-stress forces

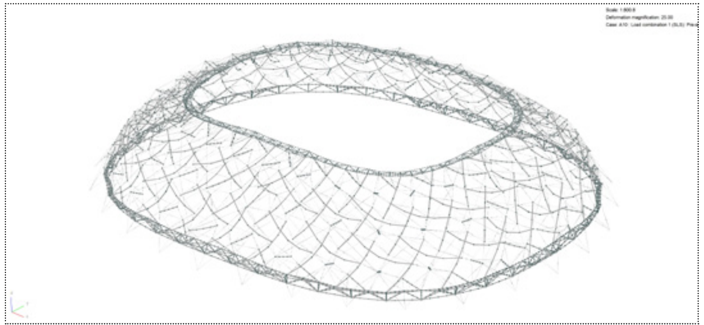

64.1(a). Load combination 1 (SLS)

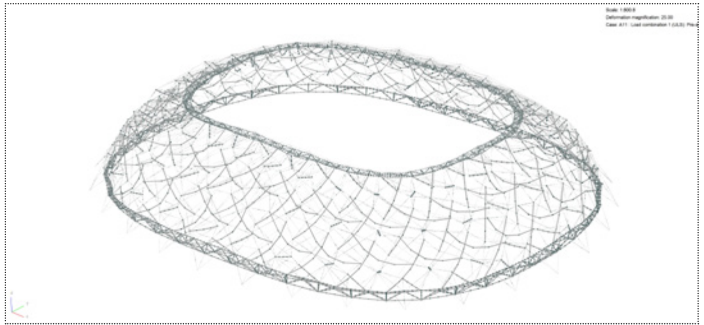

64.1(b). Load combination 1 (ULS)

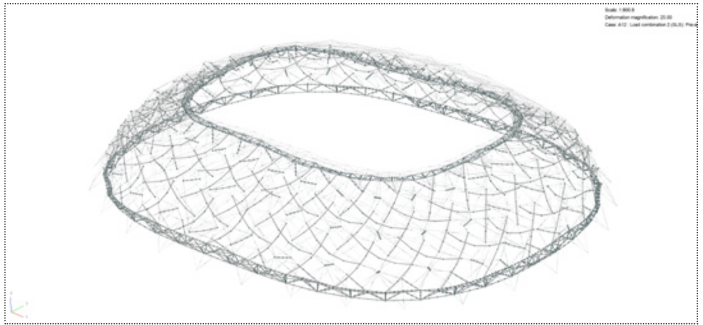

64.2(a). Load combination 2 (SLS)

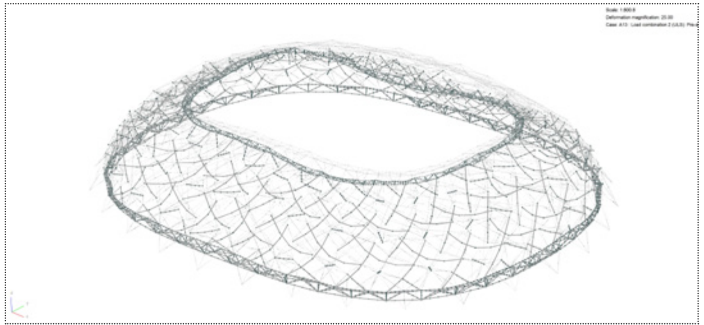

64.2(b) Load combination 2 (ULS)

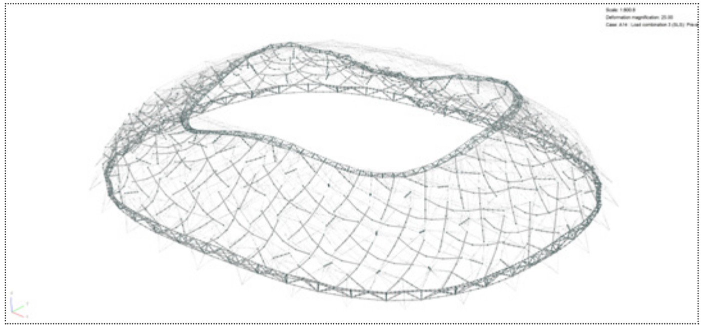

64.3(a).Load combination 3 (SLS)

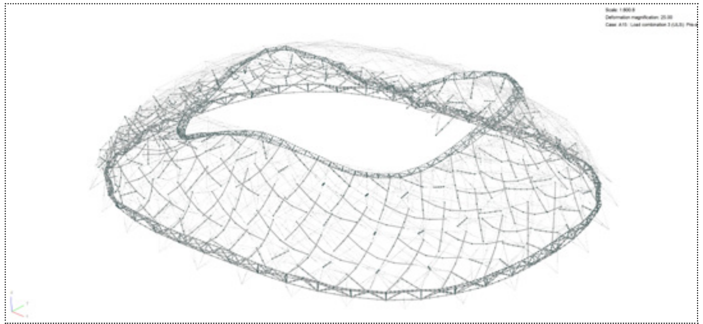

64.3(b). Load combination 3 (ULS)

Load combination 1: Pre-stress forces, self-weight and dead loads (LC1 + LC2 + LC3)
Ultimate Limit State (axial forces, weights, and support reactions):
LC1 + 1,35*LC2 + 1,35*LC3
Serviceability Limit State (node displacement):
LC1 + LC2 + LC3

Load combination 2: Pre-stress forces, self-weight, dead loads, and snow load (LC1 + LC2 + LC3 + LC4)
Ultimate Limit State (axial forces, weights, and support reactions):
LC1 + 1,2*LC2 + 1,2*LC3 + 1,5*LC4
Serviceability Limit State (node displacement):
LC1 + LC2 + LC3 + LC4

Load combination 3: Pre-stress forces, self-weight, dead loads, and wind load (LC1 + LC2 + LC3 + LC5)
Ultimate Limit State (axial forces and support reactions)
LC1 + 0,9*LC2 + 0,9*LC3 + 1,5*LC5
Serviceability Limit State (node displacement):
LC1 + LC2 + LC3 + LC5

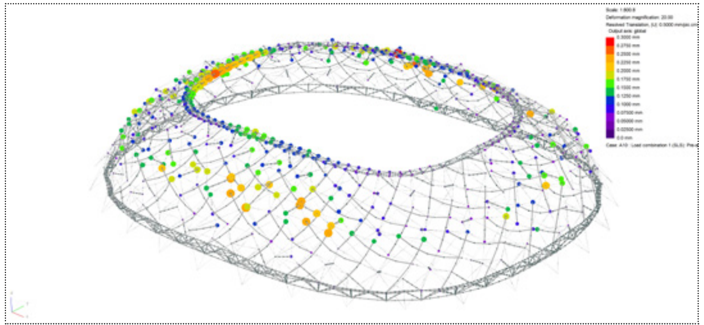

65.1(a). Load combination 1 (SLS)

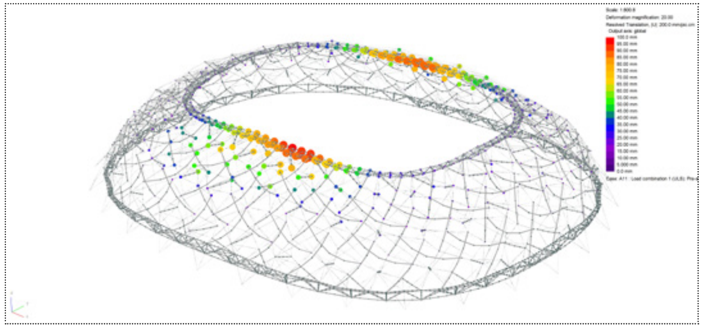

65.1(b). Load combination 1 (ULS)

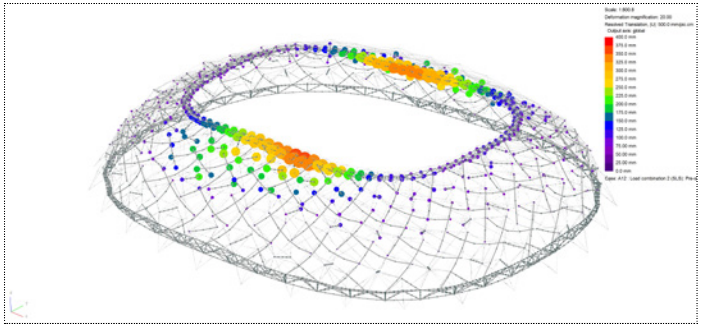

65.2(a). Load combination 2 (SLS)

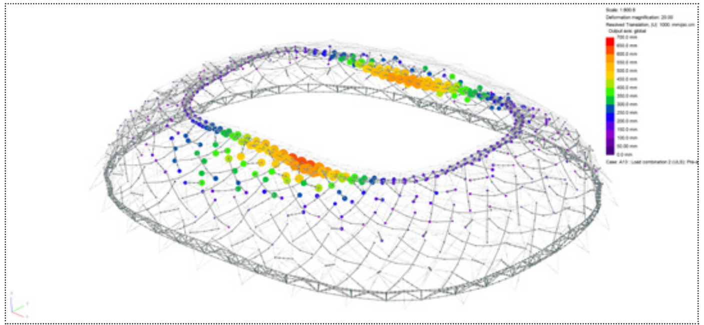

65.2(b) Load combination 2 (ULS)

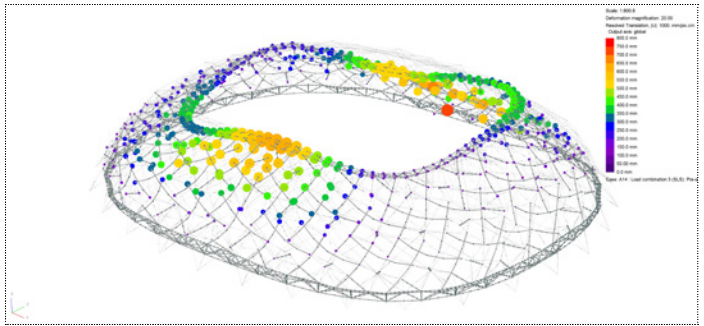

65.3(a).Load combination 3 (SLS)

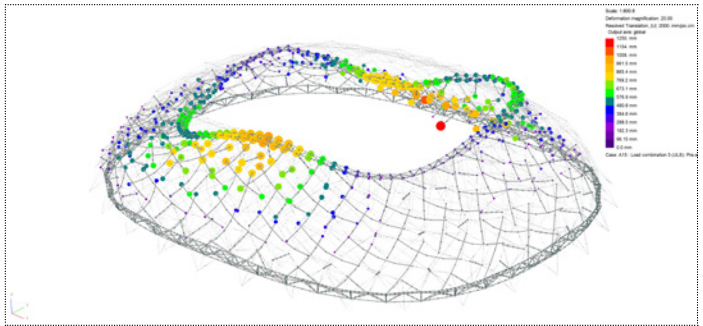

65.3(b). Load combination 3 (ULS)

Load combination 1: Pre-stress forces, self-weight and dead loads (LC1 + LC2 + LC3)
Ultimate Limit State: 100mm
Serviceability Limit State: 0.3mm

Load combination 2: Pre-stress forces, self-weight, dead loads, and snow load (LC1 + LC2 + LC3 + LC4)
Ultimate Limit State: 700mm
Serviceability Limit State: 400mm

Load combination 3: Pre-stress forces, self-weight, dead loads, and wind load (LC1 + LC2 + LC3 + LC5)
Ultimate Limit State: 961mm
Serviceability Limit State: 600mm

These results are acceptable for such a flexible system with 45m high.

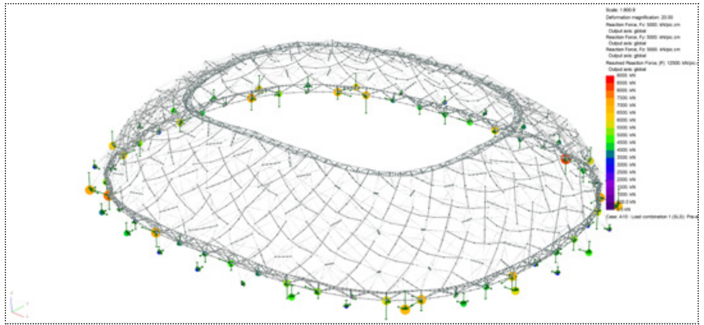

66.1(a). Load combination 1 (SLS)

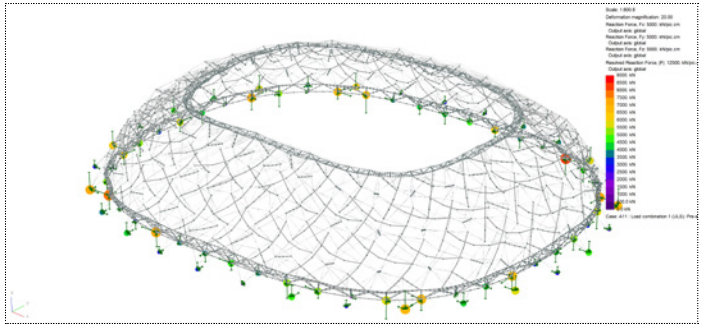

66.1(b). Load combination 1 (ULS)

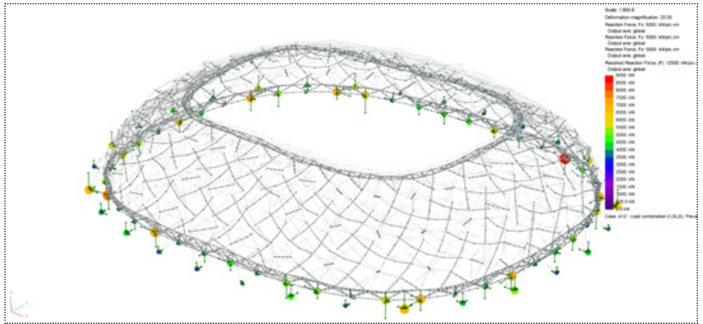

66.2(a). Load combination 2 (SLS)

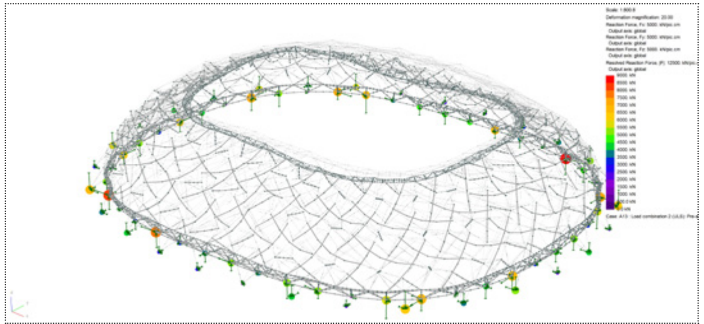

66.2(b) Load combination 2 (ULS)

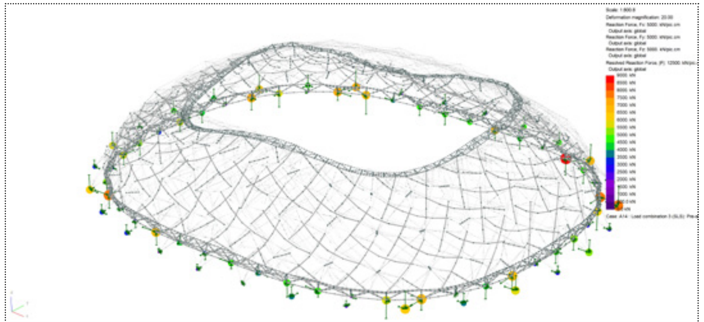

66.3(a).Load combination 3 (SLS)

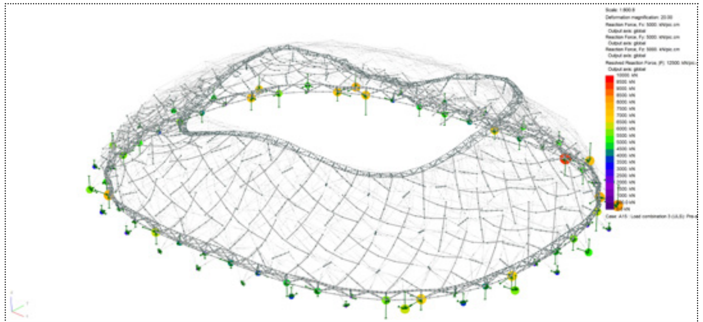

66.3(b). Load combination 3 (ULS)

Load combination 1: Pre-stress forces, self-weight and dead loads (LC1 + LC2 + LC3)
Ultimate Limit State: 9000 kN
Serviceability Limit State: 9000 kN

Load combination 2: Pre-stress forces, self-weight, dead loads, and snow load (LC1 + LC2 + LC3 + LC4)
Ultimate Limit State: 9000 kN
Serviceability Limit State: 9000 kN

Load combination 3: Pre-stress forces, self-weight, dead loads, and wind load (LC1 + LC2 + LC3 + LC5)
Ultimate Limit State: 9000 kN
Serviceability Limit State: 10000 kN

Support reactions do not change largely when the load cases changed. Pre-stress forces play an important role in this system.

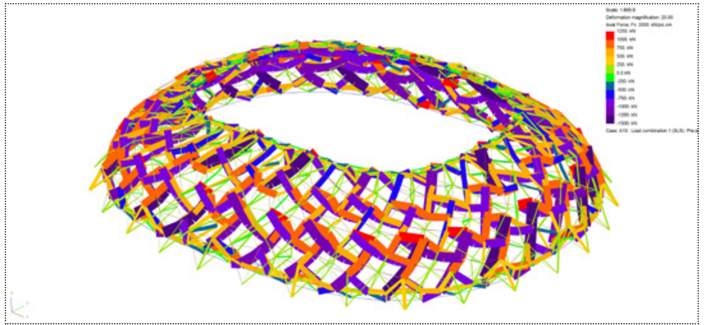

67.1(a). Load combination 1 (SLS)

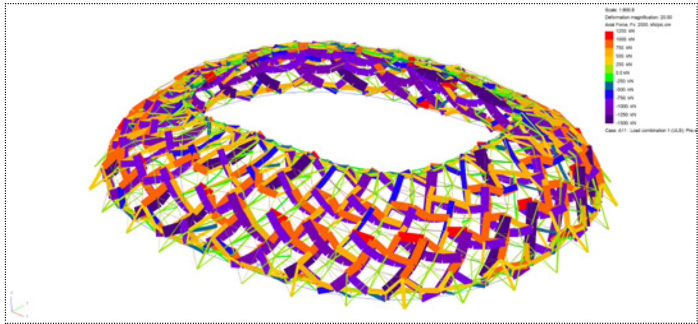

67.1(b). Load combination 1 (ULS)

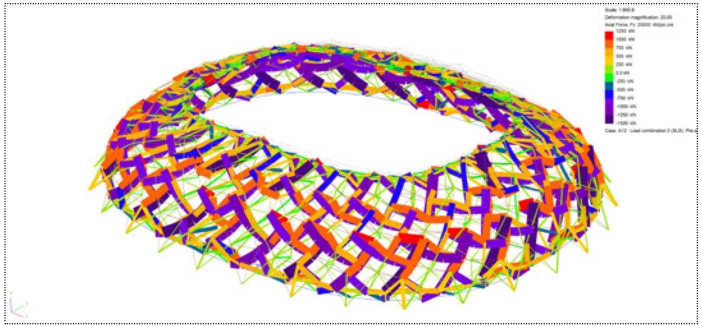

67.2(a). Load combination 2 (SLS)

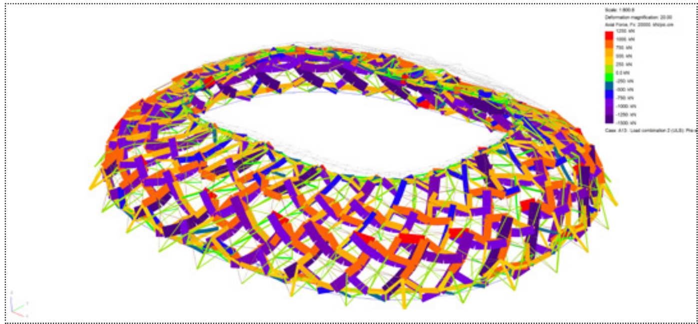

67.2(b) Load combination 2 (ULS)

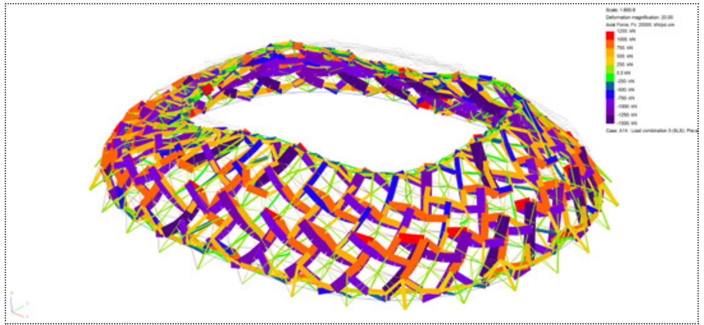

67.3(a).Load combination 3 (SLS)

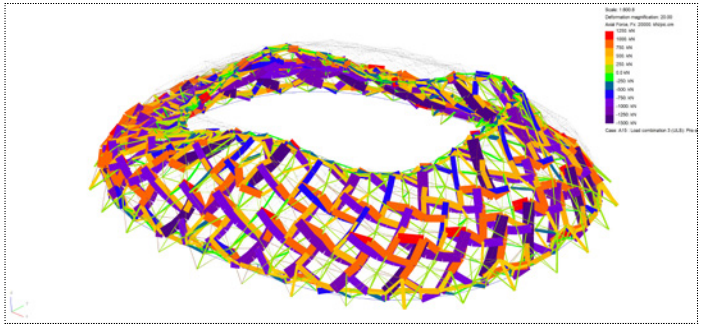

67.3(b). Load combination 3 (ULS)

Load combination 1: Pre-stress forces, self-weight and dead loads (LC1 + LC2 + LC3)
Ultimate Limit State: -1500 kN - 1250 kN
Serviceability Limit State: -1500 kN - 1250 kN

Load combination 2: Pre-stress forces, self-weight, dead loads, and snow load (LC1 + LC2 + LC3 + LC4)
Ultimate Limit State: -1500 kN - 1250 kN
Serviceability Limit State: 9-1500 kN - 1250 kN

Load combination 3: Pre-stress forces, self-weight, dead loads, and wind load (LC1 + LC2 + LC3 + LC5)
Ultimate Limit State: -1500 kN - 1250 kN
Serviceability Limit State: -1500 kN - 1250 kN

GF GALFAN Coated Steel - Full Locked Strands

PFEIFER

VVS-1 VVS-2 VVS-3

Material: Unalloyed quality steel
Modulus of Elasticity: 160 ± 10 kN/mm²
Tolerance Wire Diameter: +3%
Corrosion Protection: Inner layers: Hot dip galvanized with inner filling
Outer layers: GALFAN coated without inner filling

NOMINAL CABLE DIAMETER	CABLE CONSTRUCTION	METALLIC CROSS SECTION AREA	MINIMUM BREAKING LOAD			WEIGHT APPROX
mm		mm²	kN	kg	lb	kg/m
21.0	VVS-1	281.0	405	25000	91040	2.4
26.0	VVS-1	430.0	621	38360	139600	3.6
31.0	VVS-2	634.0	916	56630	205920	5.3
35.0	VVS-2	808.0	1170	72340	263020	6.8
40.0	VVS-2	1060.0	1520	93970	341710	8.9
45.0	VVS-2	1340.0	1930	119380	433880	11.2
50.0	VVS-2	1650.0	2380	147140	535040	13.8
55.0	VVS-3	2090.0	3020	186730	678920	17.2
60.0	VVS-3	2490.0	3590	222040	807060	20.5

68.1. Pfeifer Cable Structure, GALFAN Coated Steel - FUll Locked Strands

SS Stainless Steel - Open Strands

1x19 1x61 1x91

Material: Grade 316

NOMINAL CABLE DIAMETER		CABLE CONSTRUCTION	METALLIC CROSS SECTION AREA	MINIMUM BREAKING LOAD			WEIGHT APPROX
mm	in.		mm²	kN	kg	lb	kg/m
7.0	9/32	1 x 19	29.2	35.0	3540	7800	0.243
8.0	5/16	1 x 19	38.2	45.4	4640	10220	0.317
-	3/8	1 x 19	54.2	64.0	6546	14434	0.446
10.0	-	1 x 19	59.7	71.0	7250	15980	0.495
-	7/16	1 x 19	73.7	86.0	8770	19335	0.624
12.0	-	1 x 19	86.0	102.0	10400	22930	0.713
-	1/2	1 x 19	96.3	119.0	12101	26678	0.804
14.0	9/16	1 x 19	117.0	139.0	14170	31240	0.971
16.0	5/8	1 x 19	153.0	182.0	18550	40910	1.270

68.2. Pfeifer Cable Structure, GALFAN Coated Steel - Open Strands

From 300 Struts to 4200 Struts

There are 300 struts in structural model due to computational expensive calculation. In reality, the structure will have 4200 struts. Therefore, the maximum axial forces and stresses will be smaller. As a result, the structural element will be more optimized. This mean diameter of cables can be decrease from 40mm to 12mm or smaller, picture 4.35-36. And the diameter of CHS struts can be decrease from 400mm to 150-100mm.

$$\frac{\text{the number of struts in model}}{\text{the number of struts in reality}} = \frac{300}{4200}$$

$$= 0,07$$

$F_{compression;max;reality} = 1500.0,07 = 105$ kN
$F_{tension;max;reality} = 1250.0,07 = 87.5$ kN
$\sigma_{compression;max;reality} = 400.0,07 = 28$ MPa
$\sigma_{tension;max;reality} = 1000.0,07 = 70$ MPa

Buckling of Struts

The longest strut is 10 [m] with two ends pinned K = 1, CHS139x10, I = 868.10^4 [mm^4]. Maximum load can be handled by strut following Euler's formula:

$F_{max\ (139.3x10)} = \pi^2.EI/(KL)^2$
$= 3,14^2.210000.868.10^4/(1.10000)^2$
$= 85810$ [N] $= 179,72$ [kN]

$F_{max(139x10)} > F_{compression;max;reality}$, so there is no buckling.

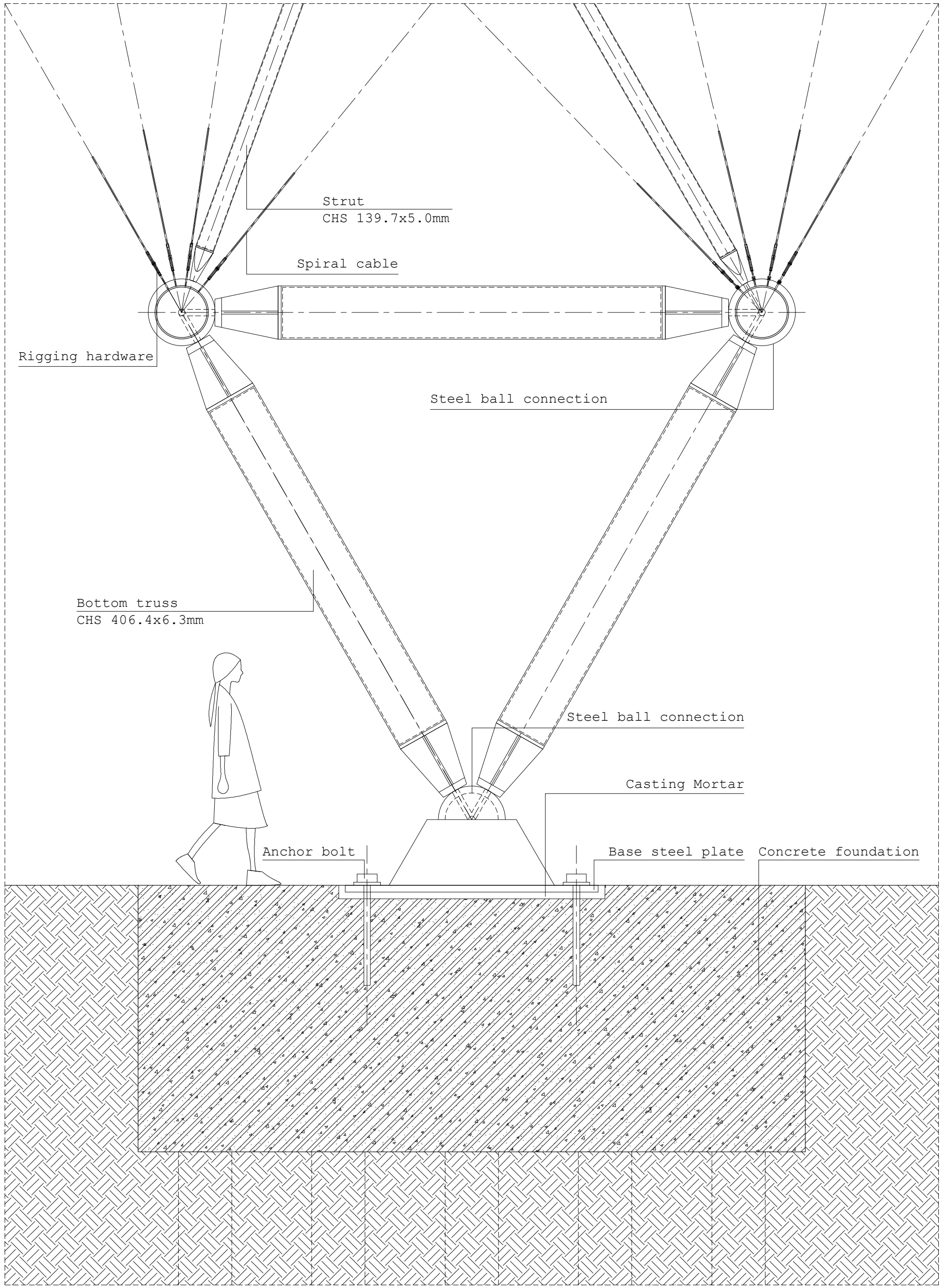

69. Foundation - Bottom truss - Tensegrity (Strut and cable network)

The connections between the tensegrity shell and the bottom truss as well as top truss are also necessary, they are pinned joints.

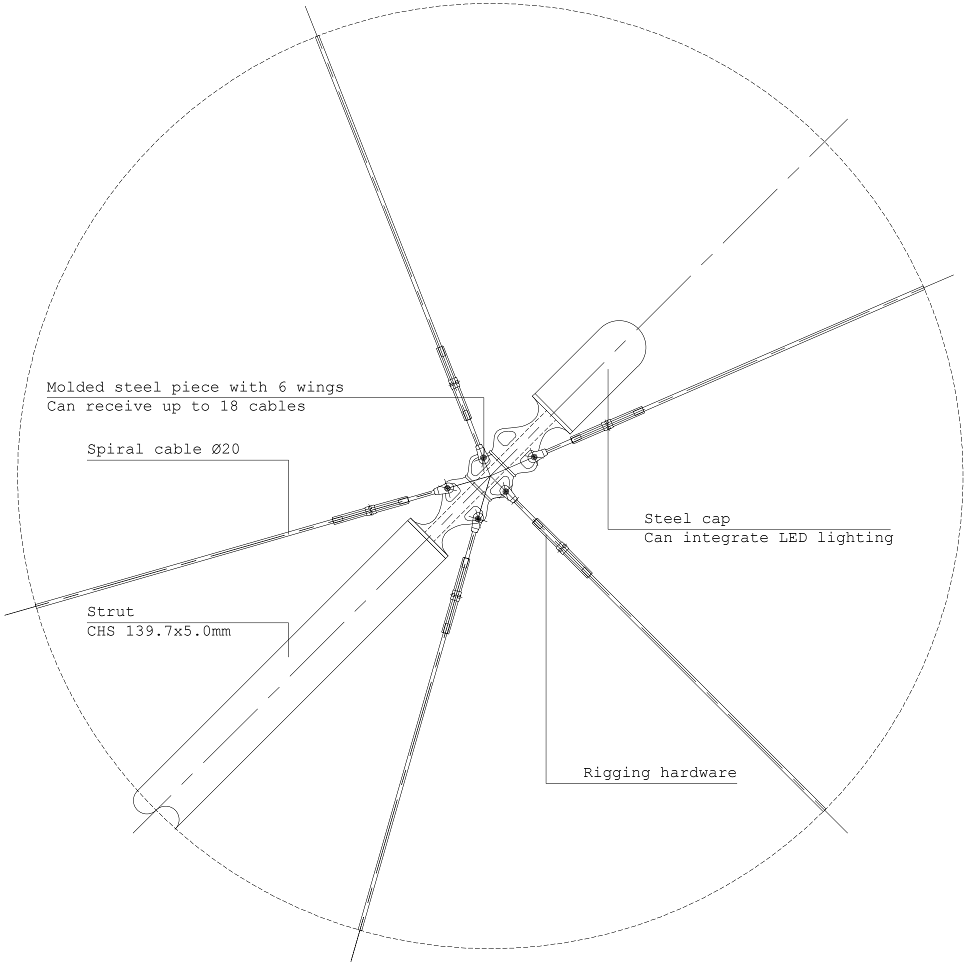

70. Tensegrity joint - Side view

In a true tensegrity system, the typical connection is the one in which there is only one strut linking with many other cables, and the minimum amount is three cables. So it is utterly essential that the connection has to accommodate forces coming from all directions but creating no bending moment. To achieve this, a connection needs to hold all the structural elements in a way that the central lines of these elements are meeting at one point. Aesthetically, the size of the joint should be as small as possible, so that it is not distinguished from the body of struts. At best, they should naturally be a part of struts to receive cables coming. Achieving this, there will be no connection anymore but only the network of struts and cables.

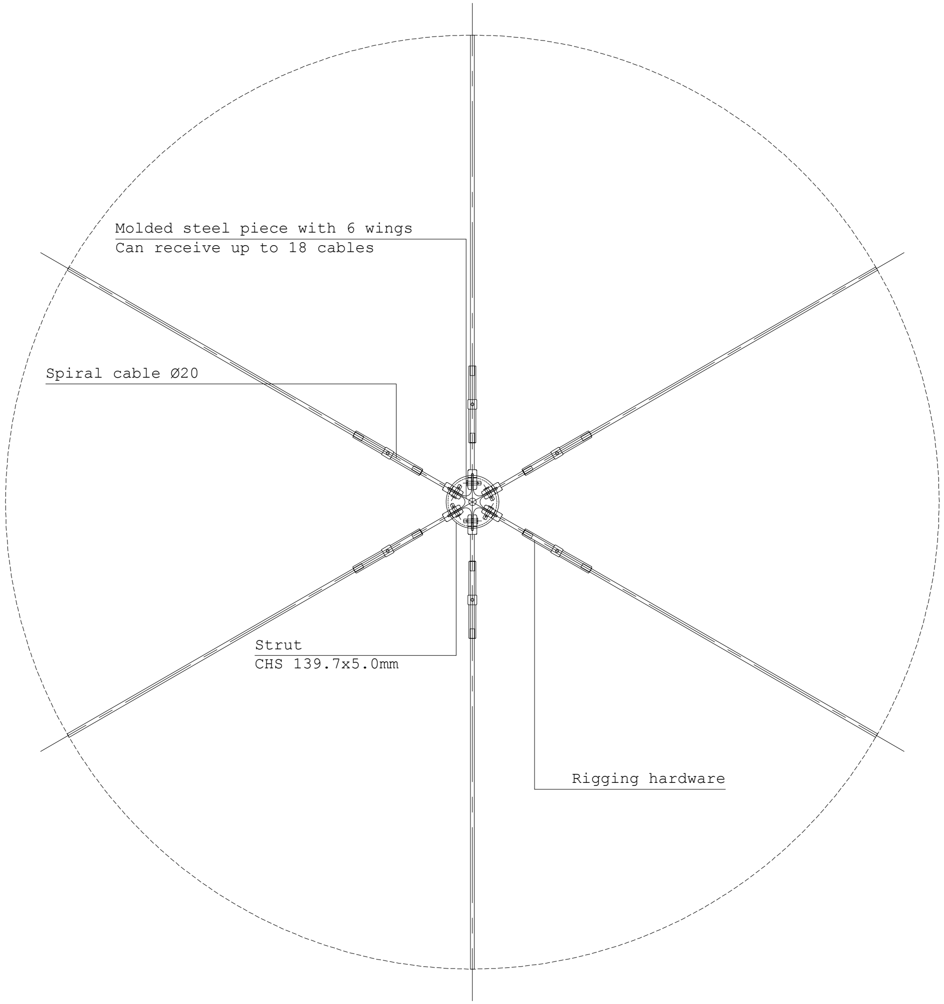

71. Tensegrity joint - Horizontal section

In a true tensegrity system, the typical connection is the one in which there is only one strut linking with many other cables, and the minimum amount is three cables. So it is utterly essential that the connection has to accommodate forces coming from all directions but creating no bending moment. To achieve this, a connection needs to hold all the structural elements in a way that the central lines of these elements are meeting at one point. Aesthetically, the size of the joint should be as small as possible, so that it is not distinguished from the body of struts. At best, they should naturally be a part of struts to receive cables coming. Achieving this, there will be no connection anymore but only the network of struts and cables.

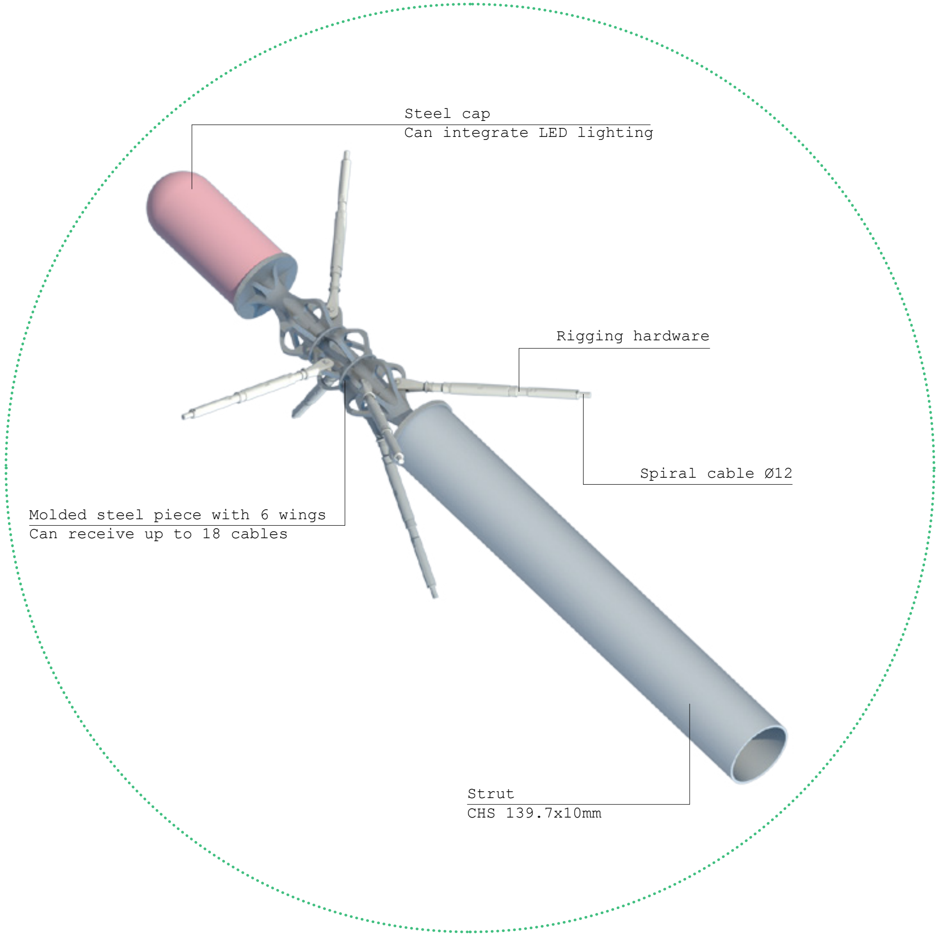

72.1. Perspective view

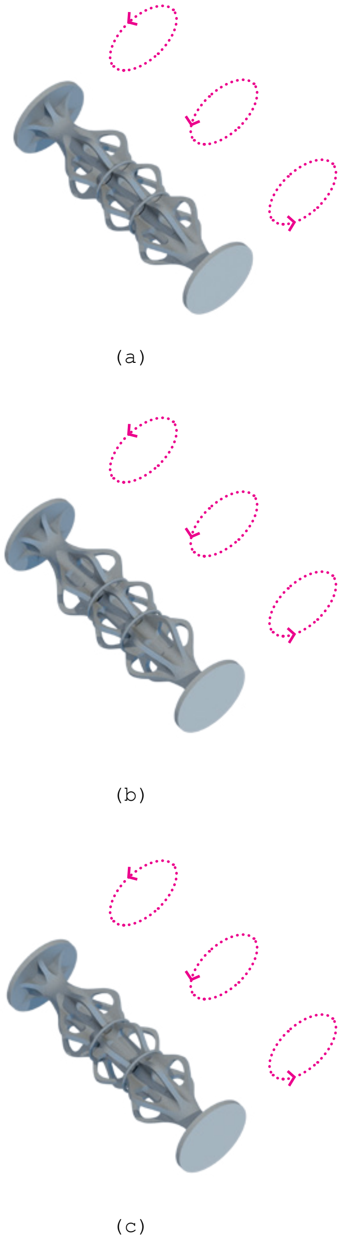

72.2. Self-rotating joint

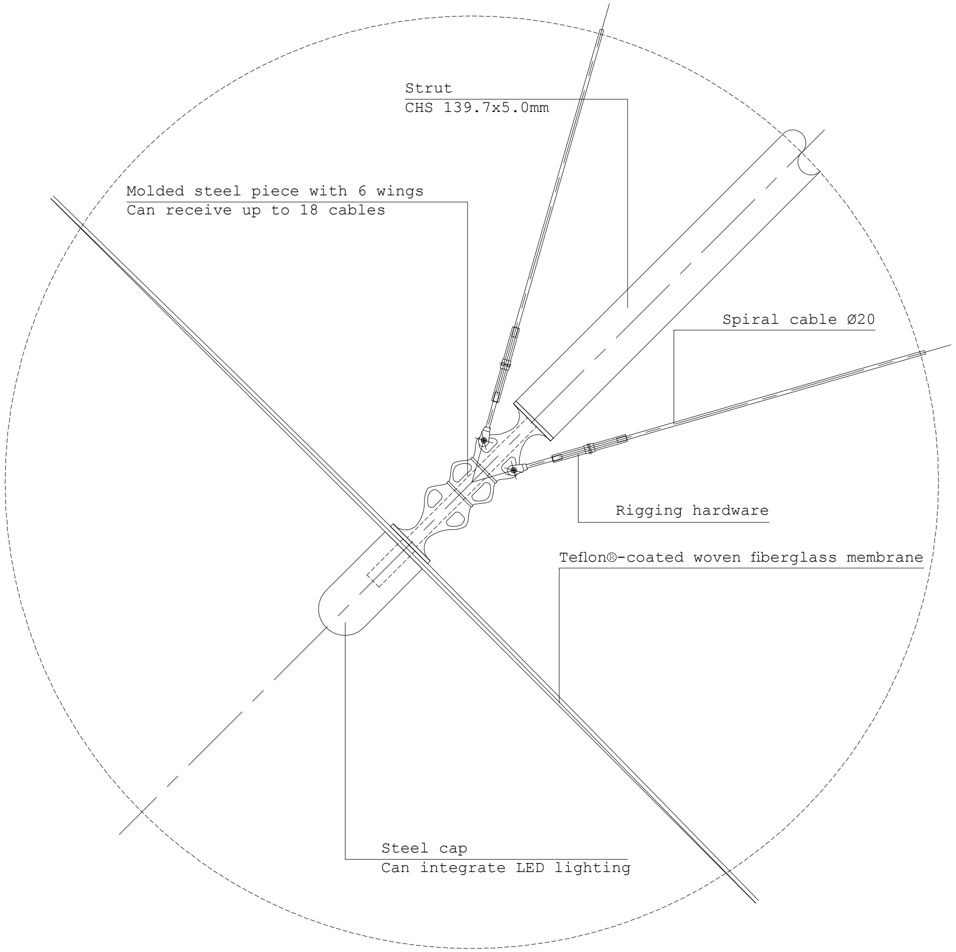

73. Connecting to the cladding at the bottom of strut

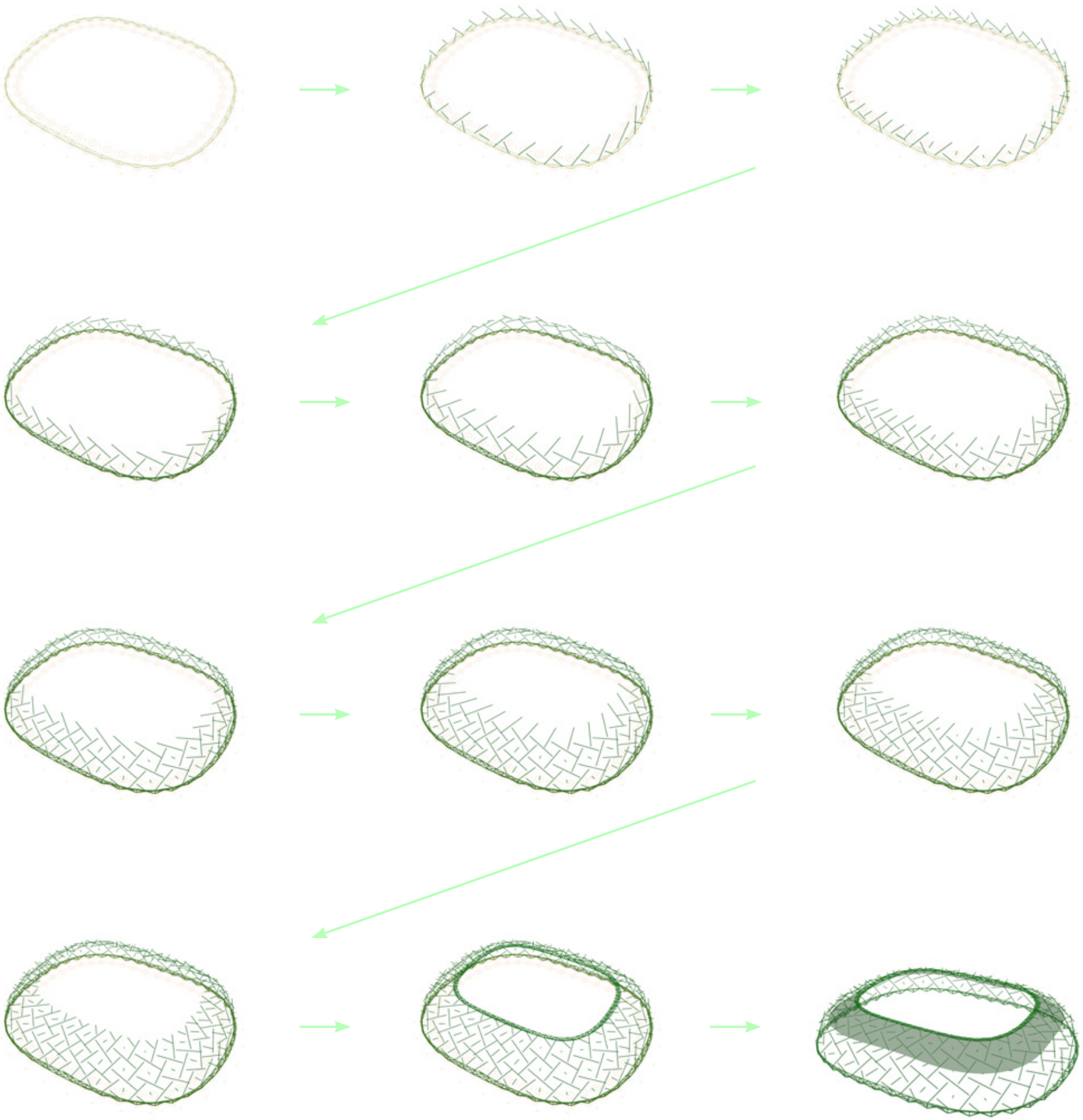

74. Construction sequence

(1) Taking off the roof and four lighting posts of the current stadium.
(2) Setting the concrete shallow foundation ring to the ground.
(3) Installing the bottom truss.
(4) Installing the first round of struts, for the first time, every longer strut will be fixed to its designed positions in space by three cables to the ground. The shorter struts will be fixed to bottom truss and longer struts by cable with measured lengths.
(5) Lifting normal struts to fix them to the first round of tensegrity by normal cables. Making sure that all cables will be in tension.
(6) Keep adding struts and cables bottom-up until the last round of tensegrity part.
(7) Installing the top truss on the ground, lifting it up to the designed level, fixing it to the tensegrity shell with pinned joints.
(8) Adjusting the tension in the cable network to get expected geometry, stiffening the entire structure.
(9) Installing ETFE roof underneath the new structure to cover all the stadium's stands.
(10) Finishing

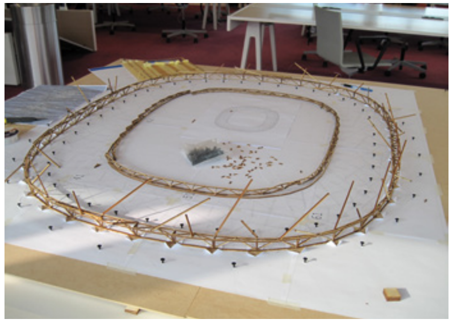
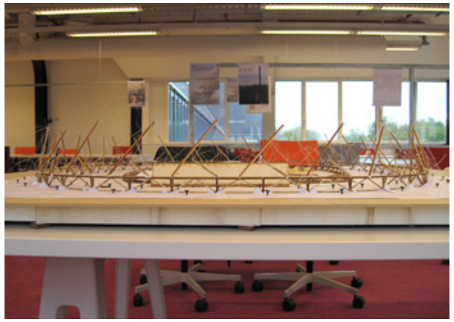
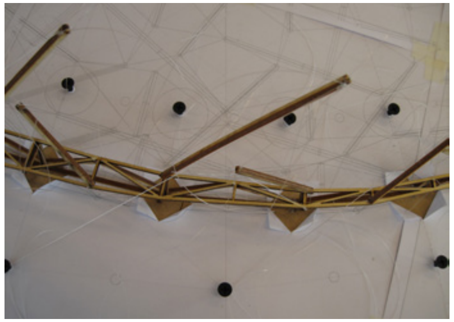


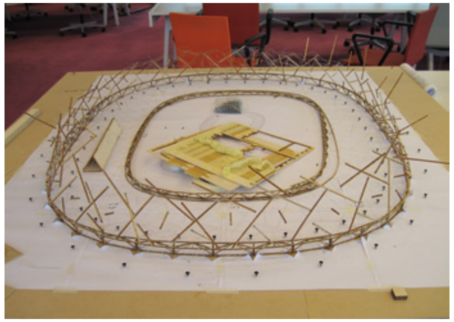



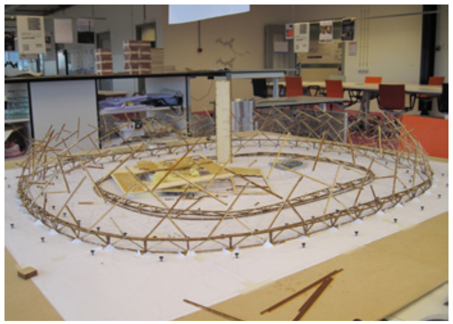
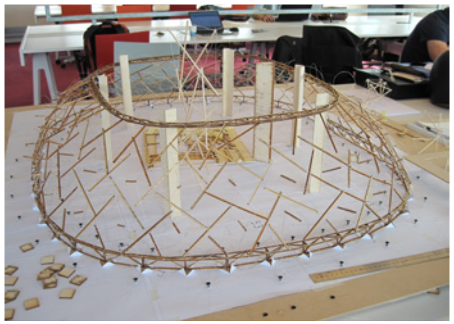
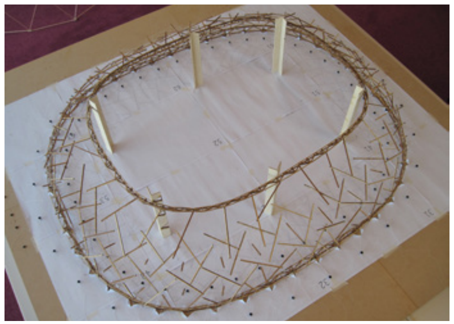

(1) The new design method for double-surface tensegrity systems is constructed along this thesis. There are two families of double-surface tensegrity structures that are discovered.

(2) Double-surface tensegrity structures are buildable.

(3) Based on a generic grid of vertices, the structural can be computationally generated by programming which will bring a lot of possibilities to develop such a system.

(4) The modeling is conducted in rhino and grasshopper, so the model is not entirely parametric yet. Structural model can be built in grasshopper along with all the structural properties, such as material, element type, sectional profile.

(5) Oasys GSA is only a calculation platform, and the design time is shortened.

(6) After form-finding, the found shapes are very stiff. The geometries handle very well its own weight as well as some other loading conditions, such as dead loads, snow load, and wind load.

(7) Finding the right pre-stress forces is the key of a successful form-finding using 'ignore form-finding properties' in Oasys GSA.

(8) The areas around inner ring deformed the most.

(9) The more elements a structure has, the smoother it is after form-finding.

(10) The process is not linear, but it is expected. There is always a need to go back to check and redo to be able to move forward.

(11) It is crucial to compare behaviors of physical models and digital model to direct the research and design to the right direction.

Thank you for your attention!